Politecnico di Torino

Master Thesis in Automotive Engineering
A.Y. 2020/2021
Graduation session October 2021

Development of a lightweight passenger cell for a highly efficient competition prototype vehicle

Thesis Supervisors:
Prof. Andrea Tonoli
Prof. Dr. Markus Zimmermann
M.Sc. Duo Xu

Candidate:
Alessandro Fruni

Abstract

In the current automotive panorama, one of the main focuses for car manufacturers is the compliance with the emissions regulations set by authorities. An improvement of vehicle efficiency leads to more environmentally friendly products without worsening vehicle performances. Considering battery electric vehicles, the efficiency is the parameter to be optimized to reach the range target, probably the most critical characteristic of the current models. Starting from these motivations, this research will investigate the efficiency optimization of the vehicle body. This is done by means of the development of the body part for the new car of TUfast Eco team, which is involved in the design of high efficiency vehicles to participate in the Shell Eco-marathon competition. The new vehicle is called MUC022 and will take part in the 2022 season.

In particular, the outer body shape of the car and the relative structural part, a monocoque in Carbon Fibre Reinforced Plastic material, will be derived in CAD environment. To increase the efficiency, the weight must be reduced while the aerodynamic performances improved. The result will be an optimization of the body shape and a reduction of the vehicle projected frontal area. These outcomes are feasible thanks to a streamlined style shaped by means of CFD analysis. The concept must comply with the competition regulations, respecting the stated vehicle external and internal dimensions while assuring accessibility and roominess for the driver and his/her luggage.

The monocoque model will be derived starting from the outer body shape and refined in order to assure enough space for the various systems and subsystems of the vehicle. Furthermore, the structural integrity must be considered during the passenger cell design. A FEM analysis allows to assess and validate the strength and stiffness performances of the structure.

The production requirements will be studied and implemented to assure the manufacturability of the described solutions. A reliable production process will be selected, and the geometry properly adapted to the manufacturing procedures. The moulds of the monocoque will be finally designed.

Table of Contents

1 Introduction

1.1 Motivations and Goals

The motivations of this research are linked to the current automotive trends, mainly focused on the reduction of vehicle emissions and electrification. The authorities in many markets are pushing toward the reduction of pollutants for the cars equipped with an internal combustion engine. At the same time, the electrification trend is more and more relevant also because of the support of different organizations, like the European Union, and single countries initiatives.

In this context, the efficiency is an important parameter since it directly influences the homologation of the new vehicle and the performances in terms of fuel consumption, a crucial characteristic for a potential final customer. This is further amplified in the case of battery electric vehicles, where the global vehicle efficiency influences the vehicle range, one of the most controversial characteristics of this typology of cars.

A proper design of the vehicle body allows to reduce the mass of the car which is directly influencing the resistance to motion. This can be done working both on the geometry of the structural part or selecting unconventional materials. It is the case of composite materials, which allow a huge mass saving with respect to traditional materials like steel and aluminium. The design of the vehicle body is also linked to the aerodynamic performances of the car. It is possible to tune aerodynamics in order to further reduce the drag acting against the vehicle.

These motivations are the basis for this research which has the goal of evaluating the vehicle efficiency in relation to car body design. This kind of study is performed by means of the design of a high efficiency vehicle characterized by an extremely reduced vehicle mass and by a shape expressly design for aerodynamics. Nevertheless, these targets must be reached without an excessive worsening of the other vehicle characteristics (visibility, accessibility, internal roominess) which are common also to passenger cars.

Indeed, even if the vehicle is designed according to competition rules, the validity of the procedures can be extended to passenger cars, whose design procedures can be influenced by this research.

1.2 TUfast Eco Team and Shell Eco-marathon

TUfast is a registered company, based in the Technical University of Munich, born in 2002 to create an environment where students can gain practical experience in the development of race cars. In particular, the racing team takes part every year in the Formula SAE, with the objective of building a new, superior TUfast race car every single year. Furthermore, thanks to the organization, students with different backgrounds can enter in contact, developing innovative solutions through interdisciplinary cooperation. Therefore, the students at the

Technical University of Munich can develop their own race car: they take control of every step, as it happens in real working experiences (TUfast, n.d.).

In 2009 the company was expanded creating a new team, focused on high efficiency vehicles, called “TUfast Eco Team”. TUfast Eco Team is taking part to international competitions, such as the Shell Eco-marathon, in which the objective is creating the most efficient vehicle among the participants. Initially, TUfast Eco Team started developing high efficiency prototypes, able to define new limits in terms of energy consumption. These vehicles are characterized by extreme outer shapes and layouts, to reduce as much as possible the resistance to motion. In 2017, with MUC017, the team passed from the prototype class of the Shell Eco-marathon to the urban concept category. Consequently, the focus during the last years was on the development of bigger vehicles, similar to small citycars, always with the target of lightweight and efficiency. With respect to prototypes, urban concept vehicles must offer a certain internal space for occupants and luggage, increasing the challenges of the project. Figure 1-1 shows the 2019 team and MUC019.

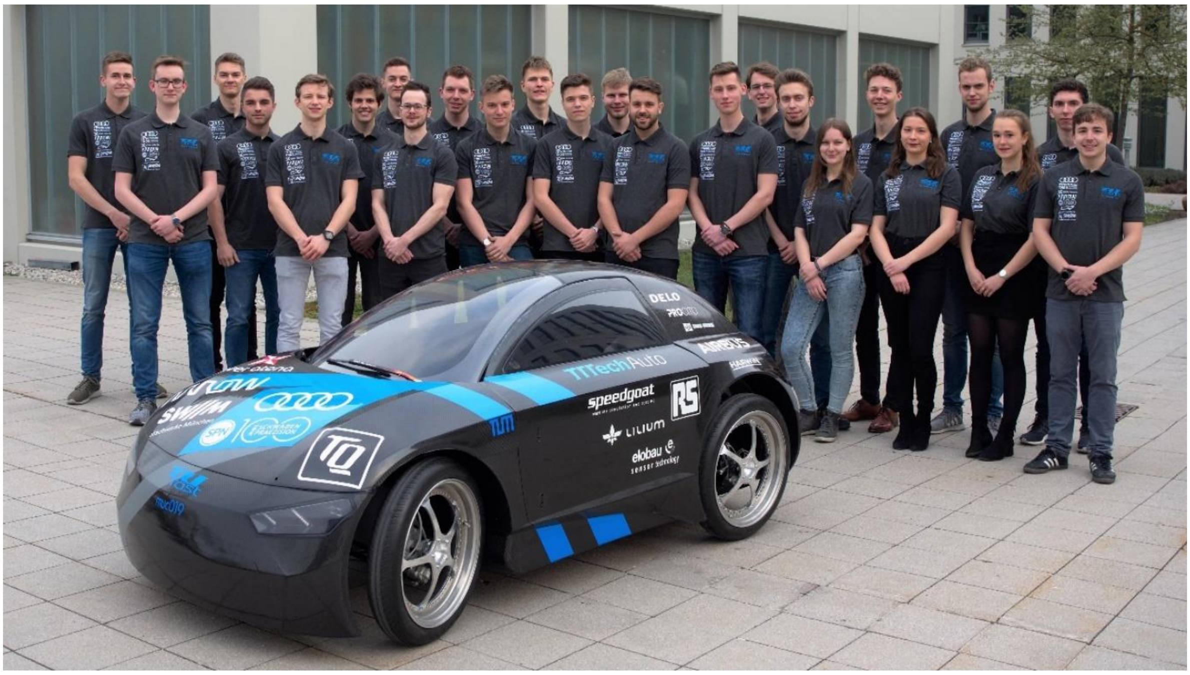

Figure 1-1 TUfast Eco Team and MUC019 (TUfast, 2019)

With its work, TUfast Eco Team wants to contribute to the creation of a "green" mobility, developing competencies in this subject and implementing the latest innovations in their vehicles. This is traduced in an active participation in the future of mobility.

It is important to point out that the team, working on MUC022, the next vehicle which will take part in the Shell Eco-marathon, has been completely renovated and has started working without a proper know-how transfer from previous projects. For this reason, the aim of this work goes beyond the development of a single vehicle, since the creation of documented methodologies and solutions is a necessity for the future team projects.

TUfast Eco Team has been taking part in different international and national competitions since it was born. In particular, the Shell Eco-marathon is the most important competition of the sector because of its age and size. For this reason, the rules the team is considering during the design phase are the ones issued for this race.

Shell Eco-marathon is an energy efficiency competition sponsored by the homonymous company. The goal of the competition is developing and building automotive vehicles to achieve the lowest possible energy consumption. The competition was born in 1939 as a bet between Shell employees to see who could drive further with one gallon of fuel. Since 1985, it becomes a design competition for students where each student team must create a vehicle to drive a certain distance while using as little energy as possible.

In order to compete at the event, each team must respect carefully the milestone presented in the rules during the design and build process. Before the track competition, a technical inspection is performed to check the compliance with Shell Eco-marathon rules (Shell, n.d.).

Because of the pandemic, the live track events of 2020 were cancelled and substituted with a virtual programme. In this way, the students have had the possibility to work on their projects, even if the traditional race was not feasible (Shell, n.d.). For 2021, a hybrid competition was announced: a virtual programme was confirmed together with an “on track” competition, called “Mini Shell Eco-marathon”. It will be characterized by smaller events across the different regions. With reference to the 2022 edition, there are not news yet, but it is expected an “on track” competition. In Figure 1-2 it is possible to see some Urban Concept vehicles during the competition.

Figure 1-2 Some Urban Concept vehicles at Shell Eco-marathon (Shell, n.d.)

1.3 Structure of the Thesis

The “State of the Art” chapter is devoted to the analysis of three themes characterizing the car body design. Initially, the vehicle body structure is introduced, highlighting its characteristics and the relative functions. Subsequently, the most relevant aspects of the car aerodynamics are reported and described. Finally, a focus on composites is required to analyse in deep the properties and the behaviour of the material.

The following section represents the effective starting point for the research. Indeed, Chapter 3 is dedicated to the analysis of the requirements (rules, efficiency targets and structural requirements). The results are presented starting from Chapter 4, where the overall outer shape of the vehicle is presented considering the concept decisions and the preliminary packaging analysis. An aerodynamic evaluation allows to highlight the differences with respect to the old model. Successively, the monocoque design is illustrated, explaining the reasons behind the geometry of the structure. At the same time, also a structural validation is required to assess the performances of the body. Finally, the manufacturing procedure is reported together with the selected assembly techniques.

2 State of the Art

An evaluation of the current standards in the car body design is fundamental to summarize and categorize relevant information for the subsequent steps of the research. This analysis is realized in three parts related to vehicle body, aerodynamics and materials.

2.1 Vehicle Body

It is important to have a clear idea about the past and current technical solutions in the field of body design. This chapter is dedicated to the evaluation of the most common body configurations and vehicle body functions.

2.1.1 Historical Evolution and Modern Monocoques

At the beginning of the 20th century, the first cars were designed conceiving the body in two main parts: the body and the chassis frame. The latter was designed to carry the majority of the loads and to provide the attachments for every mechanical system. On the contrary, the body part was conceived as a sort of dead weight (Morello, Rosti Rossini, Pia, & Tonoli, 2008a, p. 5). From the point of view of the materials, the chassis was built using wood or steel. In particular, steel was used in the form of bent and cut sheets or by means of tubes. The body part was initially made of wood to realize complex shapes and to use the same manufacturing techniques previously adopted for carriages. The geometric layout of the chassis portion passed from the original "grillage" solution to most advanced "X" shaped chassis. This one was able to withstand the torsion of the whole car in a better way because the beams forming the "X" were subjected to bending, improving the global performance of the structure even if an open cross section was adopted. Figure 2-1 reports the two configurations.

A

B

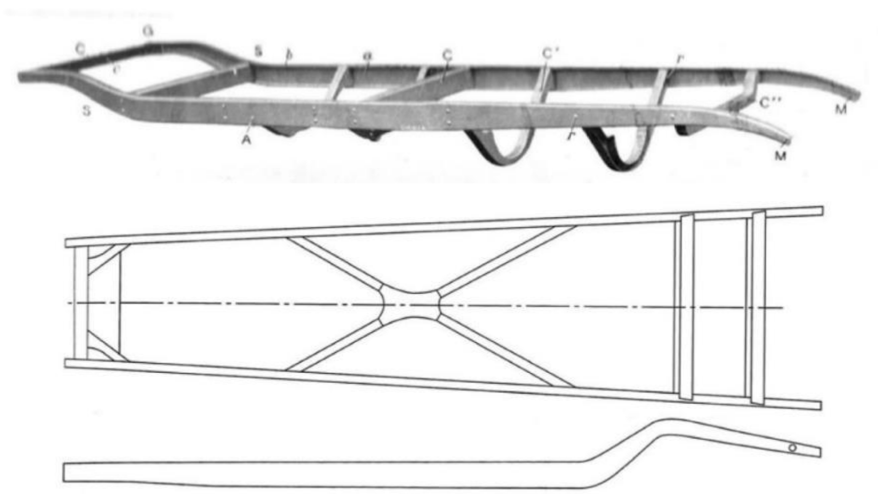

Figure 2-1 The grillage (A) (Morello, Rosti Rossini, Pia, & Tonoli, 2008a, p. 6) and X-shaped chassis (B) (Morello, Rosti Rossini, Pia, & Tonoli, 2008a, p. 13)

In 1935, Fiat presented the 1500, a very advanced car with a new layout characterized by a partial integration of the body with the chassis. In this solution the chassis frame was bolted and not welded. Nevertheless, the body started to contribute to torsional performances. At the same time, the “X” shape of the chassis helped to reduce the overall height of the vehicle with a consequent reduction of the aerodynamic drag.

The last step in the evolution of the structural part of the car, was obtained with the integration of chassis and body with the aim of improving the stiffness while reducing the overall mass. A first example of this idea can be found in the Lancia Lambda (1922). In this car the chassis was integrated with the body and the dimensions of the doors were reduced to have bigger sills to increase the overall stiffness (Morello, Rosti Rossini, Pia, & Tonoli, 2008a, p. 19). A picture of its chassis is reported in Figure 2-2.

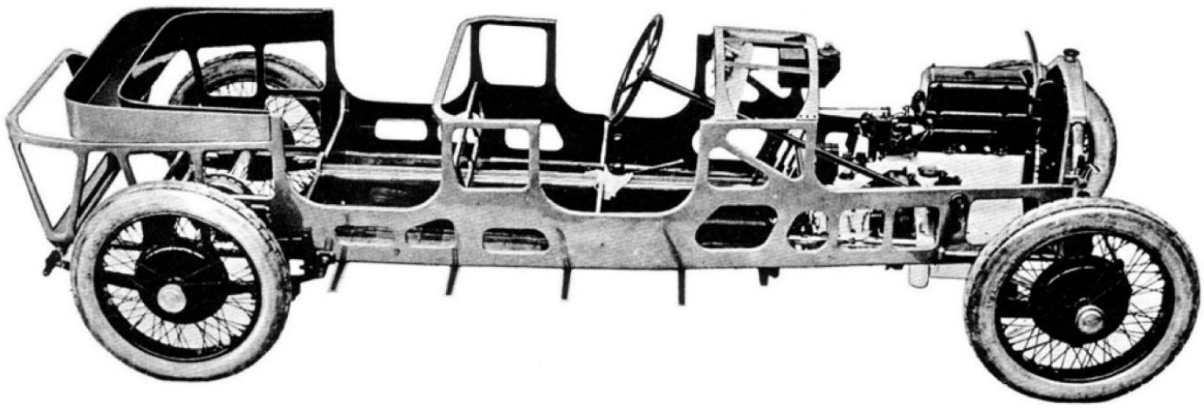

Figure 2-2 Lancia Lambda chassis (1922) (Morello, Rosti Rossini, Pia, & Tonoli, 2008a, p. 20)

Today, most of the passenger cars use the unibody configuration with ancillary subframes. The variety of materials used is increasing, passing from steel (mostly adopted in the form of sheets) to aluminium and new advanced materials. The aluminium can be implemented as sheets, exploiting die casting (common for the A pillar) or by means of extrusion. Generally, a theoretical weight saving around 45% (Scattina, 2020) can be achieved passing from steel to aluminium. Nevertheless, the use of aluminium leads to additional problems like the reduced formability of the sheets and the necessity of using an inert gas environment to avoid oxidization.

A new strong trend in the material field is related to the use of composite materials, indeed, they allow to reduce drastically the weight while assuring excellent mechanical performances. Currently, they cannot be introduced easily in mass production vehicles design because of the longer cycle times and the high human contribution during the production. On the contrary, it seems extremely beneficial in the case of race cars and high-performance vehicles. In fact, it is a consolidated option for the realization of the chassis of Supercars and Hypercars.

The Alfa Romeo 4C (2013) is an example of car adopting a carbon fiber monocoque with the aim of reducing the overall mass. Indeed, this car weighs only 895 kg thanks to the use of a monocoque of 65 kg. This latter is created by means of the “pre-preg” process and, after the curing cycle in the autoclave, allows to obtain a single element that works in a compact way against external loads.

Then, two additional frames are attached to the front and rear structure of the monocoque, to provide a connection for the suspensions and for the powertrain. These structures are realized in aluminium while the cross section is varying according to the load applied to the different areas of the frame. In Figure 2-3 the structural part of the car is depicted.

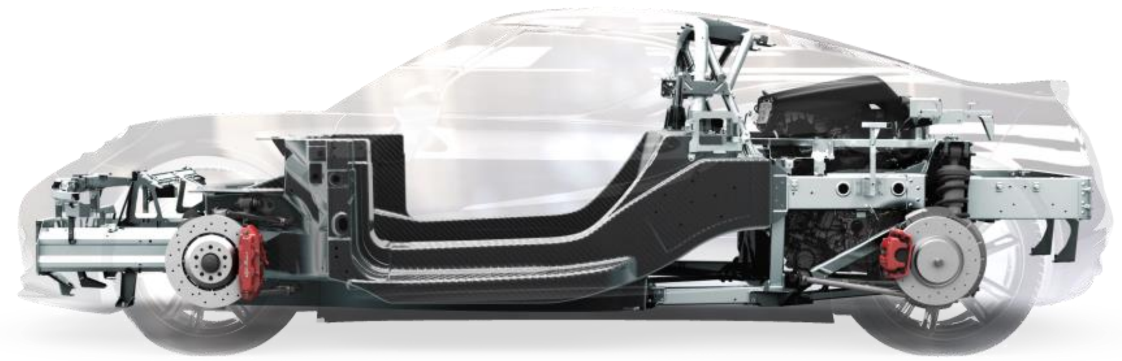

Figure 2-3 Alfa Romeo 4C structural part (Auxibito, n.d.)

A completely different concept characterizes the BMW i3. It is a Battery Electric Vehicle with a citycar body style. Indeed, it is long less than 4 metres, and is conceived as a premium mass production car. This is one of the few applications of carbon fiber in a car which is not completely focused on performances, since the use of composite materials in this BMW has the goal of counterbalancing the additional mass provided by the batteries. This solution leads to a curb mass around 1200 kg (BMW, 2013, p. 22), a very good result which allows good dynamic performances and increased battery range.

The carbon fiber is used to realize the upper part of the body, the so called “life module”, which is then joined to another module made in aluminium. This latter is then linked to the mechanical systems of the vehicle.

The life module is made up of 150 carbon fibre reinforced plastic parts (BMW, 2013, p. 41), which is a number significantly lower with respect to the parts in a conventional body in white. Another advantage of carbon fibre is the enhanced freedom in the design due to the strength of the material. Consequently, BMW had the possibility of removing the B pillar, creating a single door opening in the structure. In Figure 2-4 it is possible to see the body structure of BMW i3.

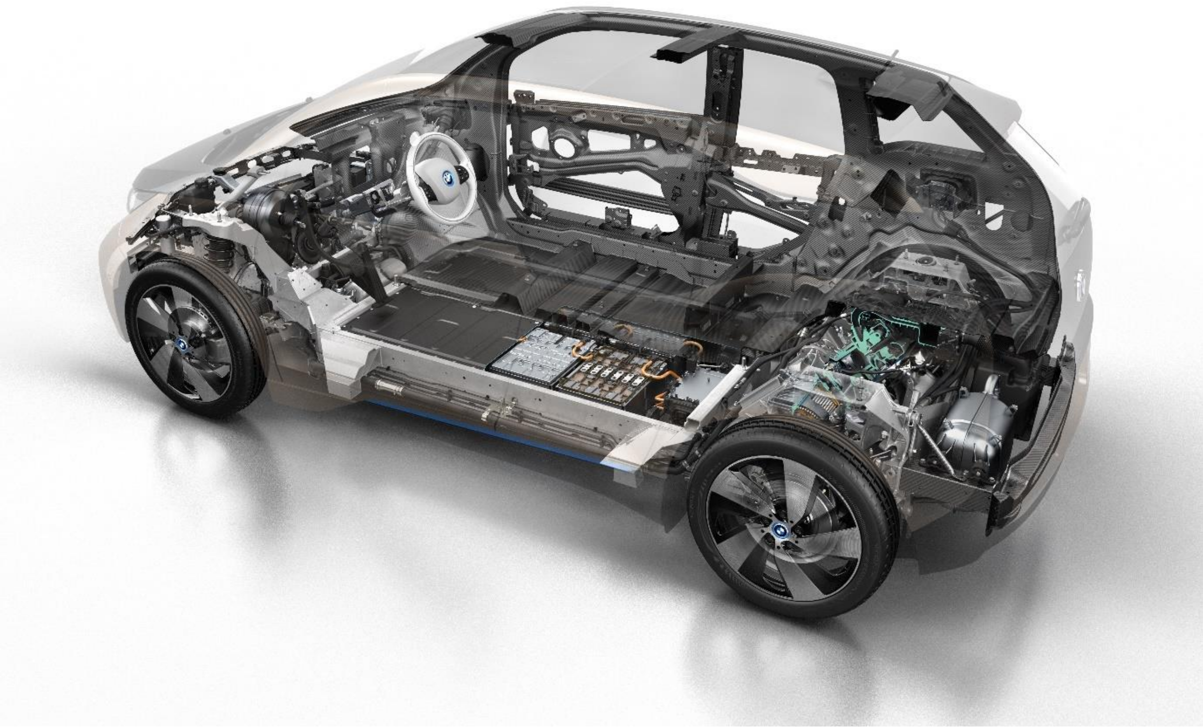

Figure 2-4 BMW i3 structure (BMW, 2013)

Another interesting vehicle, adopting a carbon fibre structure is the Rimac C_Two. The information in this paragraph is entirely referred to a video, published by Rimac itself (Rimac, 2020a). It is again a Battery Electric Vehicle but designed for high performances since it is a Hypercar with a power near to 2000hp. Rimac engineers designed the monocoque, in CFRP, starting from the driver position and taking into account the boundaries imposed by regulations and by the performance targets. The battery pack has a "H" shape: the modules are installed in the tunnel, behind the two passengers and in front of their feet. The first outcome of this choice is an aerodynamic improvement since the absence of battery modules under the occupants allows to reduce the H point height and consequently leads to a lower roof. The second outcome regards vehicle dynamics because the battery module in front of the passengers feet allows a tuning of the centre of gravity position. Indeed, it can be moved forward, with respect to equivalent vehicles, to improve the grip at the front axle. In Figure 2-5 the Rimac C_Two assembly line is depicted.

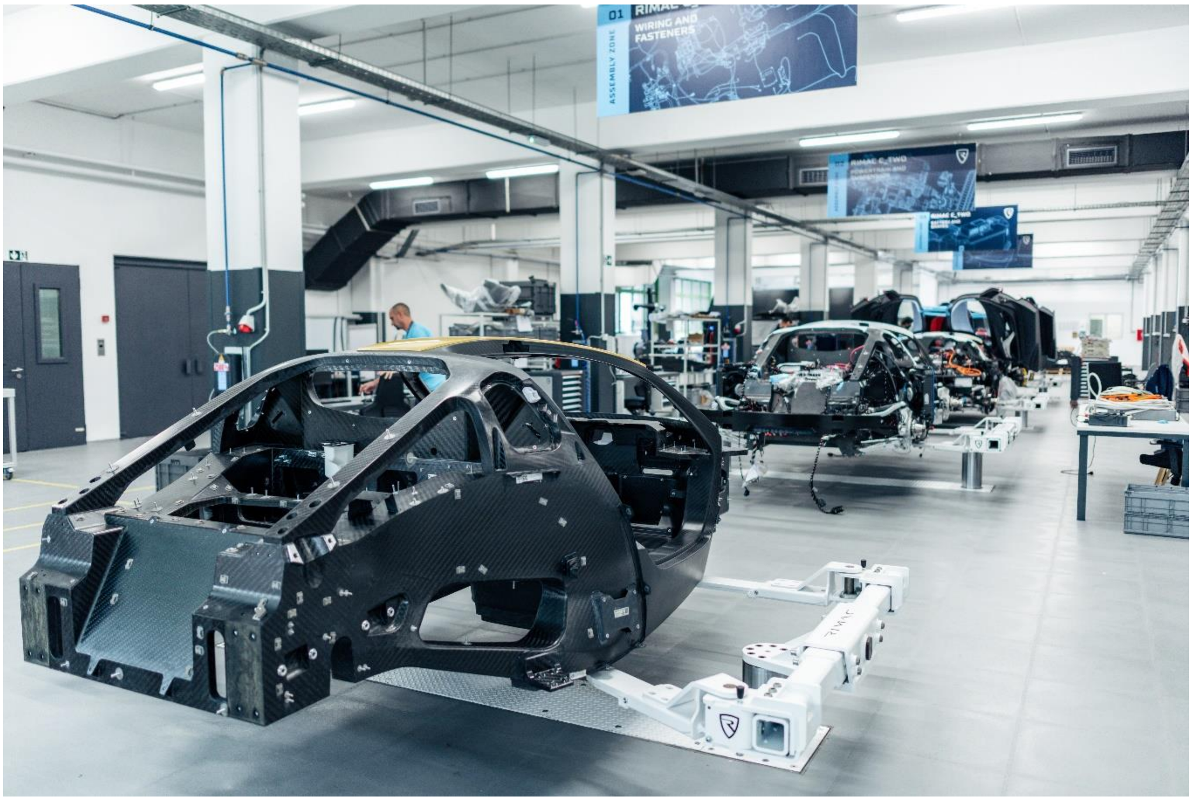

Figure 2-5 Rimac C_Two assembly line (Rimac, 2020b)

The lower part of the monocoque is made in a single part, cured in autoclave, to avoid concentration of stresses and to reduce the weight. This part is then bonded to the roof and to the upper structure. The roof is characterized by an "X" shape, which leads to a load path designed to exploit the roof when bending and torsion loads are applied. Two beams at the rear are included to improve bending performances and, therefore, to sustain the weight of the rear powertrain (Rimac, 2020a).

2.1.2 Definition and Configurations

The body is the part of the vehicle aimed to contain and to isolate from external agents the passengers and their luggage. The design of this part has changed during the years and different solutions were developed in relation to the various vehicle classes. According to the literature, there are different methods to integrate the underbody with the rest of the structure. It is possible to distinguish between four main configurations.

In Figure 2-6 the technical scheme of the four configuration is reported. The following section is referred to the classification described in "The Automotive Body" (Morello, Rosti Rossini, Pia, & Tonoli, 2008a, pp. 92-94).

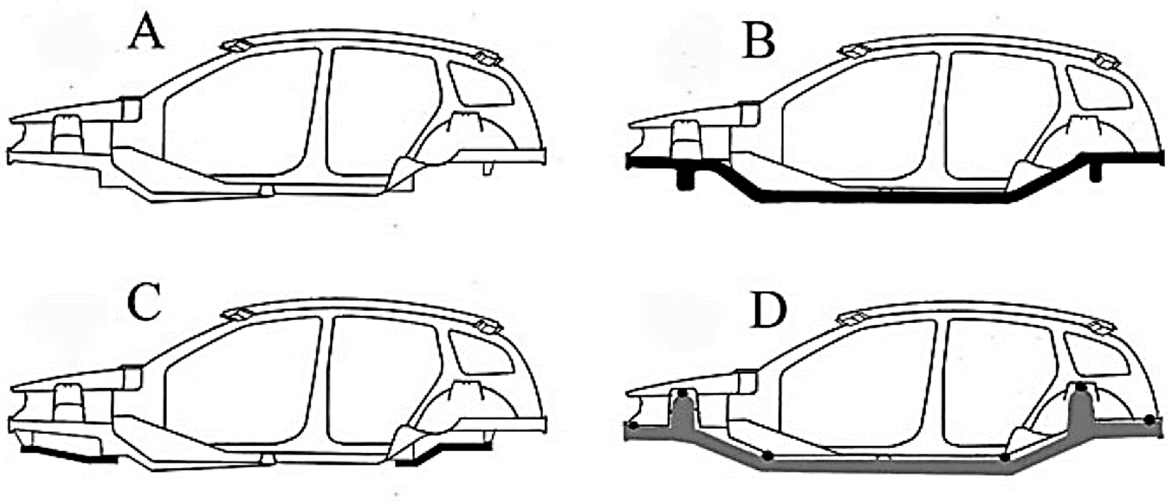

Figure 2-6 Common body configurations (Morello, Rosti Rossini, Pia, & Tonoli, 2008a, p. 93)

A) Unibody

In this case the underbody cannot be physically detached from the upper parts of the body, obtaining a weight reduction with respect to equivalent solutions. Nevertheless, because of the sequence of parts joined together, it is difficult to obtain a good dimensional precision at the level of the suspension attachment points. This solution is not so flexible during the assembly process in the case of mass production passenger cars. The monocoque of MUC022 can be seen as a unibody configurations since it will present unique structure comprising all the required attachment points for the suspension system.

B) Body on frame

The “Body on frame” configuration is obtained when the underbody is connected to the upper part by means of rigid links, like bolts. This solution is usually adopted in commercial vehicles because it leads to a higher flexibility in the assembly process. Indeed, commercial vehicles are usually characterized by many variants, therefore, the possibility to maintain the same mechanical part, changing only the upper portion of the body, allows to simplify both the design and logistic setup. A first drawback is the greater floor hight which is obtained with respect to the unibody solution, even if it is not a major problem in case of commercial vehicles. The second disadvantage regards the total mass of the solution since it is greater compared to the unitized body configuration.

C) Body with ancillary subframes

This is the solution usually adopted in passenger cars. It consists in a sort of unitized body solution with two detachable subframes for the fastening of powertrain and suspension system. This configuration leads to a better modularity for the assembly process. The weight is slightly higher with respect to the unibody configuration.

D) Dual frame body

In this case the chassis portion is separated from the body. The connection between the two parts is obtained by means of elastic joints which lead to a better insulation from road asperities. The structural, safety and propulsion targets are optimized on the frame part, so the increment in weight with respect to the unibody solution is partially counterbalanced by the weight reduction of the upper body.

2.1.3 Body Functions

The body is a vehicle part designed to fulfil different requirements at the same time. Most of the time the objectives are contrasting, therefore, the right equilibrium between them must be found. This section is based on the body functions listed in "The Automotive Body" (Morello, Rosti Rossini, Pia, & Tonoli, 2008a, pp. 105-135).

The first body function is the aesthetical one. Indeed, the outer panels determine the style of the vehicle according to the concept decisions of the project. The aerodynamics is strictly linked to the style: this is a body function of growing importance because of the latest emission regulations for passenger cars and because of the necessity to increase as much as possible the range of electric vehicles. Usually, the aerodynamic directives are in contrast with the style necessities, leading to solutions which are a trade-off between the two inputs. In the case of MUC022, the appearance of the vehicle is important for the team sponsors. Nevertheless, it is a minor problem with respect to what happens in passenger cars, where the style is one of the most important factors for the market success of the product.

It is clear that the weight of the passengers and the loads at which the car is subjected are completely sustained by the vehicle body. Probably, the structural function is one of the most relevant for the body because it is necessary to assure all the connections to the mechanical parts. At the same time, the structural function is assured also with a good support to concentrated loads.

The body must also assure good ergonomics and roominess for the occupants. This is obtained selecting the proper dimensions to host the passengers and their luggage. A packaging analysis is required to select the dimensions able to assure the expected level of comfort. The accessibility requirement is generally in contrast with the structural one since a good stiffness level is usually achieved by means of bigger sections. These latter could, for example, reduce the door openings area, leading to a worst accessibility. In the case of TUfast Eco Team, the ergonomics and accessibility are important functions since they are essential to develop a car of the urban concept class. While in passenger cars the movement of the occupants is studied to determine the required door opening, in the case of urban concept class, a minimum dimension is stated by the rules. Nevertheless, a certain degree of freedom in the design of the vehicle side is assured by the possibility of rotating this area. In this way, it is possible to tune the sill dimensions and, therefore, the stiffness of the car.

Also the visibility is a function of the vehicle body, because the extension of the panels determines the height of the belt line and the area of the windshield. The pillars are a relevant source of blind spots but their contribution is crucial for the stiffness target. Also in this case, a good compromise between these opposing trends must be found to be compliant with the rules.

Another function is the insulation from the external environment to minimize noise, vibration and thermal transmission. The vibration of the vehicle body panels is not directly considered during the design of MUC022. Nevertheless, a proper connection of each panel (in particular movable parts) must be assured by means of adequate hinges and locking mechanisms.

The last analysed requirement related to vehicle body is safety. The vehicle body must be designed to absorb part of the energy during an impact and to assure the presence of an undeformable passenger compartment which assures enough space for the occupants in the event of a crash. In the case of urban concept cars taking part to the Shell Eco marathon, the passive safety feature is verified thanks to the roll bar around the driver.

2.2 Aerodynamics

The aerodynamics has a direct influence on the performances of a vehicle in terms of handling, comfort and global efficiency. The aerodynamics contribution to the resistance to motion can be quantified considering the following expression:

$$F_{aer} = \frac{1}{2} \cdot C_d \cdot \rho \cdot A \cdot V^2 \qquad (2\text{-}1)$$

Different factors are present in Formula (2-1) but only a few are controllable and optimizable to reduce the drag force. Obviously, the air density is not a parameter to be tuned while the speed factor in the formula expresses only a relation between the drag force and the vehicle velocity. On the other hand, the drag coefficient and the frontal area are the objects of this dissertation since they can be modified and optimized.

The frontal area is obtained as shown in Figure 2-7. The projected frontal area is usually influenced by design requirements like roominess, comfort, ergonomics, manufacturability and others. This is what usually happens in passenger cars, while, in the case of Shell Eco-marathon vehicles, the area can be tuned more freely, but considering the minimum dimensions for the driver's compartment and for the whole vehicle. The coefficient C_d is a dimensionless coefficient which defines the aerodynamic quality of the shapes of the vehicle. It is important to point out that the drag coefficient alone is not indicating the whole aerodynamic optimization, indeed, the parameter to be considered is usually the product between the frontal area and the drag coefficient.

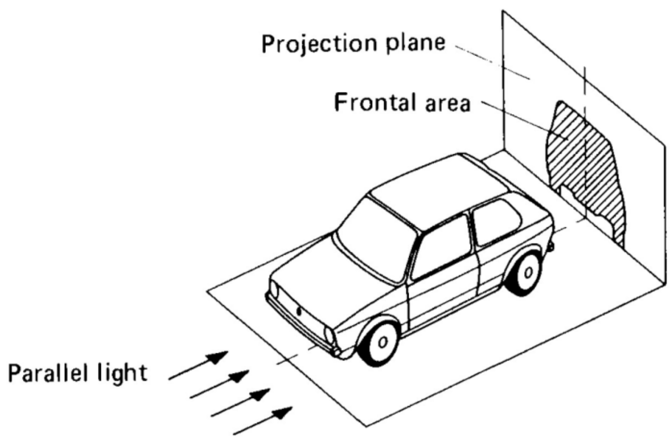

Figure 2-7 Projected frontal area definition (Hucho, 1987, p. 3)

Talking about the aerodynamic drag in general, it is possible to consider a first distinction between Parasitic Drag and Lift-induced Drag. This latter is the consequence of the work to create lift forces while the Parasitic Drag is made up of: Form Drag, Skin Friction and Interface Drag. The Form Drag is due to the pressure around the object and strongly depends on body shape. The Skin Friction is linked to the viscous shear stress on the surface of the body while the Interface Drag is caused by the interconnection of multiple bodies. Depending on the fact that the body is a Bluff Body (characterized by advanced separation of the boundary layer) or an Aerodynamic Body (boundary layer completely attached), each drag contribution can be more or less relevant. In the case of cars, similar to bluff bodies, the form drag is the highest contribution. Some trends, regarding body shapes, can be analysed to derive some guidelines during the definition of the outer vehicle shape. In the following, the most relevant are described.

2.2.1 Aerodynamic Trends

For the front-end shape, a trend, based on stagnation point height, can be related to the variation of drag coefficient. In Figure 2-8, this latter is shown.

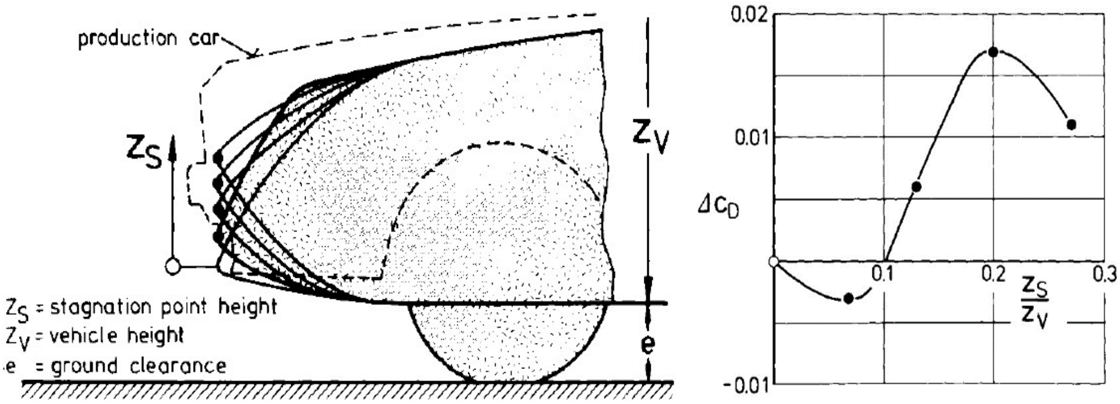

Figure 2-8 Effect of stagnation point position on drag (Hucho, 1987, p. 132)

The stagnation point vertical position determines the amount of flow going to the underfloor and to the upper part of the vehicle. It is possible to select an optimum stagnation point which usually is close to the ground (Hucho, 1987, p. 133).

In Figure 2-9 another guideline is depicted. It regards the bonnet and windscreen inclination. Once a proper inclination of the bonnet is set, a further inclination is not leading to big improvements (Hucho, 1987, p. 133). Furthermore, the validity of this tendency should be evaluated also in case the two angles are varied together, since it is possible to have an interaction between the two trends.

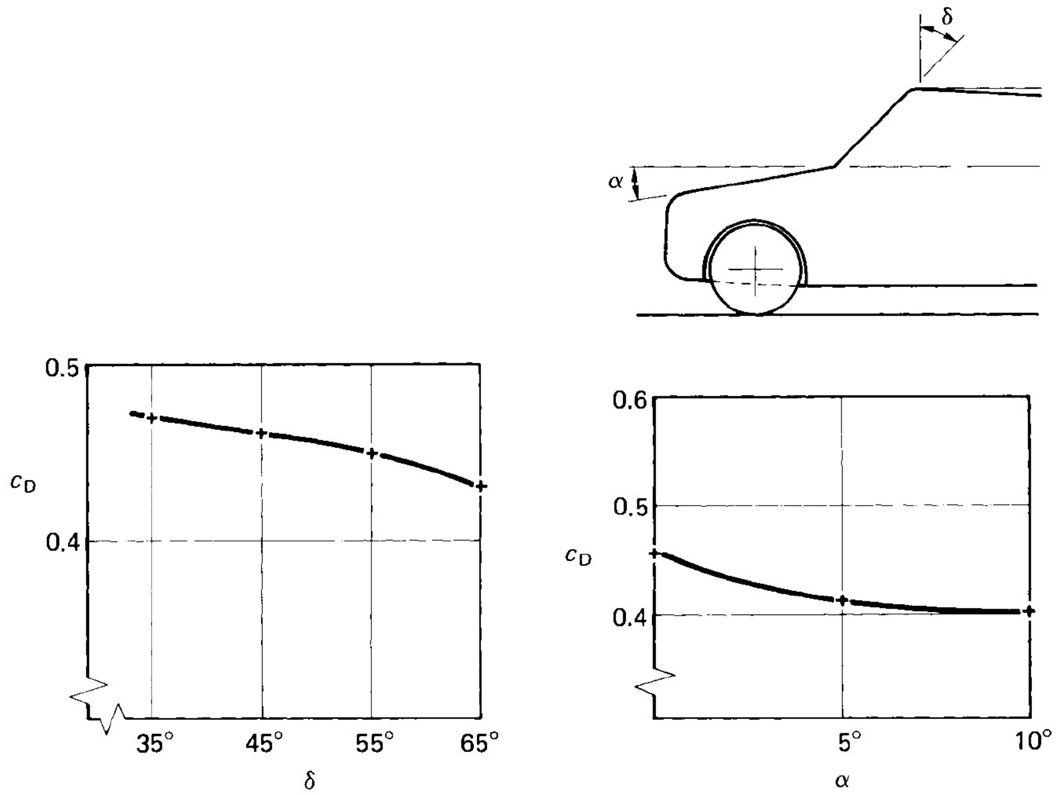

Figure 2-9 Effect of bonnet slope α and windshield rake δ on drag (Hucho, 1987, p. 132)

Another body part which highly influences the aerodynamic performances is the roof. A common design procedure is selecting the most advanced position for the maximum height of the roof. This guideline allows to create a bigger surface and length on the roof for pressure recovery since a high pressure close to flow separation is in favour of low drag. Nevertheless, the modification of the roof hight leads also to a variation of the frontal area value. Indeed, it is always advisable to evaluate the result as the product between C_d and frontal area variation. The case of side curvature is peculiar to understand the necessity of evaluating both parameters. In Figure 2-10 the relation between the variation of side curvature and $C_d \cdot A$ product is reported. It is evident that a proper balance between C_d decrease, and frontal area increase must be found.

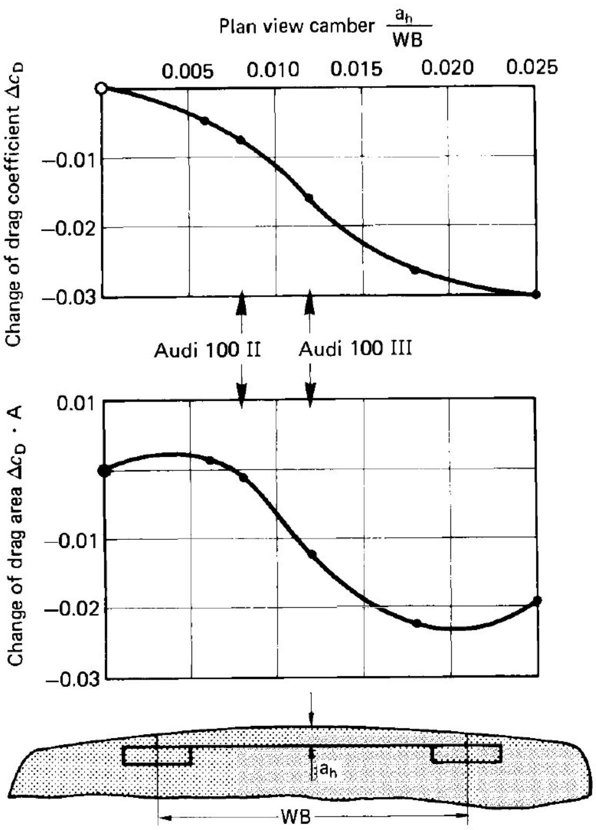

Figure 2-10 Effect of side curvature variation for a notchback car (Hucho, 1987, p. 160)

2.2.2 Modern Applications

Currently, the improvement of the aerodynamic performance is a central topic in the automotive field since the reduction of fuel consumption is fundamental to achieve the emission target fixed by the European Union. At the same time, it is crucial to increase as much as possible the range of Battery Electric Vehicles, one of the most critical aspects of this typology of cars.

Volkswagen XL1 outer shape is designed to achieve an extreme aerodynamic drag reduction. It is a limited production car developed to achieve the target of 100 km with 0.9 litre of diesel (Volkswagen, n.d.). To reach this level of efficiency, a refinement of vehicle weight, drivetrain efficiency and aerodynamic is required. The result is a car with a drag coefficient of 0.189 (Volkswagen, n.d.), an outstanding value obtained thanks to specific aerodynamic details. For example, two panels are adopted to cover the rear wheels, with a consequent improvement of the flow quality on the side. The tail is cut sharply at a certain point, setting the flow detachment region and, consequently, wake dimensions. At the same time, the profile of the vehicle is characterized by soft changes in curvature in order to keep the flow attached until the end of the tail. The underbody is completely flat thanks to plastic panels that extend to cover part of the suspension system. In Figure 2-11 the outer shape of Volkswagen XL1 is depicted.

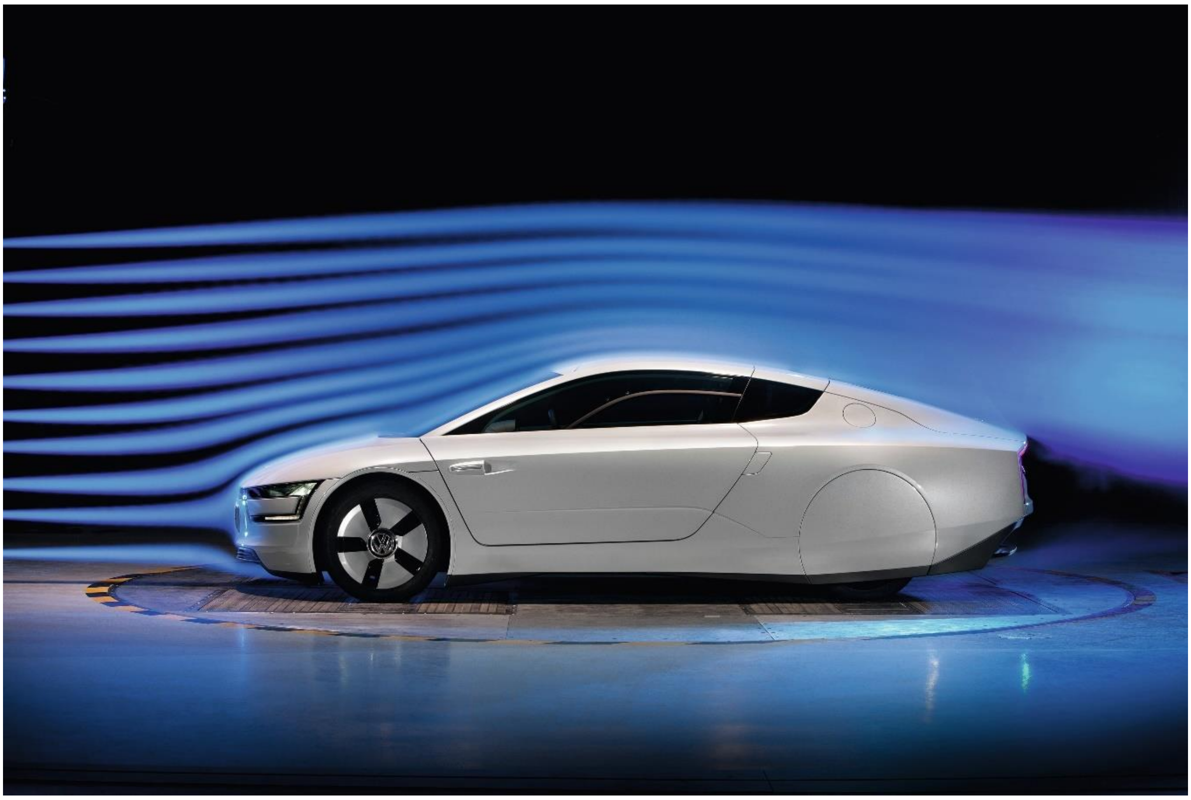

Figure 2-11 Volkswagen XL1 outer shape (Volkswagen, 2018)

Talking about Battery Electric Vehicles, it is worth mentioning the Mercedes EQS, currently the production car with the lowest drag coefficient on the market (Daimler, 2021a). With respect to Volkswagen XL1, characterized by extreme dimensions and concept choices, the Mercedes EQS is a production vehicle offering a greater interior space and enhanced comfort. Therefore, it is an example which shows how a car with conventional proportions can be optimized from aerodynamic point of view. It reaches a drag coefficient of 0.2 and a frontal area of 2.51 m^2 which leads to an effective air resistance of 0.5 m^2 (Daimler, 2021b).

The design of the A pillar is done to create a rounded shape which is able to reduce the turbulences which characterize this body area. Thanks to the battery positioning, an extremely flat underbody can be realized. Another aerodynamic benefit coming from the electric powertrain regards the front of the vehicle since it is completely sealed. This characteristic reduces drastically the drag contribution coming from the front of the vehicle. In Figure 2-12 the side of the Mercedes EQS is shown.

Figure 2-12 Mercedes EQS side (Daimler, 2021c)

2.3 Composites and Carbon Fibre Manufacturing

The analysis of the material is fundamental for the design process. For this reason, an evaluation of the characteristics and behaviour of composite materials is required. Furthermore, a description of the available manufacturing processes will be included.

2.3.1 Composites

Composite materials are obtained through the combination of two materials which have different chemical and mechanical properties. Exploiting the peculiar characteristics of each composite constituent, it is possible to optimize the overall properties of the resulting material. In this way, it is possible to increase the stiffness, to reduce the weight or to improve specific characteristics like the conductivity of the material. The two constituents are usually classified in two families: the matrix and the reinforcement. While the matrix is used to surround the reinforcement and to maintain it in position, the reinforcement, thanks to its peculiar qualities, is used to improve the mechanical performance of the composite.

It is possible to categorize composite materials in different ways, nevertheless, a useful classification, considering the application treated in this dissertation, is shown in Figure 2-13. A first distinction regards composites reinforced by fibres and composites reinforced by particles. It is important to focus the attention on the first branch of the classification since it is related to the material type which will be used in MUC022. In the case of fibre reinforced composites, fibres (usually of carbon or glass type) are surrounded by a matrix (usually epoxy resin) modifying the mechanical properties depending on fibres orientation. The fibres are grouped in layers according to various patterns, chosen with the purpose of tuning the properties on a specific axis. These layers can be stacked together to obtain a laminate. This latter can be obtained orienting, also in this case, each layer in a different direction, optimizing the overall composite depending on the necessities of the project.

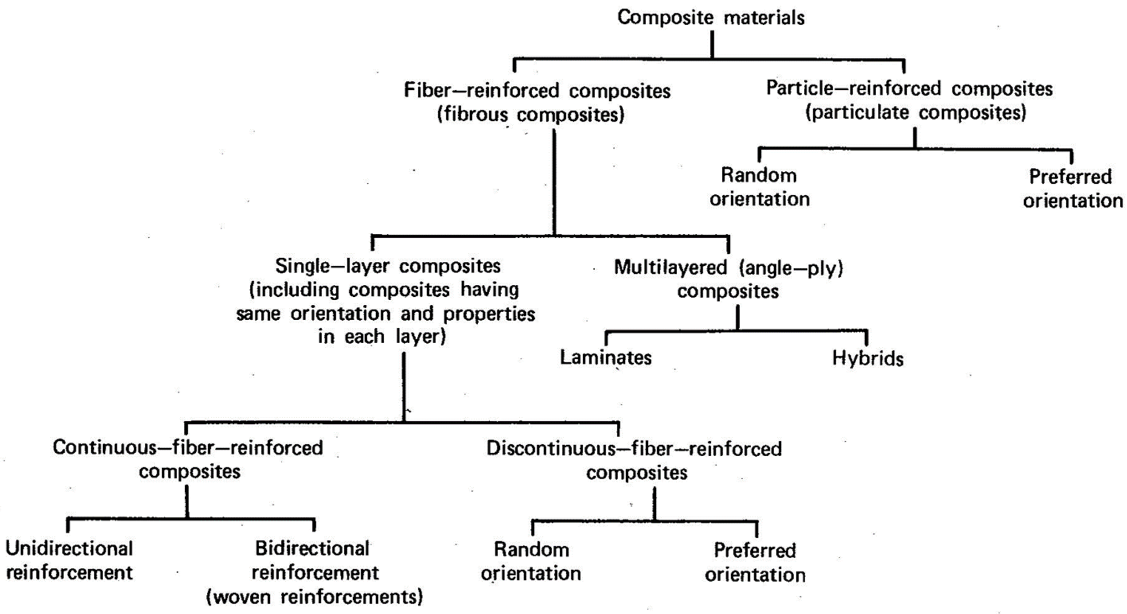

Figure 2-13 Classification of composite materials on the basis of type and orientation of the reinforcement (Belingardi, 2021, p. 1)

As already explained, it is common to face non isotropic characteristics talking about composites. This leads to the necessity of analysing them differently with respect to traditional isotropic materials like steel or aluminium. In particular, it is common to indicate 3 directions to characterize the layer or lamina. In this way, the most important parameters can be referred to a specific direction, as shown in Figure 2-14.

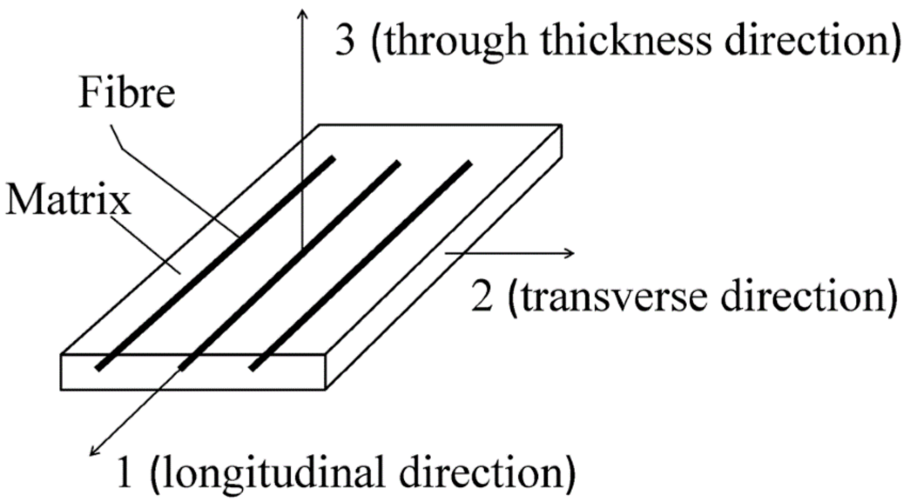

Figure 2-14 Lamina co-ordinate system (Chunguang, Shiquan, Mingyu, Zhirong, & Baomin, 2019, p. 4)

The most important parameters to be considered are the five elastic constants:

- Young modulus in the longitudinal direction E_1 or E_L.
- Young modulus in the transversal direction E_2 or E_T.
- Shear modulus in the lamina plane G_{12} or G_{LT}.
- Poisson coefficient in the lamina plane ν_{12} or ν_{LT}.
- Poisson coefficient in the transverse plane ν_{23} or ν_{TZ}.

At the same time, the strength of the lamina is characterized by five values:

- Tensile strength $\sigma_{R,L}$ in the longitudinal direction L.
- Compressive strength $\sigma'_{R,L}$ in the longitudinal direction L.
- Tensile strength $\sigma_{R,T}$ in the transverse direction T.
- Compressive strength $\sigma'_{R,T}$ in the transverse direction T.
- Shear strength $\tau_{R,LT}$ in the lamina plane.

In order to obtain these parameters, the calculation starts from the values referred to the matrix and reinforcement. So doing, the volume ratio, defined as shown in Formula (2-2) and in Formula (2-3), is used to combine the characteristics of the two composite constituents.

$$V_f = \frac{v_f}{v_c} \tag{2-2}$$

$$V_m = \frac{v_m}{v_c} \tag{2-3}$$

Where V_f and V_m are respectively the fibre volume ratio and the matrix volume ratio while v_f, v_m and v_c refer to the volume of fibre, matrix and composite.

For example, the mixture rule is used for the computation of the Young's modulus of the composite and to obtain the strength of the composite in longitudinal direction. In this case the strength value considered for the matrix is the one at the failure strain of the fibres. This last computation is shown in Formula (2-4).

$$\sigma_{c,R} = \sigma_{c,f} \cdot V_f + \sigma_m \cdot V_m \tag{2-4}$$

Different theories were developed to estimate the parameters previously introduced. Furthermore, many other factors, like the thermal expansion coefficient, can be studied in detail to derive a model able to describe the orthotropic behaviour of the composites. This study is usually performed for a single lamina, which is then connected to other laminas, stacked one upon the other using the matrix itself. Laminas can have all the same direction, or they can be stacked orienting differently each layer. The ordering sequence adopted to stack the laminas is said "stacking sequence". This type of approach allows to customize the material behaviour depending on the loads applied to the vehicle body.

In order to understand the relation between stress and strain in composite materials, it is firstly necessary to analyse the stress-strain relationship at the level of the lamina. The following dissertation is entirely referred to "Basic Mechanics of Laminated Composite Plates" (Nettles, 1994, pp. 6-21).

In Formula (2-5) it is reported the equation in plane stress condition. The subscripts are referred to the directions previously introduced; indeed, it is worth noticing this expression is valid considering the lamina reference system. In this case, it is evident there is no relation between the shear stress and the normal strain. In accordance with Nettles publication (Nettles, 1994, p. 6), in position 3,3, subscript 6,6 is used.

$$\begin{bmatrix} \sigma_1 \\ \sigma_2 \\ \tau_{12} \end{bmatrix} = \begin{bmatrix} Q_{11} & Q_{12} & 0 \\ Q_{12} & Q_{22} & 0 \\ 0 & 0 & Q_{66} \end{bmatrix} \cdot \begin{bmatrix} \varepsilon_1 \\ \varepsilon_2 \\ \gamma_{12} \end{bmatrix} \tag{2-5}$$

Then it is possible to express this matrix in a general reference system, not aligned with the one of the lamina and, for this purpose, a rotation matrix is adopted. A fully populated matrix is obtained.

$$\begin{bmatrix} \sigma_x \\ \sigma_y \\ \tau_{xy} \end{bmatrix} = \begin{bmatrix} \bar{Q}_{11} & \bar{Q}_{12} & \bar{Q}_{16} \\ \bar{Q}_{12} & \bar{Q}_{22} & \bar{Q}_{26} \\ \bar{Q}_{16} & \bar{Q}_{26} & \bar{Q}_{66} \end{bmatrix} \cdot \begin{bmatrix} \varepsilon_x \\ \varepsilon_y \\ \gamma_{xy} \end{bmatrix} \tag{2-6}$$

To continue the study of laminated composites, five assumptions must be considered (Nettles, 1994, p. 11):

1. “The laminate thickness is small compared to the other dimensions.”
2. “The lamina of the laminate are perfectly bonded.”
3. “Lines perpendicular to the surface of the laminate remain straight and perpendicular to the surface after deformation.”
4. “The laminae and laminate are linear elastic.”
5. “The through-the-thickness stresses and strains are negligible.”

These assumptions are generally reasonable if the laminate is not damaged. The next step is the definition of strains and displacements. The nomenclature adopted for this dissertation is the following:

- u is the displacement of the plate in x direction;
- v is the displacement of the plate in y direction;
- w is the displacement of the plate in z direction.

The total in-plane displacement can be expressed as a sum of normal displacement plus the one introduced by bending.

$$u = u_0 - z \cdot \frac{\partial w}{\partial x} \tag{2-7}$$

$$v = v_0 - z \cdot \frac{\partial w}{\partial y} \tag{2-8}$$

Using Formulas (2-7), (2-8) and the general definition of strain it is possible to write:

$$\begin{bmatrix} \varepsilon_x \\ \varepsilon_y \\ \varepsilon_z \end{bmatrix} = \begin{bmatrix} \varepsilon_x^0 \\ \varepsilon_y^0 \\ \varepsilon_z^0 \end{bmatrix} + z \cdot \begin{bmatrix} K_x \\ K_y \\ K_z \end{bmatrix} \tag{2-9}$$

The strain will be the sum of the membrane behaviour of the laminate at the midplane (superscript 0) plus the bending behaviour of the laminate (K is indicating the curvature).

Consequently, it is possible to derive the Stress-strain relationship of the lamina in the stack.

$$\begin{bmatrix} \sigma_x \\ \sigma_y \\ \tau_{xy} \end{bmatrix} = \begin{bmatrix} \bar{Q}_{11} & \bar{Q}_{12} & \bar{Q}_{16} \\ \bar{Q}_{12} & \bar{Q}_{22} & \bar{Q}_{26} \\ \bar{Q}_{16} & \bar{Q}_{26} & \bar{Q}_{66} \end{bmatrix} \cdot \begin{bmatrix} \varepsilon_x^0 \\ \varepsilon_y^0 \\ \gamma_{xy}^0 \end{bmatrix} + z \cdot \begin{bmatrix} \bar{Q}_{11} & \bar{Q}_{12} & \bar{Q}_{16} \\ \bar{Q}_{12} & \bar{Q}_{22} & \bar{Q}_{26} \\ \bar{Q}_{16} & \bar{Q}_{26} & \bar{Q}_{66} \end{bmatrix} \cdot \begin{bmatrix} K_x \\ K_y \\ K_{xy} \end{bmatrix} \tag{2-10}$$

To analyse the overall behaviour of the laminate, the next step is the calculation of the resultant normal and shear forces, as well as of the resultant bending and twist moments. The forces are obtained integrating the stresses along the thickness of the laminate while, for the moments, the stresses are multiplied by the distance from the midplane. It is important to underline that in this way the forces and the moments are expressed in terms of N/m and N respectively since they are divided by the width of the laminate. Combining these calculations about forces and strains, it is possible to derive the expressions of forces and moments which can be summarized in a single relation.

$$\begin{bmatrix} N_x \\ N_y \\ N_{xy} \\ M_x \\ M_y \\ M_{xy} \end{bmatrix} = \begin{bmatrix} A_{11} & A_{12} & A_{16} & B_{11} & B_{12} & B_{16} \\ A_{12} & A_{22} & A_{26} & B_{12} & B_{22} & B_{26} \\ A_{16} & A_{26} & A_{66} & B_{16} & B_{26} & B_{66} \\ B_{11} & B_{12} & B_{16} & D_{11} & D_{12} & D_{16} \\ B_{12} & B_{22} & B_{26} & D_{12} & D_{22} & D_{26} \\ B_{16} & B_{26} & B_{66} & D_{16} & D_{26} & D_{66} \end{bmatrix} \cdot \begin{bmatrix} \varepsilon_x^0 \\ \varepsilon_y^0 \\ \gamma_{xy}^0 \\ K_x \\ K_y \\ K_{xy} \end{bmatrix} \tag{2-11}$$

where

$$A_{ij} = \sum_{k=1}^{n} \left[\bar{Q}_{ij}\right]_k \cdot (h_k - h_{k-1}) \tag{2-12}$$

$$B_{ij} = \frac{1}{2} \cdot \sum_{k=1}^{n} \left[\bar{Q}_{ij}\right]_k \cdot (h_k^2 - h_{k-1}^2) \tag{2-13}$$

$$D_{ij} = \frac{1}{3} \cdot \sum_{k=1}^{n} \left[\bar{Q}_{ij}\right]_k \cdot (h_k^3 - h_{k-1}^3) \tag{2-14}$$

The meaning of *h* is shown in Figure 2-15.

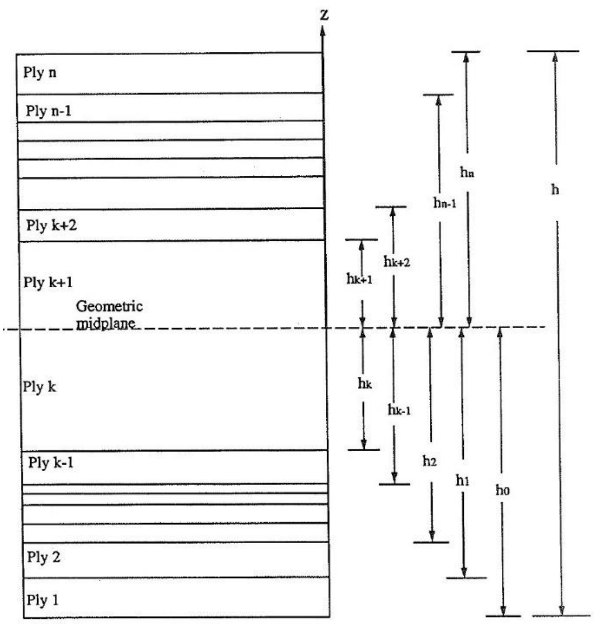

Figure 2-15 Cross section of a laminate (Nettles, 1994, p. 19)

In general, the forces and the moments depend both on strains and curvatures. This is not what typically can be seen for metallic materials where the elastic modulus is constant through the thickness of the plate. On the contrary, in composite materials the difference of Young's modulus in the various laminas generate the dependency on the curvature.

The B matrix puts in relation the forces with the curvatures and the moments with the strains at the midplane. Depending on the stacking sequence, the stiffness matrix can be fully populated or can be strongly simplified, as it happens in the case of symmetric laminates.

2.3.2 Failure

Different kinds of failure modes characterize composite materials. One possibility is the failure of the fibre itself because of a tensile load (or due to buckling). Another option is debonding failure: in this case the damage is linked to a failure in between the fibre and the matrix. Sometimes, because of fatigue, the cracks regard micro-fractures in the composite. This last case is linked to tensile, compressive or shear loads. Figure 2-16 reports a typical compressive side of fracture region of specimens showing splitting (dark arrows) and fibre buckling (top).

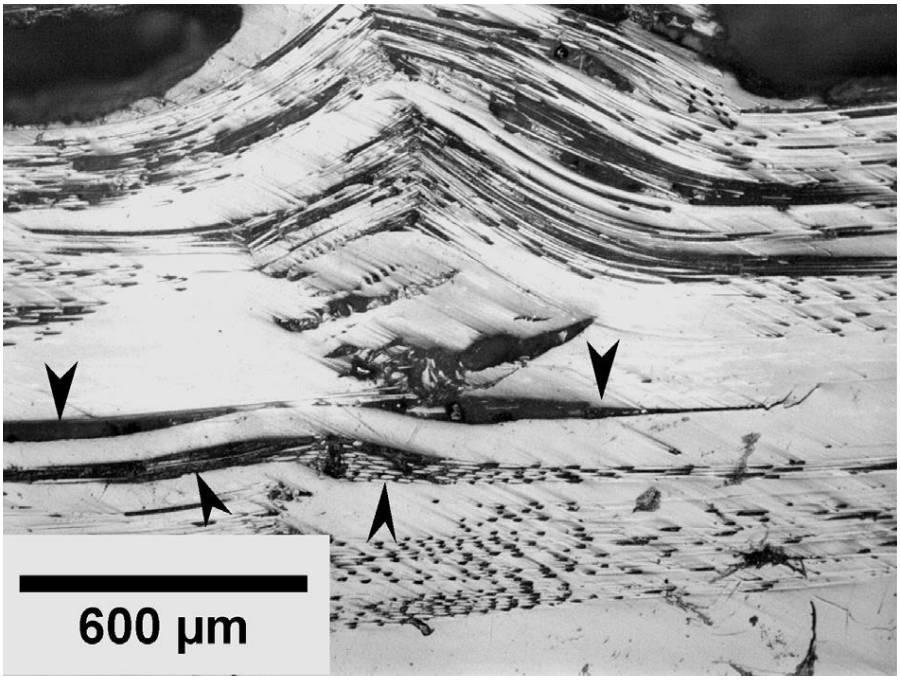

Figure 2-16 Example of fracture region of a specimen. (Sudarisman, 2009, p. 215)

Another failure mode is the "delamination" where the separation regards the laminas within a laminate.

The failure criteria should be adapted to the behaviour of composite materials, considering their orthotropic characteristics. One of the best criteria is called "Tsai-Wu". Tsai-Wu, with respect to the other criteria, allows to predict failure exploiting a single equation, including all the failure mechanism at the same time. The formulation is quite complex, but it is usually included in different FEM solvers. The Tsai-Wu criterion predicts failure when the failure index in a laminate reaches 1. In Formula (2-15) the general formulation of the criteria is shown (Tsai & Wu, 1972, p. 38).

$$\sum_{i,j} F_{ij} \cdot \sigma_i \cdot \sigma_j + \sum_i F_i \cdot \sigma_i < 1 \qquad (2\text{-}15)$$

Where ij=1,2,…,6 and F_i, F_{ij} are experimentally determined material strength parameters.

2.3.3 Manufacturing Techniques

The selection of the proper composite material is not only related to the typology of fibre and matrix, indeed, the final characteristics of the material are also function of the way in which the composite is processed. Usually, in order to produce carbon fibre parts, the matrix and the fibres are shaped into components and then cured. For this reason, a mould, which can be realized according to different techniques, is required for the process. A first important distinction regards wet and dry processes. While dry production processes adopt pre-pregs or impregnated resin fibres, the so called “wet techniques” use carbon fibre which is hand coated with resin before the product is actually finished (Scopione, n.d.).

This section will deal with the two techniques will be evaluated for the production of the components of MUC022: the *VAP process* and the *Pre-preg (Autoclave)* process.

VAP Process

The Vacuum Assisted Process (VAP®) is a technique to manufacture composite parts using vacuum injection. It is a wet process that uses vacuum to coat the dry fibres with the resin. Since VAP® is a variant of the traditional Vacuum Infusion Process (VIP), it is convenient to start analysing this latter. In the traditional VIP, the dry fibres are placed into the mould and then are seal closed using a vacuum bag. Next, vacuum is created inside the bag through a vacuum pump. The dry fibres are wet by the resin infused into the mould (Performance Composites, n.d.).

The main limitation of this method is related to the determination, or prediction, of the flow fronts in order to avoid any kind of “dry spot”, so areas where the resin is not present. Furthermore, the vacuum should also be reduced due to the risk of matrix boiling. Fluctuation in the fibre volume content and greater components porosity are the outcomes of these limitations. In the case of VAP®, a specific sequence of layers behind the bag and the presence of a dedicated membrane, allow to create a more uniform vacuum, removing dry spots. In fact, under vacuum condition, the VAP® semi-permeable membrane allows to remove molecules of air and gas keeping the resin under the membrane itself (Trans-Textil GmbH, n.d.). In Figure 2-17 the part lay-up is reported.

Since this process is cheaper than the pre-preg one, it could be used to create the carbon fibre moulds required for monocoque lamination. This aspect will be evaluated in detail in section 5.3.

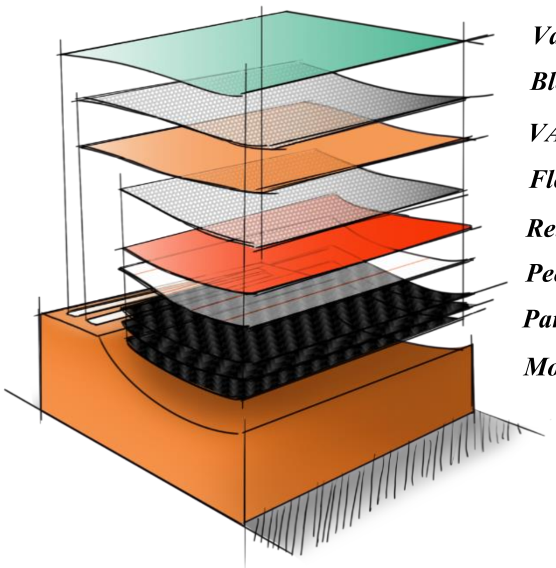

Figure 2-17 VAP® technique layers (Composyst, n.d.)

Pre-preg (Autoclave)

In this case, fabrics and fibres are pre-impregnated by the manufacturer with a pre-catalysed resin. For this reason, it falls in the category of the "dry processes" since it is not required to apply the resin separately. This section is completely referred to Gurit "Guide to composite" (Gurit, n.d.).

When stored for long time, prepregs are generally frozen to preserve the characteristics of the material. Since the catalyst is latent at ambient temperature, the material can be used for several weeks after the defrosting. The prepregs can be then laid by hand into a mould. Very complex shapes can be realized and, generally, the lamination is easier with respect to wet processes. After the lamination, the result is vacuum bagged and heated to 120-180 °C to allow resin reflow and curing. Usually, this process is performed in an autoclave in order to apply additional pressure to the laminate. This latter is generally required for a good curing, even if the autoclaves are expensive and slow. The price of the pre-impregnated fabrics is usually higher with respect to the dry ones and the overall cost is even higher considering the necessity of adopting tools able to withstand high temperature. For this reason, carbon fibre moulds are usually selected for the scope. On the other hand, the use of pre-preg leads to important advantages. High fibre contents can be achieved with low voids content since the amount of resin is set by the manufacturer itself. This technique will be used to produce the entire monocoque.

3 Requirements

The analysis of the requirements represents the starting point for the effective development of the research. Three typologies of requirements will be considered in this section: the competition rules, the efficiency targets and the structural needs.

3.1 Rules

The first aspect to be considered during the development of a new vehicle is the compliance with the rules of the competition for which the car is designed. The rules which are considered in this dissertation are the ones referred to the urban concept class of Shell Eco-marathon. “Chapter I” and “Chapter II” are the two documents issued by Shell: the first one is reporting the Shell Eco-marathon official rules while the second is focused on the guidelines of the “on-track” event. The most relevant section is the “Part 3”, related to Vehicle Design, contained in “Chapter I”. In the following, only the most important and pertinent rules will be presented and commented. As already mentioned, the following section are entirely referred to Shell Eco-marathon 2021 Official Rules Chapter 1 (Shell, 2020).

3.1.1 Vehicle Design

In the case of Urban Concept vehicles, it is mandatory to use 4 wheels (in constant contact with the ground). This is a first relevant insight for the preliminary concept decisions and is in line with the philosophy of the Urban Concept class, whose rules are defined to obtain a design similar to passenger cars. The external trims must present a certain level of stiffness since aerodynamic appendages which deform and change shape because of wind are not allowed. At the same time, the edges of the external components must not be sharp: a minimum of 50 mm of radius must be considered for safety reasons.

Another rule, which is directly influencing the vehicle body, states that the energy compartment (where the drivetrain is located) should be easily accessible. It means it is required a bonnet which can be dismounted or opened in a simple way. Furthermore, the drive train and related components (as the fuel tank, hydrogen system components, etc.) must be covered by the body parts. It is required a bulkhead to isolate the energy storage and propulsion system from the cockpit. In case of problems (fuel leak, fire, etc.), it avoids the driver to enter in contact with flames or liquids.

3.1.2 Chassis Solidity, Roll Bar and Safety Belts

All the cars which participate to the Shell Eco marathon must have a chassis or monocoque to protect the driver’s body in a safe way. An important rule, which has a big effect in terms of safety and packaging, is the one related to the roll bar around driver’s helmet. Indeed, it is required to integrate a roll bar around the head of the driver to act as a protection when he/she is positioned in a normal way. In particular, 50 mm between the roll bar and the helmet must be always assured. This last consideration is fundamental to properly design the outer shape of the vehicle since it is the main constraint during the design of the upper part of the cockpit. It is worth mentioning that MUC022 will integrate a monocoque to comply with the structural requirements, therefore, the roll bar is the monocoque itself. Furthermore, this rule specifies that the roll bar cannot impair driver visibility, in fact, the head or the torso must not be raised above the roll bar to pass the visibility test.

The roll bar must also extend transversally beyond the driver's shoulders (when the driver is positioned with fastened safety belts). In terms of load, this roll bar must withstand a static load of 700 N applied in a vertical, horizontal, and/or perpendicular direction, without deforming in any direction.

The car must be equipped with an effective safety harness with at least five mounting points (certified or compliant with FIA standards) to maintain the driver in his/her position in a safe way. Consequently, the five belts must be firmly attached to the vehicle structure. From structural point of view, each safety harness mounting point must be able to withstand a 200 N force in any direction.

3.1.3 Visibility and Accessibility

Visibility is another requirement which is considered during the technical inspection at the Shell Eco-marathon competition. First of all, "the driver must have access to a direct arc of visibility ahead and to 90° on each side of the longitudinal axis of the vehicle" (Shell, 2020, p. 16). This level of visibility must be reached without the use of any optical or electronic device. Nevertheless, the driver can move the head to achieve this field of vision but always maintaining the helmet at 50 mm from the roll bar. Furthermore, the vehicle must have rear view mirror on each side. They cannot be substituted by electronic devices and the minimum allowed surface area is 2500 mm^2 (e.g. 50 mm x 50 mm). This norm has a huge impact in the design of the cockpit. MUC022 would have internal side view mirrors to improve aerodynamics. This choice sets constraints for the shape of the passenger compartment; indeed, it should have a transversal dimension at the level of the belt line which decreases progressively from the front part to the back.

The accessibility is another factor characterizing the urban concept design with respect to the solutions adopted in prototype class vehicles. It is required to design this aspect to assure that a driver, fully harnessed, can vacate the vehicle at any time without assistance in less than 10 seconds. It is not a precise rule since it gives a certain degree of freedom to set the driver position and the door opening mechanism. Additionally, the driver compartment must include a single opening mechanism per door. This latter must be operable both from the outside and inside in an intuitive way. The opening method have to be clearly marked by a red arrow while it is forbidden to use adhesive tape to close the driver's opening from the outside.

3.1.4 Dimensions

The most relevant guidelines for the design come from the rules related to the dimensions. They are directly influencing the final shape and consequently aerodynamics and packaging. In Table 3-1 the rules related to the dimensions are reported.

Table 3-1 Dimensions stated in Shell Eco-marathon rules

Vehicle characteristic	Minimum	Maximum	Unit of measure
Height	1000	1300	mm
Width	1200	1300	mm
Length	2200	3500	mm
Front track	1000	-	mm
Rear track	800	-	mm
Wheelbase	1200	-	mm
Driver's compartment height	880	-	mm
Driver's compartment width	700	-	mm
Ground clearance	100	-	mm
Mass	-	225	kg

It is also important to remember that all vehicle dimensions must not be achieved by body extensions such as “stuck-on” appendages or cut-outs.

From the point of view of the whole vehicle body, the rules state that all mechanical parts must be fully covered, including suspensions and wheels. A wiper for the windscreen must be integrated because the car should be able to be driven safely also in case of rain.

A big constraint during the design is imposed by the necessity of including an area to host a rigid box with dimensions of 500 x 400 x 200 mm (L x H x W). This area must be easily accessible. A floor and sidewalls must be included to hold the luggage in place when the vehicle is moving. This requirement is a big limitation if not previously taken into account in the preliminary concept decisions. Therefore, it is required a careful packaging analysis to allocate enough space.

3.1.5 Wheels and Lighting

The wheels must be located inside the vehicle and a bulkhead should be present to make the wheelhouse inaccessible to the driver. The wheel must not enter in contact with the body during its motion. Finally, the rims must be between 15 and 17 inches in diameter.

As real passenger cars, the vehicle must be equipped with a functional external lighting system. In Figure 3-1 it is displayed the rear of MUC018, characterized by a single big taillight which extends horizontally. In particular, the rules give the following indications for the lighting system design (Shell, 2020, p. 23):

- two front headlights;
- two front turn indicators;
- two rear turn indicators;
- two red brake lights in the rear;

- two red rear running lights;
- “the centre of each headlight unit must be located at an equal distance and at least 300 mm from the centreline of the vehicle”;
- “the mandatory red indicator light for the self-starter operation must be separate from any of the above”;
- “a hazard light function must be included in the vehicle system”.

Figure 3-1 MUC018 taillights (TUfast, 2018)

3.2 Efficiency Targets

The result achieved in the competition depends on the forces acting against the motion of the vehicle during the race. The design of the vehicle must be integrated with a proper driving strategy in order to exploit the peculiar characteristics of the final car. For example, depending on the motor and drivetrain type, it is possible to select a level of acceleration in line with the motor efficiency map. Not all the aspects regarding the strategy can be decided during the development since the location of the competition is defined and communicated too late to design the vehicle expressly for the track. Therefore, the general mechanisms behind energy consumption are considered and correlated with the data coming from previous competitions.

The reference for the development of MUC022 is the previous urban concept, called MUC019. Even if it was well designed (it achieved the second place in the design competition), the efficiency results were not satisfactory since it placed ninth in the overall competition with 130.4 km/kWh. In order to decide which aspects should be improved in the new vehicle, it is convenient to analyse the forces acting on the vehicle during its motion.

Formula (3-1) shows the general equilibrium (D'Ambrosio, 2020, p. 7).

$$F_{trac} - F_{res} = m_e \frac{dV}{dt} \tag{3-1}$$

F_{trac} is the driving torque available at the wheels while F_{res} is the total driving resistance. The term at the right, called equivalent mass m_e, is taking into account the inertia coming from the mass itself and the contribution given by the rotating components of the vehicles (like the wheels).

If the traction force F_{trac} is greater that the resistance force F_{res}, the difference is used to accelerate the vehicle. On the other hand, if the speed is constant, the two contributions are equal. Since the term F_{trac} depends on the residual braking force when the brake pedal is not pushed and by the efficiency of the driveline, the most important contributions related to the vehicle body are inside the term F_{res} and in the equivalent mass m_e. The terms which made up the resistance force are the aerodynamic resistance (F_{aer}), the rolling resistance (F_{rr}) and the climbing resistance (F_{cli}). Formula (3-2) summarizes this relation (D'Ambrosio, 2020, p. 8).

$$F_{res} = F_{aer} + F_{rr} + F_{cli} \tag{3-2}$$

The climbing resistance is difficult to be considered since the road grade could change depending on track topology. Nevertheless, the mass of the car is the controllable parameter to reduce this term.

The rolling resistance is influenced by many factors, like the weight applied on the wheel, the speed, the wheel dimensions and the air pressure of the tire. The tire characteristics and material are probably the most important factors to be considered: for this purpose, specific Eco tires can be selected to reduce the impact of rolling resistance.

The last factor to be considered is the aerodynamic resistance. It is dependent by the square of the speed, by the frontal area and by the shape of the car, summarized in the drag coefficient.

In case of acceleration, the inertia becomes a predominant factor. In these conditions, the mass of the vehicle and the inertia of the wheels are the parameters to be reduced to improve the vehicle efficiency.

From this general analysis it is evident that the two most important aspects to be inspected for the design of the body are the mass of the vehicle and the aerodynamics. Additionally, new more efficient tires could be selected to equip MUC022.

3.2.1 Aerodynamic Prospective

From aerodynamic point of view, MUC019 is a hatchback characterized by a big wake at the back and consequent low aerodynamic performances. Indeed, as depicted in Figure 3-2, the typical aerodynamic flow of a hatchback body style ends with a big low-pressure area, called wake, which is source of aerodynamic drag. Furthermore, MUC019 has a 2 seats configuration, and, for this reason, its cockpit is quite large. The improvements should deal with a reduction of the frontal area and with an optimization of the shape. A longer rear overhang will be introduced with the purpose of reducing the extension of the wake. The frontal area is constrained by the outer minimum dimensions set by Shell Eco marathon rules. Nevertheless, a single seat position could be adopted to reduce the dimensions of the cockpit. Many other aerodynamic details can be introduced or modified to reduce the drag of the vehicle. For example, the junction between bonnet and monocoque can be modified, aligning the two panels, to decrease the turbulences characterizing this area. Furthermore, rear wheels covering panels can be integrated in the design to contain the drag induced by the wheel during its rotation. This solution is feasible thanks to the reduced rear wheel track.

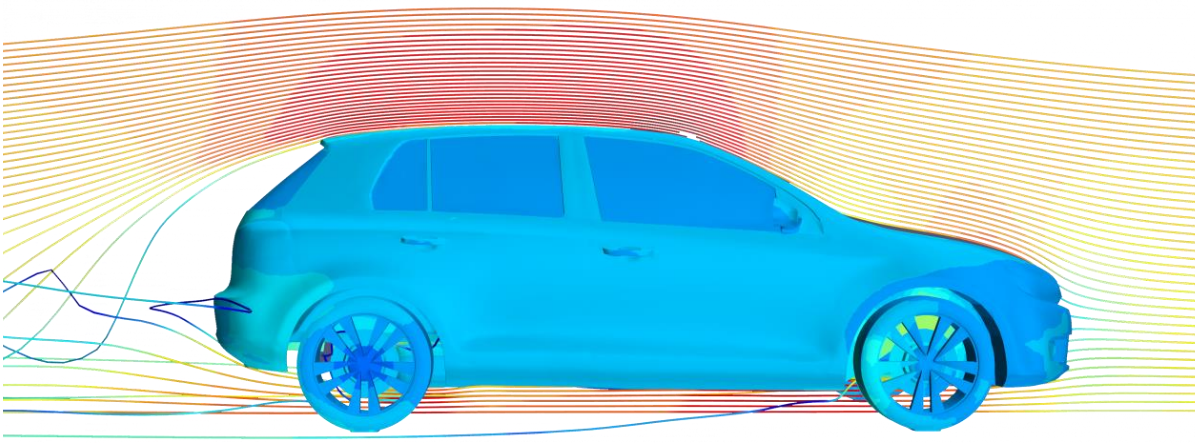

Figure 3-2 Typical aerodynamic flow of a car with a hatchback body style (Thermo Analytics, n.d.)

3.2.2 Weight Prospective

The mass of MUC019 is around 70kg thanks to the dimensions and to the manufacturing technique adopted. Indeed, the monocoque is manufactured as a single part avoiding the use of glue to join different panels.

The increase of the length of the car, because of aerodynamic purposes, has a negative effect on the total mass of the vehicle. It is possible to contain this tendency reducing the dimension of the monocoque while creating separate modules for front and rear. In this way, a reduced number of carbon fibre layers can be used for these areas which do not carry any load. At the same time, the manufacturability is simplified since the most difficult and time-consuming part, the monocoque, is smaller. In fact, as explained in section 5.3, the monocoque requires a double passage for the production of its tools. Nevertheless, the increased number of parts will lead to a higher assembly complexity. Several components can be redesigned to keep the mass of the vehicle competitive. It is the case of the belts and of the rims which together can lead to a reduction of mass around 10kg.

3.3 Structural Requirements

The monocoque is the vehicle part expressly designed to withstand the loads at which the car is subjected. Usually they are operative loads, therefore forces acting according to the profile of use of the vehicle. Nevertheless, also other loads are considered during the design, such as the forces generated in case of misuse and the ones occurring in case of crash. The aim of this section is to compute a set of loads that can be used as reference for the preliminary design. In order to do that, an assumption is required: dynamic loads are considered as quasistatic and, therefore, induced vibratory motions are neglected.

The load cases that will be considered are:

- maximum lateral force;
- maximum braking force;
- vertical loads because of an obstacle.

For the calculation of the forces some of the data introduced in section 4.2 will be used. In Table 3-2 the values used for the calculations are summarized.

Table 3-2 MUC022 datasheet for dynamic calculations

Parameter	**Symbol**	**Value**	**Unit of measure**
Empty mass	m_e	70	kg
Driver mass	m_d	70	kg
Mass distribution	η_{cg}	55%	-
Centre of gravity height	h	0.4	m
Front track	t_1	1.08	m
Rear track	t_2	0.85	m
Wheelbase	l	1.55	m
Braking force distribution	η_b	55%	-
Maximum speed	V_{max}	40	km/h

It is worth noticing that the position of the centre of gravity in longitudinal and vertical direction is difficult to be estimated precisely at this stage of the project, therefore, an approximation based on MUC019 setup will be used. In the following the subscript "1" will refer to the front axle, while the subscript "2" to the rear one. Furthermore, all the values are referred to forces present at the contact point between road and tires.

The first step for the computation of the maximum lateral forces is the calculation of the lateral acceleration of the vehicle. For this purpose, the maximum lateral acceleration the vehicle can sustain is selected. The following formula, derived from a simple lateral dynamic model (Genta & Morello, 2008b, p. 258), is used to compute the minimum radius for the maximum vehicle speed. According to the model, the maximum acceleration is dependent by the minimum between the two parameters in the brackets. The first one refers to the adhesion limit, the second one to the capsizing condition. μ_{yp} indicates the maximum lateral friction coefficient (peak value).

$$(a_y)_{max} = g \cdot min\left\{\mu_{yp}, \frac{t}{2 \cdot h}\right\} \tag{3-3}$$

$$R_{min} = \frac{V_{max}^2}{(a_y)_{max}} \tag{3-4}$$

μ_{yp} is unknown and it cannot reach high values, therefore, the most conservative choice is considering the rollover condition as determinant for the computation of the maximum acceleration. In order to be more conservative, the front track t_1 is selected for the track parameter in Formula (3-3). Because of the difference between front and rear track dimension, the rear inner wheel will be already raised when the front inner one is going to detach from the ground.

The result is a minimum radius R of 9.32m.

The mass distribution is computed considering the driver and the additional weights (required to reach 70kg in case of lighter driver). The total mass m is computed according to Formula (3-5).

$$m = m_e + m_d \tag{3-5}$$

After setting simple moments and forces equilibrium, it is possible to obtain the following formula to compute the vertical forces on the inner and outer wheel of the car at the front and rear axle.

$$F_{N1,outer} = \frac{1}{2} \cdot m \cdot g \cdot \eta_{cg} + \frac{h}{t_1} \cdot m \cdot a_y \cdot \eta_{cg} \tag{3-6}$$

$$F_{N1,inner} = \frac{1}{2} \cdot m \cdot g \cdot \eta_{cg} - \frac{h}{t_1} \cdot m \cdot a_y \cdot \eta_{cg} \tag{3-7}$$

$$F_{N2,outer} = \frac{1}{2} \cdot m \cdot g \cdot (1 - \eta_{cg}) + \frac{h}{t_2} \cdot m \cdot a_y \cdot (1 - \eta_{cg}) \tag{3-8}$$

$$F_{N2,inner} = \frac{1}{2} \cdot m \cdot g \cdot (1 - \eta_{cg}) - \frac{h}{t_2} \cdot m \cdot a_y \cdot (1 - \eta_{cg}) \tag{3-9}$$

Assuming the lateral friction coefficient allows to have enough grip in this condition, the lateral force is completely balanced by the two inner wheels.

$$F_{S1,outer} = a_y \cdot m \cdot \eta_{cg} \tag{3-10}$$

$$F_{S2,outer} = a_y \cdot m \cdot (1 - \eta_{cg}) \tag{3-11}$$

The traditional way of computing the braking load case is through the analysis of the adherence and capsize limit. Nevertheless, considering the specific application of MUC022, these conditions are not representative. An old Shell Eco-marathon rule will be considered as reference. The braking force is computed considering an initial velocity equal to the maximum vehicle speed and 15m of stopping distance *sd*. The computation is referred to the force developed on a single wheel at the front and rear axle.

$$F_{B1} = \frac{1}{2} \cdot m \cdot \frac{V_{max}^2}{2 \cdot sd} \cdot \eta_{cg} \tag{3-12}$$

$$F_{B2} = \frac{1}{2} \cdot m \cdot \frac{V_{max}^2}{2 \cdot sd} \cdot (1 - \eta_{cg}) \tag{3-13}$$

In Table 3-3 all the results (rounded up) are reported.

From structural point of view, both stiffness and strength targets must be set. Indeed, a good stiffness of the structure allows to improve the dynamic performance of the vehicle, enhancing the suspensions capabilities. At the same time, a reduced deflection of the body in the elastic field is optimal to assure a proper matching with the movable parts of the body (doors, tailgate, etc.). As a matter of fact, big deformations of the door openings affect the capability of opening and closing the movable parts when the vehicle is subjected to loads (i.e. parking on an uneven terrain). On the other hand, the strength of the body is related to the capability of the structure to deform without breaking. The necessity of reducing as much as possible the weight of the car, makes difficult to reach the target in terms of strength and stiffness. Furthermore, the visibility requirements reduce the degrees of freedom during the design of critical areas, such as the A and B pillars. For these reasons, also the structural target must be optimized taking in mind the conflicting objectives of the different body functions.

Table 3-3 Load cases

Force	Symbol	Value	Unit of measure
Normal force front outer wheel	$F_{N1,outer}$	760	N
Normal force front inner wheel	$F_{N1,inner}$	0	N
Normal force rear outer wheel	$F_{N2,outer}$	705	N
Normal force rear inner wheel	$F_{N2,inner}$	-85	N
Lateral force front wheel	$F_{S1,outer}$	1020	N
Lateral force rear wheel	$F_{S2,outer}$	835	N
Braking force front wheel	F_{B1}	160	N
Braking force rear wheel	F_{B2}	130	N

Together with the load cases reported in Table 3-3, also other forces should be taken into account during the design and the validation:

- forces applied at the attachment points of the safety belts;
- forces applied by the driver;
- forces applied by door and movable parts;
- forces due to misuse (i.e. people laying on the car).

Furthermore, the overcoming of obstacles can be considered. In this case, it is common to assume a 3g maximum acceleration in z direction. Due to tyre characteristics, when the car overcomes sharp obstacles, also horizontal forces are created. A reference value of 45° can be selected as inclination of the resultant force, obtaining 3g of acceleration also in horizontal direction.

4 Outer Shape Definition

In this section the outer shape of the car will be presented and described. At the same time, also the reasons behind specific design choices will be highlighted and explained. The analysis of the concept decisions and the packaging evaluation are the starting points for the creation of the outer body shell. This latter is presented in a dedicated section and subsequently validated through an aerodynamic analysis.

4.1 Tools

The software used to create the models is CATIA V5. It is a computer program for CAD, CAE and CAM, developed by Dassault Systèmes®. It allows to work on parts in different modes. The classical way of managing body parts is using surfaces and, for this reason, the "Generative Shape Design" mode is selected for the majority of the components. On the other hand, when dealing with solid parts, the "Part Design" mode is usually selected. It is the case of the monocoque moulds which, starting from monocoque outer shape, are then designed as solids. CATIA can be also used for checks and analysis. Indeed, a draft angle analysis can be easily included to check the draft angles during moulds design while curvature and porcupine analysis are used to check surface quality.

During the design process, it is important to keep the colleagues constantly updated about the state of the work. For this purpose, CIM database is used. It is a software which allows CAD files sharing. It is used to categorize, to link and to store the CAD files of the different systems of the vehicle. In particular, the files can be linked together by means of a series of connections between files. The models are automatically updated in case of modifications of a linked part, simplifying the work. Indeed, it is always important to use the correct constraints during the setup of the CAD model in order to avoid unwanted effects after a modification.

A specific part is used to host all the references of the project and to clarify the most relevant constraints in terms of competition regulation and interfaces. It is called "Masterpart" and has the goal of creating a summary for the most important interconnections between systems. It is reported in Figure 4-1.

As it is possible to see, the Masterpart is used to report the interface information like the position of the bolts, their orientation and the eventual presence of an insert. Furthermore, it displays basic information like the position of the wheels and their characteristic angles, the luggage position or the door opening location. On the left size of the picture, it is also possible to observe some of the "publications" in the Masterpart file. They are used to create references and links between CAD models.

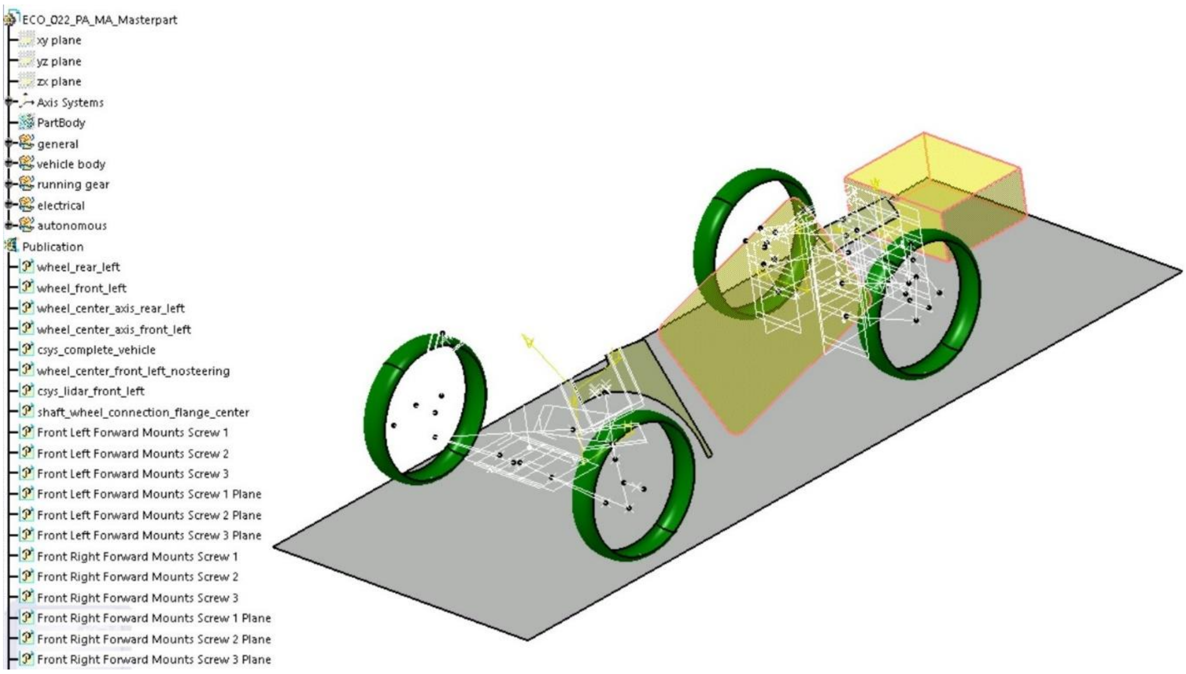

Figure 4-1 Masterpart

Another important aspect influencing the relation between CAD parts, is the selection of a common reference system. The standard adopted for the project is a right-handed coordinate system placed in the middle of the front axle, at the level of the wheel hub. The x axis is pointing towards the direction of motion, the z axis is pointing to the sky while the y axis is consequently derived.

4.2 Concept Decisions

Some constraints for vehicle body development are set by the preliminary concept decisions. First of all, the layout chosen for the powertrain influences the proportions of the car since a certain volume must be allocated to host the motors and vehicle electronics. In the case of MUC022, an electric propulsion configuration with wheel hub motors will be adopted. Even if the use of motors in the hubs leads to an increased flexibility, the related electronics should be placed near the motor themselves to avoid energy losses and to simplify the packaging. Since a front wheel drive configuration is selected to maximize the energy recuperation in braking conditions, the electronics must be placed at the front. Consequently, the choice was a classic arrangement with the front compartment dedicated to the powertrain. In order to increase the front compartment space, McPherson suspensions will be used at the front axle.

With regard to the vehicle body concept, the idea is to conceive the car in 3 modules: a light front module, the monocoque at the centre and a light rear module. Figure 4-2 shows the overall vehicle body setup and the components belonging to each module. This layout has the purpose of containing the overall weight of the car, reducing the material where no loads are applied, and to simplify the moulds manufacturing since monocoque moulds are the most critical. This is mainly due to the manufacturing process that, as explained in section 5.3, is based on the creation of foam moulds (positive of the car) from which carbon fiber moulds (negative of the car) are obtained. This double passage is time consuming and expensive, so small monocoque moulds are preferred. On the contrary, the remaining moulds (tailgate, bonnet, fenders, bumpers etc.) are obtained directly from a foam mould reproducing the negative of the parts, speeding up the process and reducing the costs. This leads to final components characterized by lower mechanical capabilities and worst surface quality with respect to using CFRP moulds. Nevertheless, these components are usually less critical with respect to the monocoque itself.

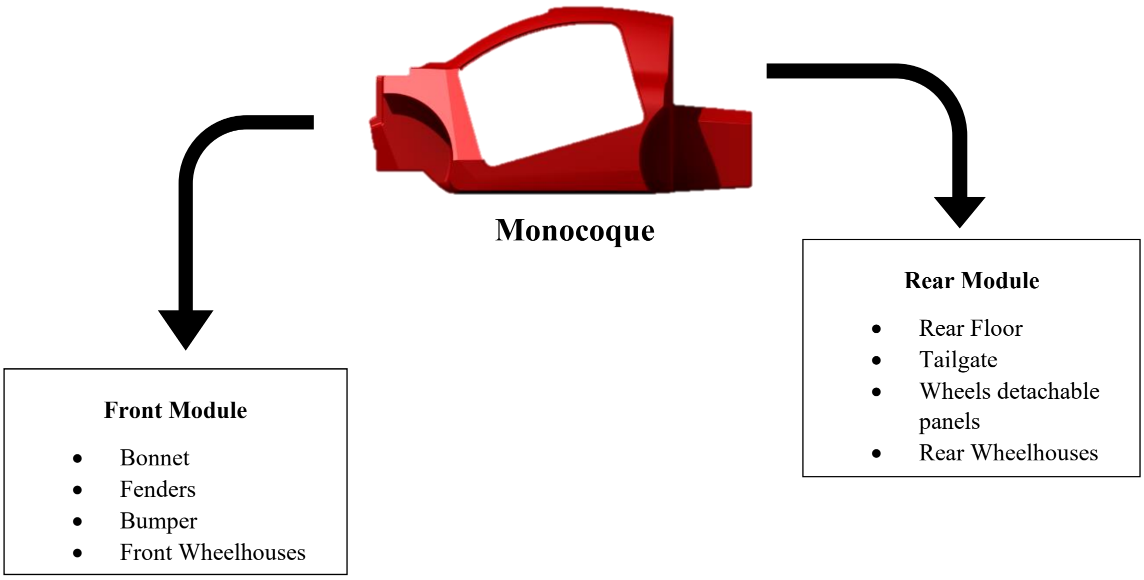

Figure 4-2 Vehicle Body layout

The luggage box to be hosted in the car is the other big constraint in the definition of the outer vehicle shape and proportions. As stated in the rules, it is a rigid box with dimensions of 500 x 400 x 200 mm (L x H x W). It represents a constraint only in terms of volume since the luggage compartment has not to sustain a specific minimum load. For this reason, the rear part was selected to host it, with the aim of exploiting the space added by the long tail. Indeed, the rear module cannot sustain high forces but can easily host the luggage box. Since the luggage compartment must be easily accessible, the rear must be equipped by an opening tailgate.

The suspension system at the back will be a double wishbone to maximize the performances. Indeed, a proper orientation of the wheel with respect to the ground allows to decrease the dissipation of energy during the motion. This is the same layout adopted by MUC019, but the kinematics requires an adaptation because the rear track passes from 1000mm to 850mm. The steering system utilizes a cable and several pulleys to move the tie rod. This system is mounted at the front of the monocoque and allows to reduce the overall volume and mass of the steering module. The brake system is hydraulic and is activated through the use of a pedal in the passenger compartment.

Finally, the driver is positioned in the centre of the vehicle, with the purpose of slightly reducing the frontal area.

In Table 4-1 the main concept decisions are reported. It is worth noting that the height, the width and the ground clearance are near the limits stated by the rules in order to reduce the frontal area of the car.

Table 4-1 Concept decisions

Vehicle characteristic	**Set value**	**Unit of measure**
Height	1000	mm
Width	1200	mm
Length	~3400	mm
Front track	1080	mm
Rear track	850	mm
Wheelbase	1550	mm
Ground clearance	100	mm
Vehicle characteristic	**Concept decision**	
Propulsion	Electric	
Traction Axle	Front Wheel Drive	
Doors	2 + Tailgate	
Seats	1	
Front Suspensions	McPherson	
Rear Suspensions	Double Wishbone	

4.3 Packaging

The design starts with a packaging analysis to define the guidelines for the outer body definition. The most important constraints must be taken into account to allocate enough space to comply with regulations, to host the driver and to locate all the functional components.

4.3.1 Driver Position

The regulations state a minimum driver mass of 70kg. In case of lighter drivers, weights on the body must be added to compensate the weight of 70kg. Considering the overall vehicle mass, a difference of 15-20kg can be easily used to tune the vehicle mass distribution. The standard used to define driver's dimensions is the DIN 33 402. In particular, the seating position is the same adopted in MUC019, designed around a 5% woman (larger than the 5% smallest women and smaller than 95% of all women).

The idea was to tilt the driver position around the hip point to avoid an unfavourable increase of the interior height. Indeed, even if the minimum height of the vehicle is not a bottleneck during the design, the necessity of having the driver head at least at 50 mm from the outer shell, sets relevant limits. The rotation around the hip point allows to save enough space to be compliant with the rule. The model is obtained through RAMSIS software and then implemented into the CAD environment. The driver model (with the helmet) is shown in Figure 4-3.

Figure 4-3 Driver model with helmet

The belt is compliant with FIA standards and has 6 attachments points. Proper attachments must be integrated to withstand the force applied to the belt in case of accident. The rules state each attachment point must withstand 200N of force in any direction. A new model of seatbelt will be selected, and it will lead to 1 kg of mass reduction. In Figure 4-4 two examples of shoulders attachment points are reported.

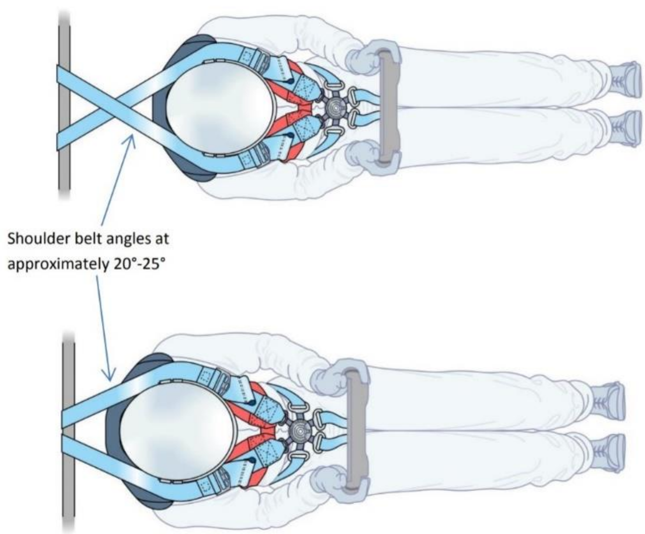

Figure 4-4 Examples of shoulder belt angles (Federation Internationale de l'Automobile, 2018, p. 9)

4.3.2 Vehicle Footprint

Different kinds of inputs and requirements must be considered designing the outer shape. For this reason, it is convenient to set the most important dimensions in a preliminary analysis. At this stage, not all the inputs from the various subsystems of the vehicle are available. Nevertheless, it is possible to exploit the information from the previous models and from literature to operate for an initial dimensioning. The outcomes of this procedure can be summarized in the following points:

- front wheelhouses dimensioning exploiting previous steering system kinematic values;
- front compartment volume from previous powertrain dimensions;
- luggage position and orientation;
- passenger cell height and width at the driver's shoulders;
- front firewall position.

A complete overview can be obtained reproducing the footprint of the vehicle. This latter can be easily created using CATIA V5 in Generative Shape Design mode. In this way, preliminary interface problems can be detected and avoided in the first steps of the project. This scheme will then be used as a guideline to set the dimension of the first concept of the vehicle.

This approach can be used to define the shape of two important sections of the vehicle: the one laying on the XZ plane (vehicle reference system) and the transversal section at the level of the driver's shoulder. Indeed, this last section is particularly relevant to offer a proper ergonomics and to comply with the rules of the competition. Particular attention is paid to leave enough space between the outer shape and driver's helmet. The necessity of assuring a minimum dimension of the cockpit (700mm) at driver's shoulders, together with the objective of frontal area reduction, leads to a cross section characterized by a big geometry change at the driver shoulders level. This choice will be recovered during the creation of the final shape. In Figure 4-5 the packaging model is reported. It is possible to observe the luggage box placed behind the suspension system and the rectangular shape representing the minimum door opening dimension. It will be oriented with a 16° angle to have the possibility to increase sill dimension at the back of the passenger compartment.

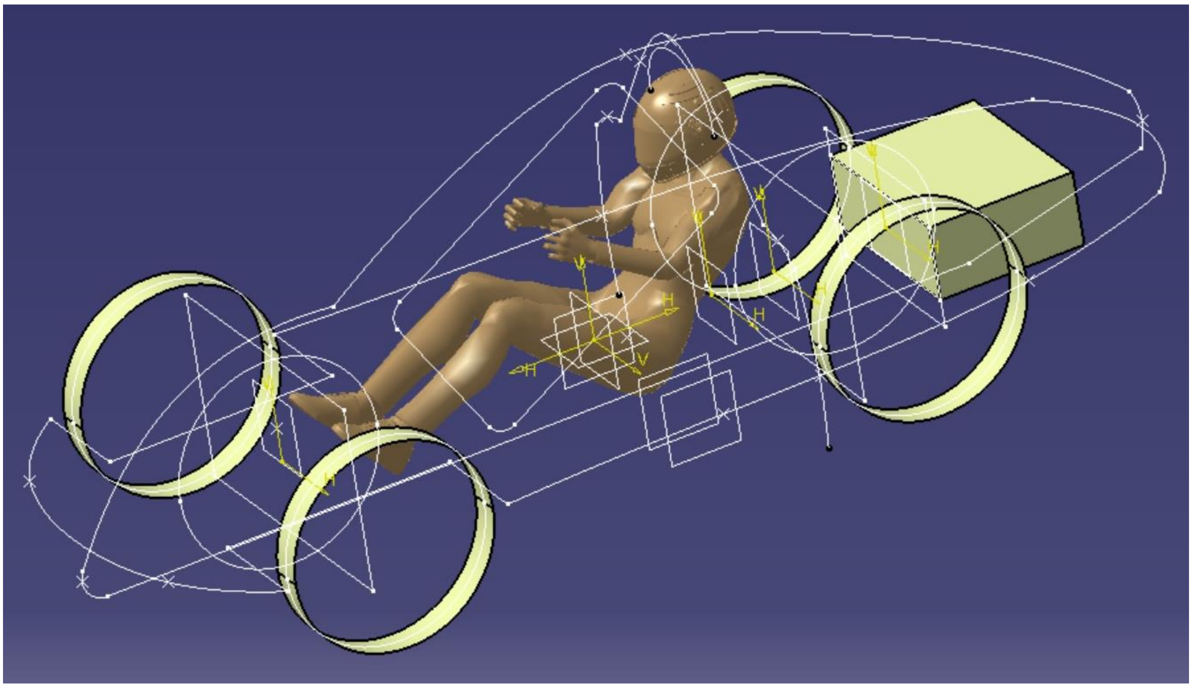

Figure 4-5 Packaging model

4.4 Concept Creation and Description

The design of the outer shape of the car is a fundamental step for the vehicle body team. The outer shape will be used to derive the single parts composing the body of the car and, at the same time, it will be used to perform aerodynamic simulations to optimize the final outline of the vehicle.

The car is characterized by a long tail at the back to be compliant to literature guidelines about streamlined shape designs. In Figure 4-6 a trend showing the influence of the boat-tailing shape on the aerodynamic drag is reported. As stated in section 3.2.1, this specific design has the purpose of reducing the rear low-pressure area at the back of the vehicle.

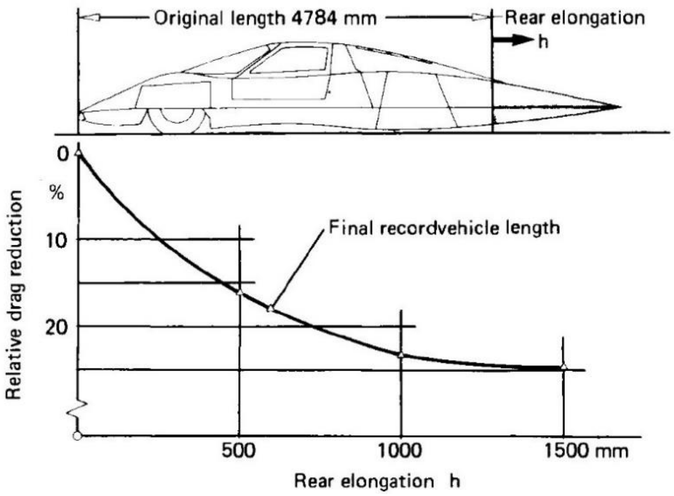

Figure 4-6 Boat-tailing applied to the Mercedes Benz C 111 III (Hucho, 1987, p. 142)

It is important to specify that the boat-tailing shape is effective only if the flow remains attached until the end of the tail. For this reason, a CFD simulation is required to validate the roof curvature to avoid an early detachment of the flow. Furthermore, it is not easy to select a dimension for the rear elongation and a proper roof curvature since the rear structure has a direct influence on the vehicle weight. Furthermore, the packaging and assembly requirements set some hard constraints in the definition of the back of the car, and, for these reasons, a trade-off is required.

As already explained, at the front of the vehicle a classical front volume is included in the design to host most of the components related to electronics and powertrain.

In Figure 4-7 the front of the car is shown in CATIA V5 environment. Indeed, the tool used for the realization of the outer shape is the mentioned software by Dassault Systèmes®. In particular, the "Generative Shape Design" mode is selected to derive the outer surfaces of the body shell. Particular attention is paid to create a smooth continuity among the surfaces, for a better final surface quality.

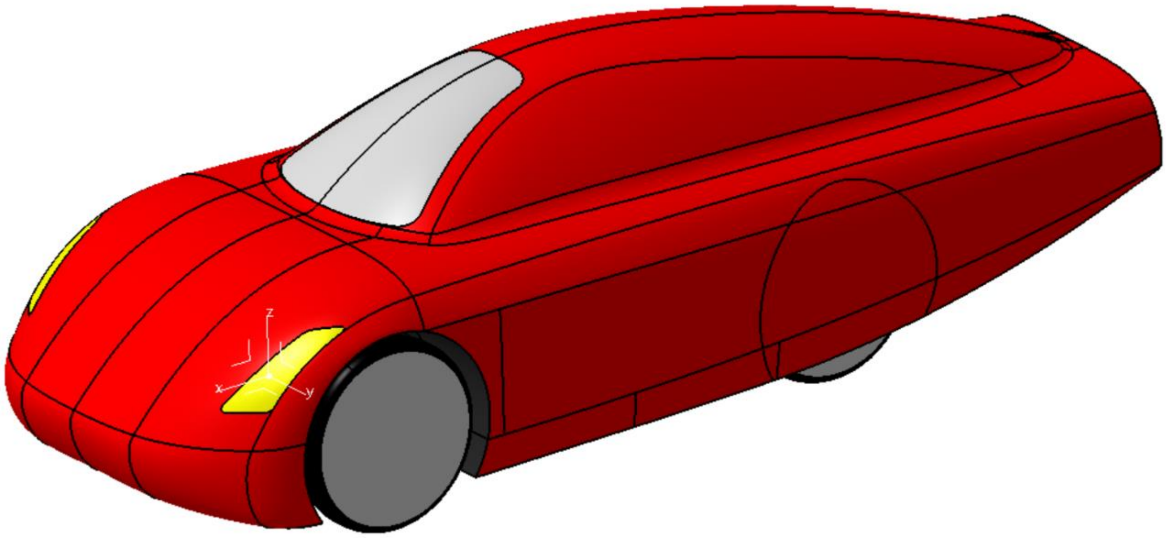

Figure 4-7 Vehicle outer shape in CATIA V5 environment (front)

From construction point of view, the body is obtained through the use of points and splines as wireframe. Then, the single surfaces are derived through "Multi-Section Surface" option or "Extrude" option. In addition, translation and projection of curves are useful techniques in case of complex surfaces.

In Figure 4-8 the rear of the car is depicted. It is interesting to point out that the style has a role in the definition of the vehicle outline. With respect to passenger cars, MUC022 is a competition vehicle so it must not comply with the current style trend and market demand. Nevertheless, the appearance of the car is a central topic when talking about sponsors and marketing.

The aesthetics of MUC022 is governed by the rear boat tailing shape which leads to a harmonious and smooth rear overhang. The panels covering the wheels enhance the "boat-appearance" and create an extremely simple and clean side. The result is a car which communicates an effect of "motion" and "movement". This is also due to the front which is, by far, the widest part of the car. The smooth lines continue until the front bumper, creating a spindly look. The width of the car is virtually extended by the headlights design which follows the bonnet curvature, giving an aggressive look at the front.

The rear taillights are not included in the CAD model, but they are shown in Figure 4-9. This latter is a modified render of the car which includes all the details of the final vehicle. It is reported to have a more realist idea of the final product and to have a preview of the splitting of body panels and movable parts.

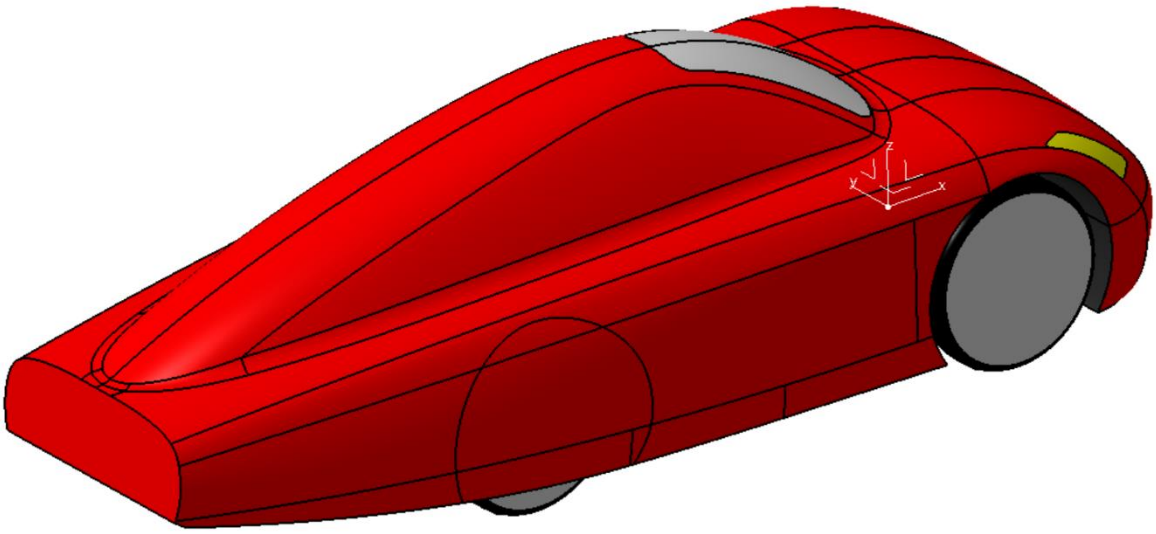

Figure 4-8 Vehicle outer shape in CATIA V5 environment (rear)

In addition, Figure 4-9 shows a relevant detail for the style: the LED light "signature" of the front headlights. Indeed, it is one of the most characterizing aspect of the look. Another detail visible in the render is the gap around the door opening which is based on the rectangular shape shown in section 4.3.2. The door hinge is placed at the rear, with the scope of creating a "Suicide Door" mechanism.

Figure 4-9 Final car preview (front)

As previously illustrated, the front is made up of a bumper (integrating the front part of the front wheelhouses), a bonnet and the fenders (integrating the rear part of the front wheelhouses). Bolts are used to connect the bumper to the front part of the wheelhouses which are then connected to the monocoque through screws. The bonnet is joined to the monocoque in the upper part by means of two hinges and it is designed to host the front headlights.

Similarly, Figure 4-10 shows a realistic render of the rear of the car. The rear module is made up of the tailgate, the rear floor and two detachable side panels. On the rear flat area, the taillights are located. As it happens with the front bonnet, the light system is integrated in the rear tailgate itself. The taillights are characterized by a single “U” shape element which incorporates all the required rear light functions. The tailgate will also be used to cover part of the rear wheels but, to allow an easy tire removal, a small detachable panel will be included in the lower part of the vehicle side.

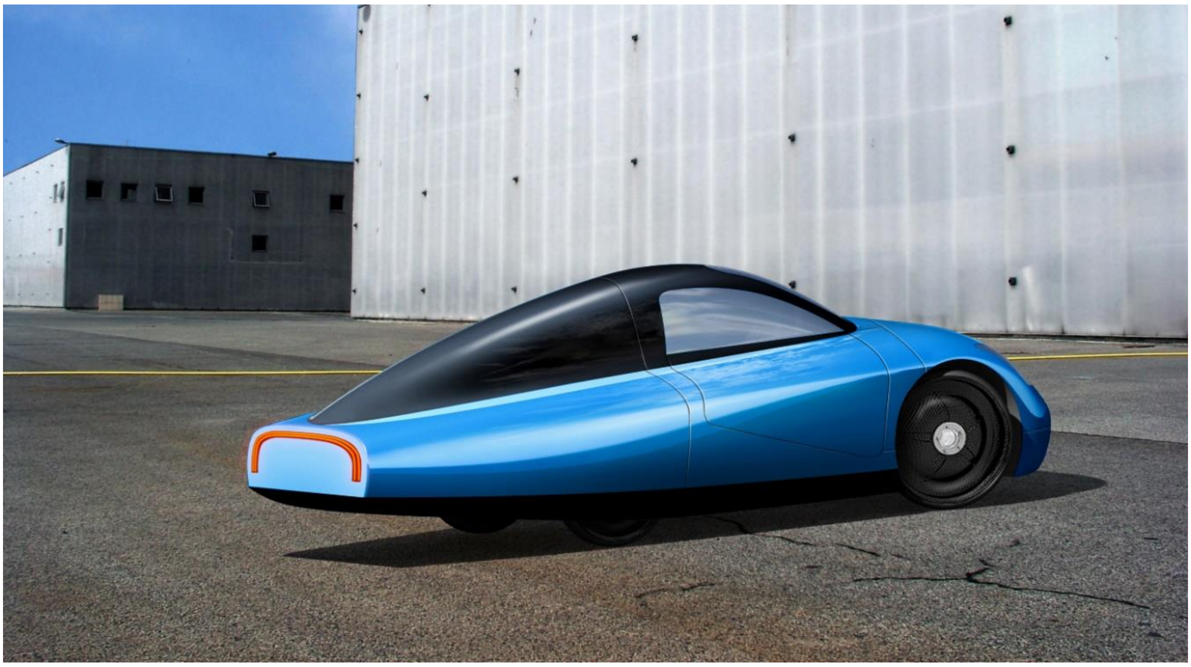

Figure 4-10 Final car preview (rear)

Finally, a brief mention to the rims. The ones showed in the last pictures are not representative of the final rims. They are based on an old MUC019 design and are included to have a preview of the final appearance of the car. Indeed, even if the new rims are based on a similar design layout, they could differ. It is worth mentioning that carbon fibre rims will be used instead of the aluminium rims which equip MUC019 with the purpose of reducing the unsprung mass value.

4.5 Aerodynamic Analysis and Optimization

As explained in section 4.4, the outer shape of MUC022 is strongly influenced by aerodynamic requirements. In fact, one of the most important targets for this new project is the improvement of the aerodynamic performances.

Without proper feedback from CFD simulations, it is difficult to predict and validate a shape, a curvature or a surface. For this reason, different iterations of simulations could be performed to improve and optimize the vehicle outline for aerodynamic purposes. It is not convenient to exploit an optimization directly derived from the software since it should always be compliant with the other vehicle body requirements and, among them, the manufacturability is the most important. Every kind of modification of the vehicle body for aerodynamic purposes, should be weighted according to the selected manufacturing technique. This passage is difficult to be implemented as constraint in a software optimization mode. For these reasons, the optimization iterations are based on a first analysis of the results, a consequent model modification, followed by a new analysis for the evaluation of the effects of the updates.

4.5.1 Velocity Planes

An example of the optimization procedure is shown in Figure 4-11, where a comparison between two different versions of the outer shape is represented. It is obtained through a CFD simulation performed by means of the Altair CFD software, with a wind velocity set at 10 m/s, which is representative of the average speed at Shell Eco-marathon competition. Rotating wheels are included in the simulation. The air density is set at 1.225 kg/m^3.

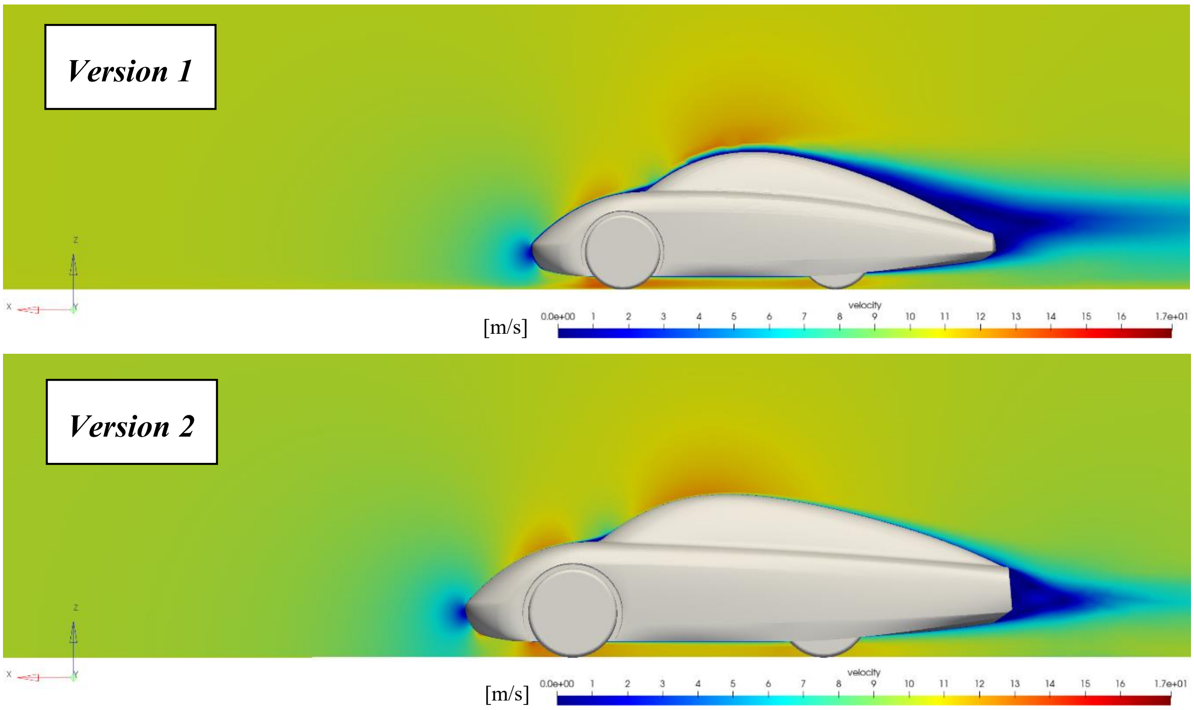

Figure 4-11 Velocity planes comparison MUC022 Version 1 and Version 2

In particular, Figure 4-11 shows the velocity plane located at the midplane of the vehicle body. This representation allows to evaluate the air flow through the vehicle silhouette highlighting eventual problems in terms of flow detachment.

Version 1 of vehicle outer shell is an old release characterized by a greater rear slope with respect to the final vehicle model. The CFD analysis of the first version shows a clear early detachment of the flow which leads to the creation of a big rear wake. In this way, the streamlined shape of the back part is useless since the flow would not follow the rear vehicle surfaces.

In order to solve this problem, the rear part has been completely redesigned, increasing the rear panel dimensions and strongly reducing the slope of the tailgate. The result is a big improvement of the flow behaviour with a delayed flow detachment and a big reduction of the rear wake. At the same time, also the "shoulder" of the vehicle, so the change in geometry at the level of the belt line, has a modified curvature. In fact, it has a more gradual slope with the goal of keeping attached the flow also on the side part of the car. The sharp cut at the back has the purpose of fixing the flow detachment, and so the wake dimensions.

In the following, the aerodynamic analysis of the final version of MUC022 will be carried out with reference to MU019 model. In this way, it is possible to highlight the improvements with respect to the old vehicle. Before starting with the aerodynamic analysis, it is important to underline that the model used to represent MUC019 is different with respect to the final one. Indeed, it has a huge spoiler at the back which is not present in the final version (that is characterized by a bigger wake because of the shorter spoiler and so early detachment of the flow).

In Figure 4-12 another velocity plane comparison is reported. In this case the picture shows the performances of MUC019 and MUC022.

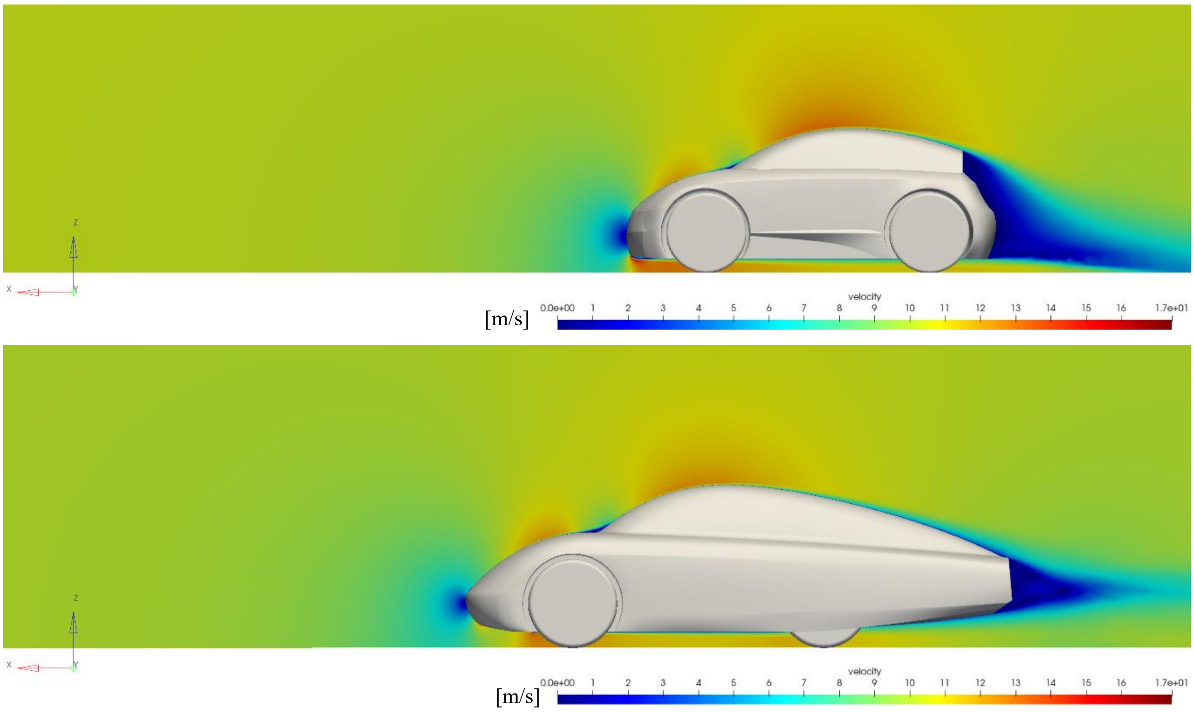

Figure 4-12 Velocity planes comparison MUC019 and MUC022

As it happened in the previous comparison, the big difference regards the back since the wake dimension is completely different in the two cases. Even with the spoiler of MUC019 model, the wake is bigger in the old car. The hatchback body style has big advantages in terms of roominess and practicality, but it is intrinsically characterized by worst aerodynamic performances. In both cases the behaviour of the underbody is good since both cars exploit a flat underbody which decrease the amount of drag.

In Figure 4-13 it is reported a comparison between MUC019 and MUC022 based on two velocity planes. Together with the midplane previously introduced, also another plane, parallel to XY (vehicle reference system), is included.

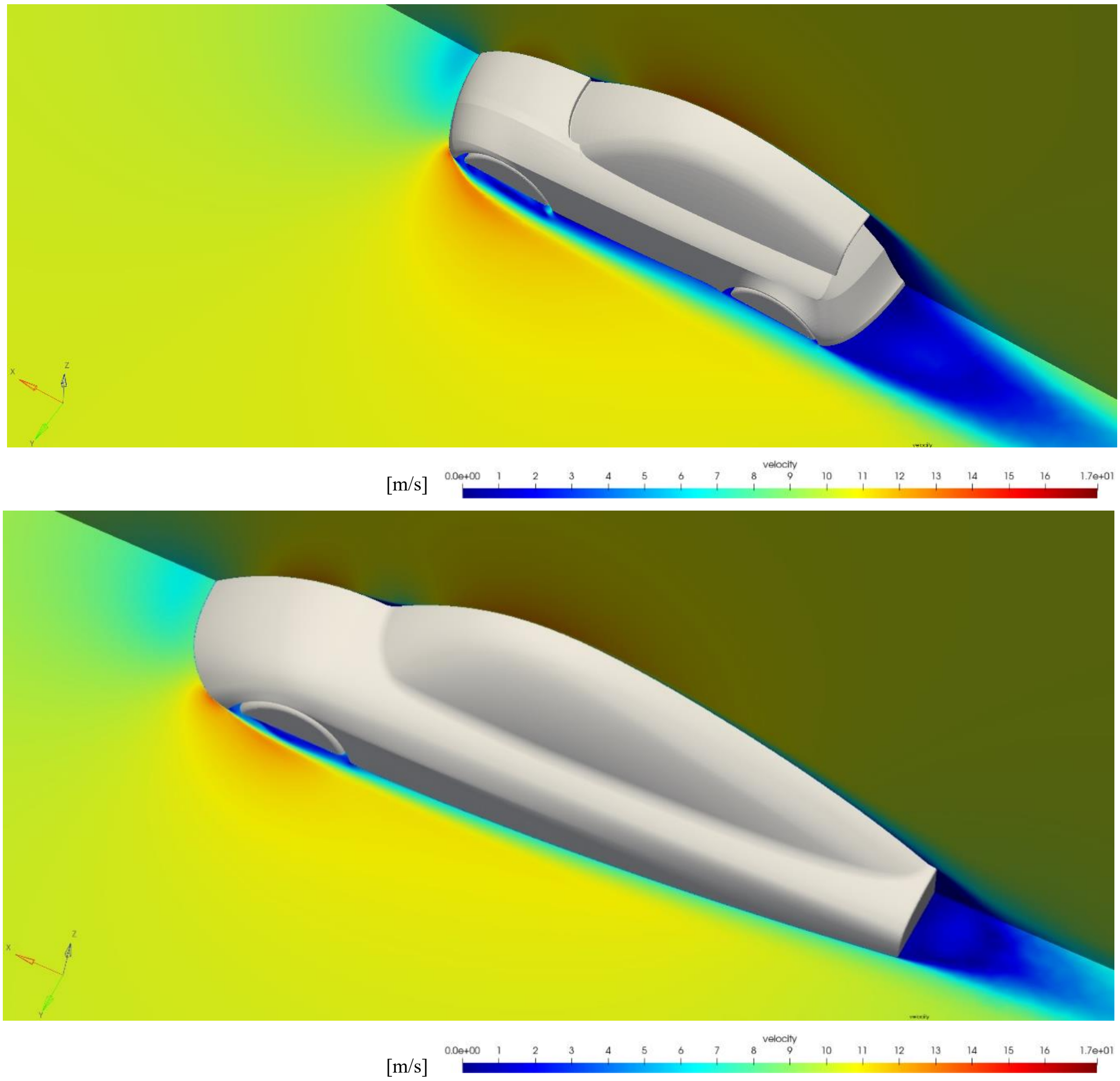

Figure 4-13 Velocity planes comparison MUC019 and MUC022 (XY plane)

Figure 4-13 allows to compare the behaviour of the flow on the side of the vehicles. As it happens for the roof, an early detachment of the flow on the sides generates drag. Furthermore, this area is also critical because of the presence of wheelhouses and wheels which strongly disturb the flow.

This last comparison highlights several differences between the two cars. First of all, the shape of the front bumper of MUC022 reduces the disturbances created by the front wheelhouse. Indeed, the blue area around the front wheel has been strongly reduced and the flow can reattach easily to the surface slightly after the end of the wheelhouse. In this way, MUC022 can exploit the surface curvature to guide the flow until the end of the car where the geometry discontinuity sets the start of the rear wake.

On the contrary, MUC019 is characterized by a big blue area (detachments) around the front wheel. The geometry of the side does not allow a reattachment of the flow, impairing the capability of the side to guide the flow until the back of the vehicle. Furthermore, the presence of panels to cover the rear wheels of MUC022, allows a smooth and clean flow of air until the back. This does not happen in MUC019 where the open rear wheelhouse further disturbs the side flow. The last information it is possible to extrapolate from Figure 4-13 is related to the dimension of MUC022 wake. In fact, it is smaller also in this new plane, further reducing the drag characterizing this region.

4.5.2 Wall Shear Stress

The following analysis regards the Wall Shear Stress. In Figure 4-14 it is reported a comparison of the front part of the two vehicles.

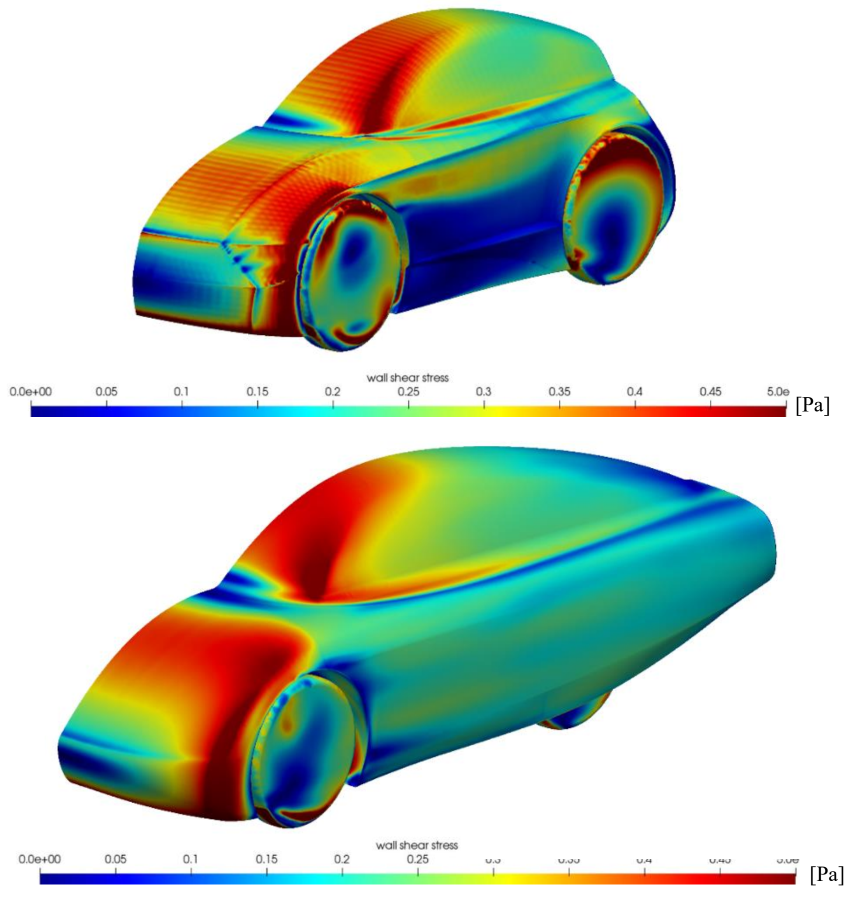

Figure 4-14 Wall Shear Stress comparison MUC019 and MUC022 (front)

The Wall Shear Stress τ_w is given by Formula (4-1):

$$\tau_w = \mu \left(\frac{\partial u}{\partial y}\right)_{y=0} \quad (4\text{-}1)$$

Where μ is the dynamic viscosity, u is the flow velocity parallel to the wall and y is the distance to the wall.

This variable is widely used in the analysis of CFD results since it is a useful indicator about flow detachment. It is related to the friction generated by the air, but it is only a small contribution in the drag generation because it accounts for a very low amount of the total aerodynamic drag (usually around 10% in passenger cars). Nevertheless, it is a relevant indicator since high values of Wall Shear Stress correspond to a flow which is significantly attached to the surface and with high velocity.

It is relevant to remember that negative pressure regions correspond to high velocity regions. The areas in which the Wall Shear Stress is the highest are: part of the tires, the windscreen-roof transition, the A pillar and the side of the front bumper. The scale in the pictures has been properly adapted to highlight the blue areas which represent the regions in which the shear stress is zero, so where the air is not attached to the vehicle.

Considering this view, the most evident difference between MUC019 and MUC020 regards the side of the car. Indeed, as already explained in the velocity plane analysis, MUC019 presents a big area of separation on the side. On the contrary, MUC022 is able to reattach the flow after the disturbances induced by the front wheelhouse.

In the front there are parts with values near to zero. These ones correspond to stagnation points. In particular, we have the central part of the front bumper where the energy is completely converted in force on the surface. Also in the lower part of the windscreen a similar phenomenon can be observed. This happens in both cars but the blue area on the bumper is smaller in MUC022. On the other hand, also MUC022 presents some minor problems. In particular, the flow near the belt line is not completely attached since a blue area is clearly visible.

Finally, it is worth noticing that the rim design is not the final one. A new design could have an impact on the result around the wheelhouse area. These potential effects will be evaluated in the future when the rim design will be finalized. In Figure 4-15 the Wall Shear Stress at the rear is shown.

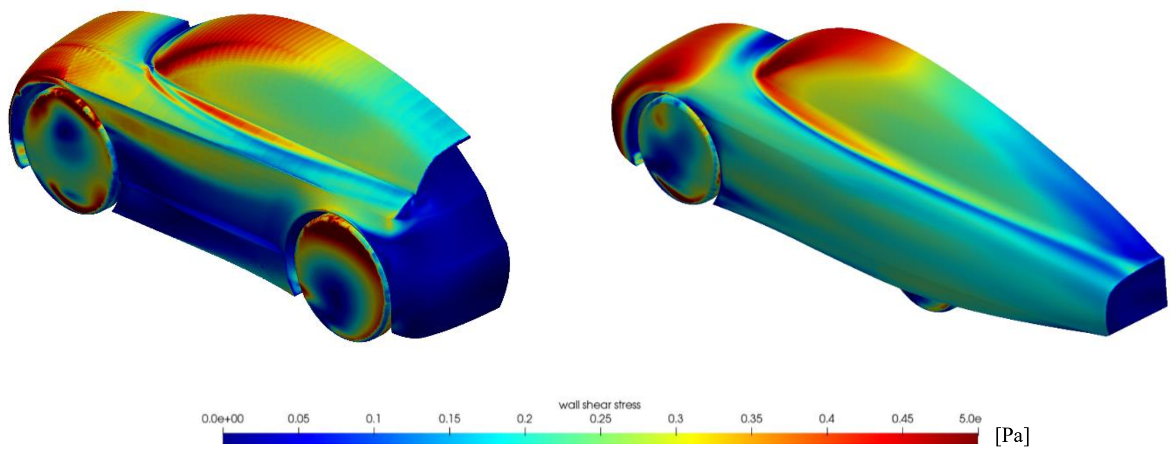

Figure 4-15 Wall Shear Stress comparison MUC019 and MUC022 (rear)

Looking at the rear, it is possible to observe the wake area of MUC019: it starts from the rear wheelhouses and extend on the whole rear. On the contrary, on MUC022, the wake is much smaller, but a certain amount of flow detaches earlier, before reaching the vertical panel at the back. This resulting behaviour is due to a trade-off between different requirements. A reduction of the rear slope can be achieved increasing the length of the vehicle or increasing the dimension of the rear flat area (and so enhancing the "truncated-tail look"). The first option is difficult to be implemented because of the maximum length set by regulations and because of the weight that a longer tail would add. At the same time, a bigger rear panel leads to problem during the milling of the tailgate mould and to an increase of weight because of the additional material needed for this structure.

The last view to be analysed is the one showing the underbody of the two vehicles. It is reported in Figure 4-16.

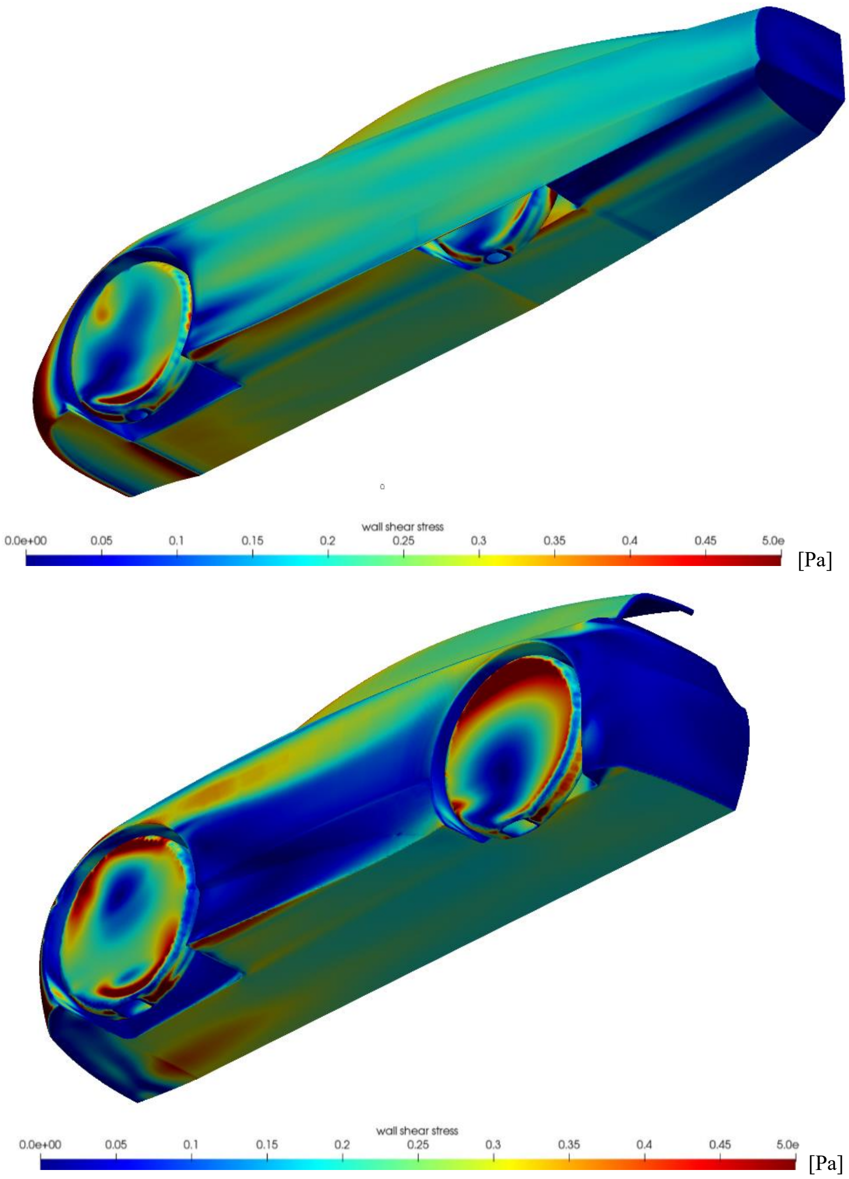

Figure 4-16 Wall Shear Stress comparison MUC019 and MUC022 (underbody)

Other differences can be highlighted looking at this view. A bigger blue area is present in MUC019 at the junction front bumper-underbody since the flow requires more space to reattach to the underbody panel. On the contrary, MUC022 presents a defect in the region behind the rear wheelhouses since a blue zone indicates that the flow cannot keep attach easily on this surface of the car.

In conclusion, a summary of the results, in terms of aerodynamic performances, is reported in Table 4-2.

Table 4-2 Aerodynamic results

Parameter	**Symbol**	**MUC019**	**MUC022**	**Unit of measure**	**% of improvement**
Drag Coefficient	C_d	0.29	0.16	-	44.8%
Projected Area	A_p	0.98	0.92	m^2	6.1%
$C_d \cdot A_p$		0.284	0.147	m^2	48.2%

5 Monocoque

This chapter is devoted to the structural part of the vehicle: the monocoque. It will be presented starting from the geometry, highlighting the most important interfaces with the different vehicle systems. Subsequently, the material will be selected and implemented in the structural validation. Finally, a section is dedicated to the explanation of the production process and assembly techniques.

5.1 Geometry Definition

After the design of the outer body shape and after having defined a concept for the splitting of the various body parts, the structural part of the car, the monocoque, has to be derived. As already explained, the vehicle outer shape will be used as starting point for the creation of the monocoque model since this latter must reproduce part of the vehicle body outer "skin". During the design of this model, it is necessary to take into account the targets and functions previously described. Indeed, the monocoque must present a structure able to withstand the loads described in section 3.3, enough visibility and doors with an opening compliant with accessibility standards. Furthermore, adequate suspension attachments must be included in the design.

In Figure 5-1 a photorealist render of the front of the monocoque is depicted.

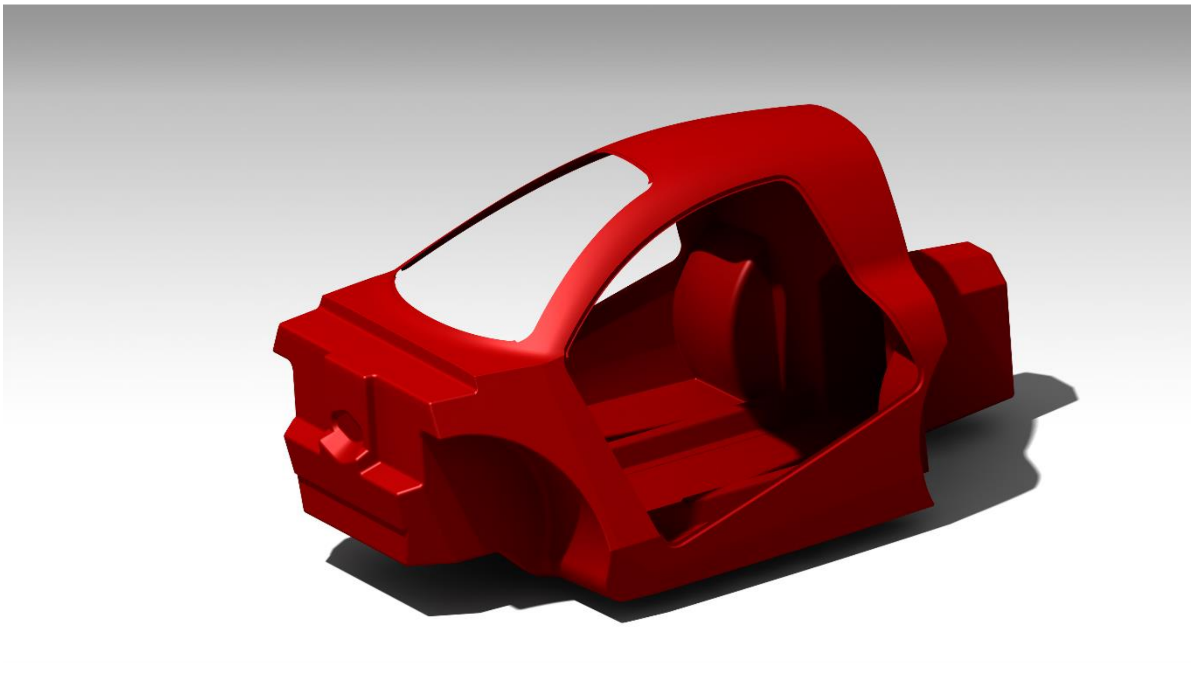

Figure 5-1 Photorealistic render of the monocoque (front)

The geometry of the monocoque is designed to assure the space for the most important components. Furthermore, the passenger cell has reduced dimensions to save mass and to decrease the costs. In Figure 5-2 it is possible to observe how the monocoque is integrated with the rest of the body.

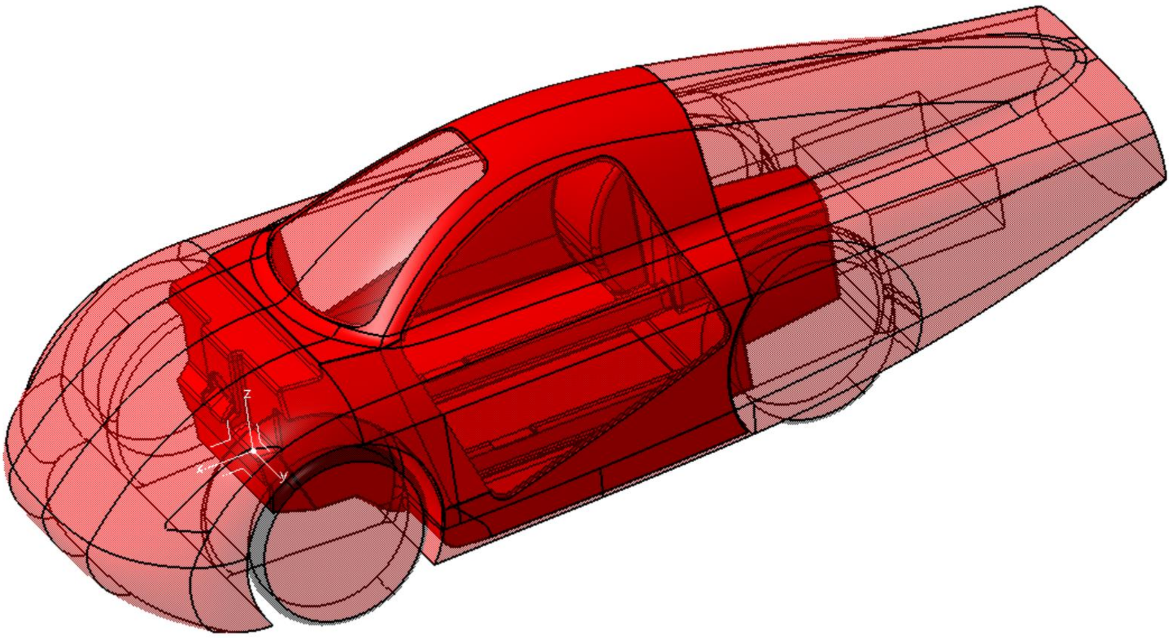

Figure 5-2 Monocoque-body integration

5.1.1 Front and central part

At the front of the car, a firewall is included to be compliant with regulations. Indeed, the passenger compartment must be separated with respect to the "powertrain compartment". Furthermore, the front firewall is hosting the attachment points for the steering system and for the electronics. The front is a very complex area from packaging point of view since it must be able to offer enough room for most of the systems of the vehicle.

A specific geometry is selected for this region to facilitate the matching with the various components. It is the case of the steering column attachment which has a dedicated shape. The same happens for the two "pockets" on the sides of the steering column interface. They are designed to increase the space allocated for the electronic components. On the lower part, two surfaces dedicated to the steering system are included. The first one is dimensioned to host the steering system pulleys, the second one to offer a region where the steering rail can move. On the upper part of the front structure, a small surface is used to host the bonnet hinges. In Figure 5-3 a scheme of the front geometry is reported.

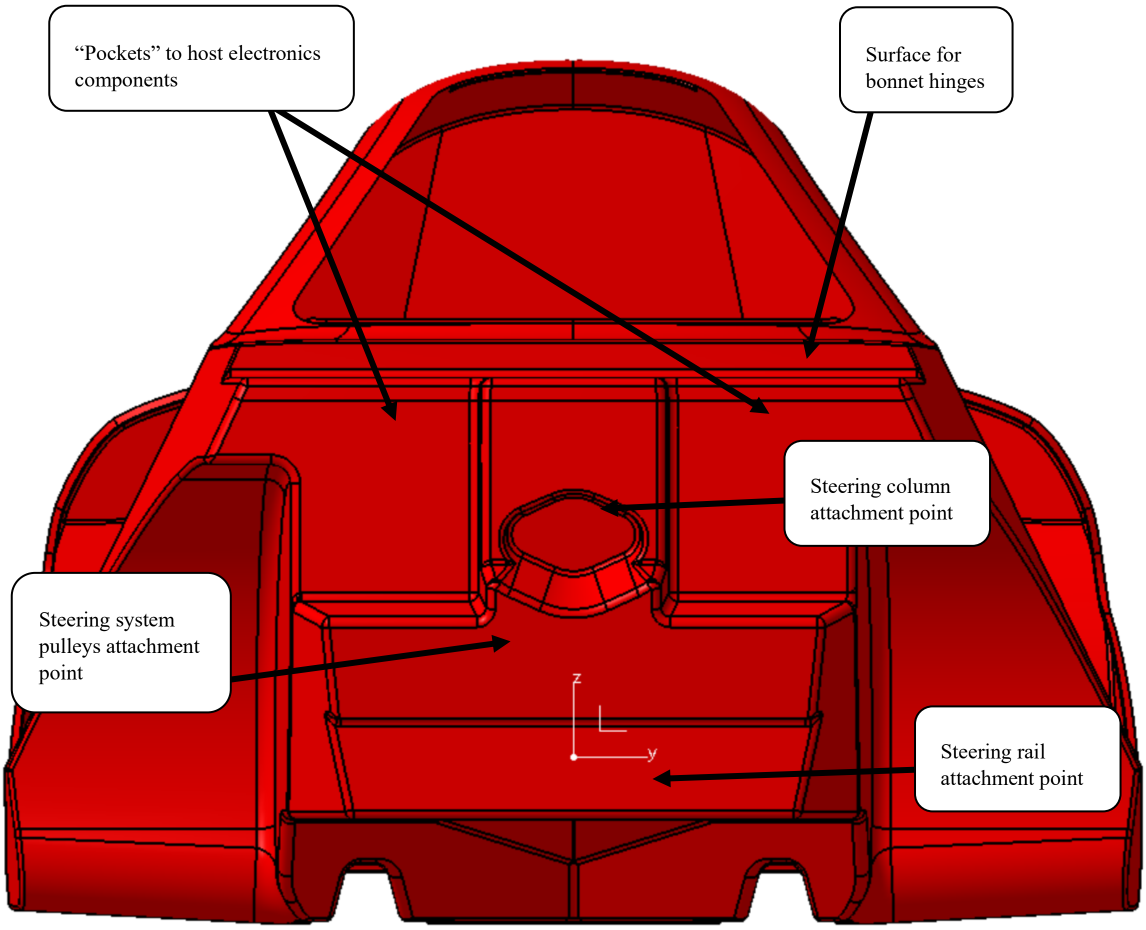

Figure 5-3 Monocoque front geometry

Another area of interest is the one around the windshield. Indeed, it should be maintained in position by the monocoque itself. For this purpose, two flanges are included in the upper and lower part of windshield opening. This detail is visible in Figure 5-4.

In the central part of the car a new configuration is introduced because of the single seat layout. In passenger cars, a tunnel must be included to increase bending stiffness and to host the exhaust line or the driveshaft. In previous TUfast urban concepts it was also considered an easy and effective way to route cables to the rear of the car (for commands and for the rear brake system). Adopting a single seat layout leads to the impossibility of integrating a single central tunnel. Therefore, two tunnels on the sides of the driver are included in the design. Furthermore, they are also incorporating some commands (windshield wiper command, emergency switch-off command, etc.), so a dedicated shape is introduced to host the control plates. In Figure 5-4 it is possible to see the two tunnels.

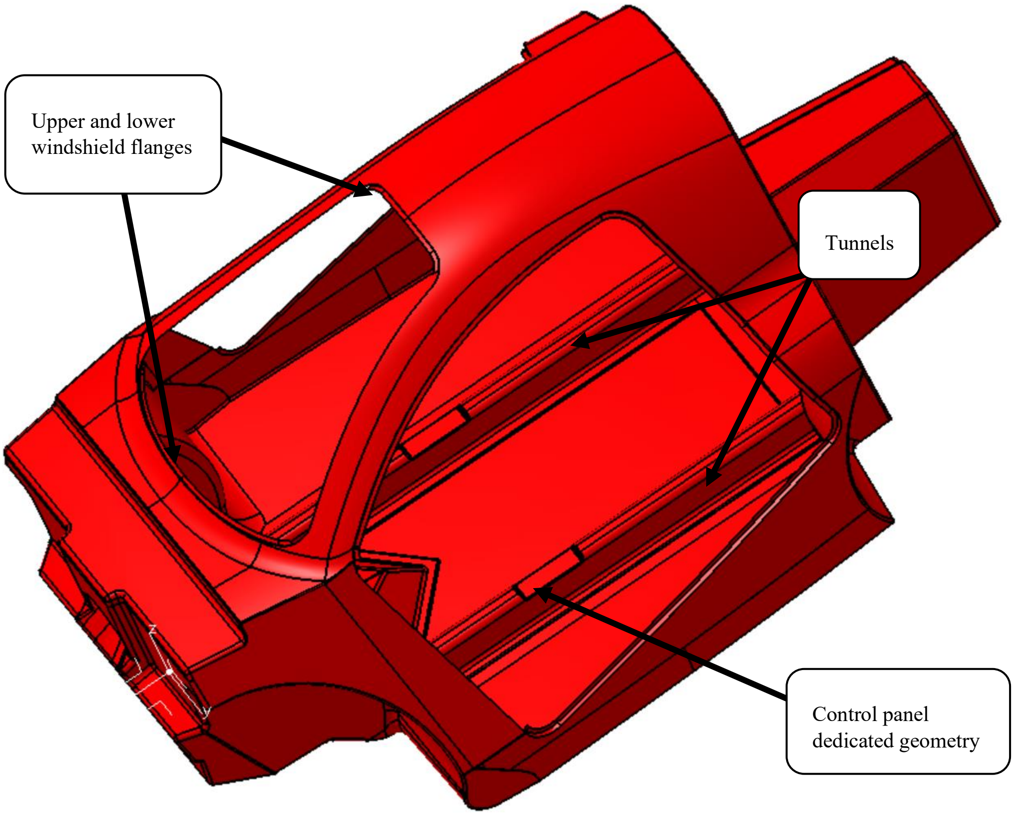

Figure 5-4 Monocoque central geometry

5.1.2 Rear part

Passing to the rear of the car, it is possible to observe a geometry governed by the necessity of incorporating rear suspension attachments. Generally, in similar monocoque solutions, a rear volume is included to offer the required space for suspension mounts. It is created joining aluminium structures or creating a smooth geometry variation to include the rear volume in the CFRP monocoque itself (see section 2.1.1). In the case of MUC022, the rear attachments must be integrated into the CFRP monocoque to save weight and to reduce the complexity. Nevertheless, because of the small wheelbase and overall vehicle dimensions, it is difficult to replicate this smooth geometry variation. Because of the low amount of load this urban concept vehicle experiences, a more extreme and cramped solution can be developed to host the rear suspension attachment points. The resultant shape is a boxy volume which simplifies the packaging, reducing, at the same time, the amount of material used at the rear of the monocoque. In the upper part of the rear "suspension box" another dedicated geometry is designed to host, more efficiently, the shock absorber mount. The rear box is also a valid option to incorporate eventual other electronic devices not initially foreseen. In Figure 5-5 a photorealistic render of the rear of the monocoque is reported.

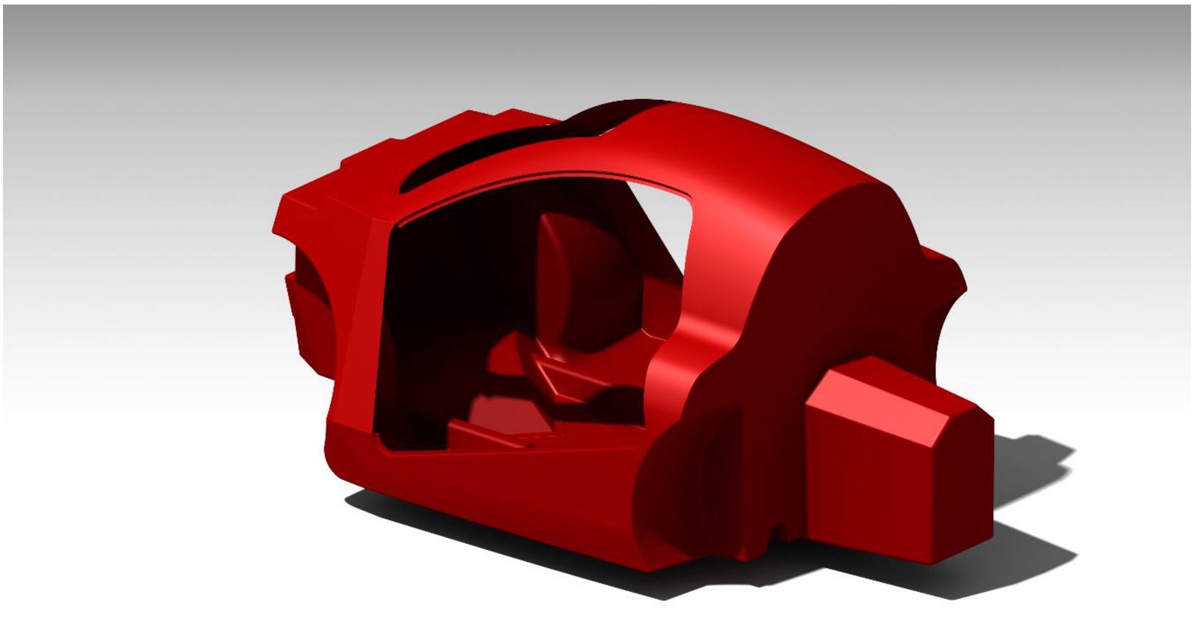

Figure 5-5 Photorealistic render of the monocoque (rear)

In Figure 5-5 it is also visible the sill. It is a crucial region to achieve the targets in terms of strength and stiffness. To maximize its dimensions, the minimum door opening area has been rotated of 16°, obtaining a sill which increase in dimensions from the front to the rear part of the car. In this way, the car is deforming less when subjected to loads while the accessibility is not drastically impaired since the passenger entering and exiting movements are mainly located at the front of the door opening.

Another interesting region at the rear of the car is the floor. A specific geometry of this area, visible in Figure 5-6, allows the matching with the rear module. Indeed, a step at the rear of the monocoque floor has the purpose of connecting the bottom surface of the rear module. This latter will be also sustained by bolts attached to the rear suspension box. Three M4 screws per side are selected for this scope. Furthermore, two cables will connect the end part of the rear floor to the monocoque rear wall. The aim is increasing the stiffness of the rear overhang in case of people laying on the rear (misuse). They will be covered by the tailgate, therefore they are not visible from outside the vehicle. The other component in the rear module is the tailgate. This big part will be firmly connected to the monocoque through a hinge located on the rear monocoque wall. For this purpose, M6 screws are selected. Additionally, magnets, placed on the matching flanges of tailgate and floor, will be used to lock the tailgate and to keep it in position.

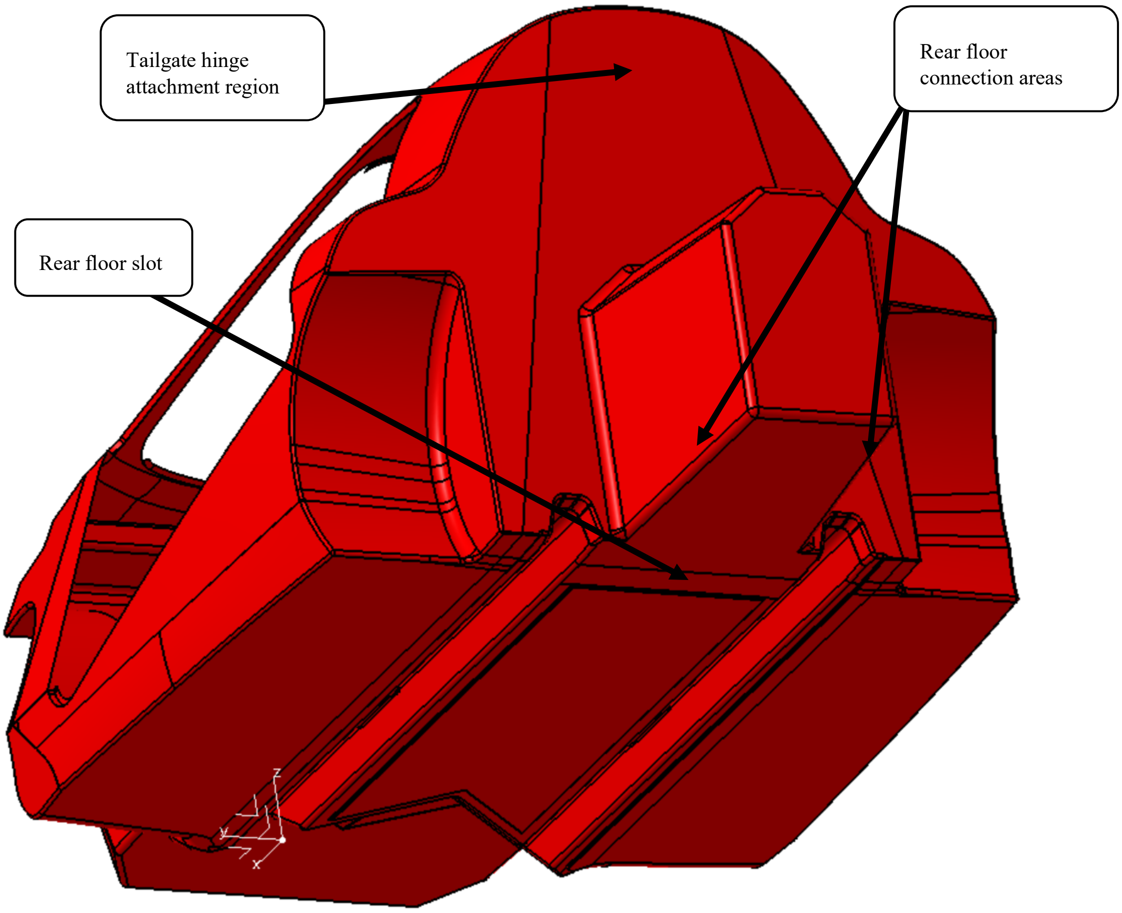

Figure 5-6 Monocoque rear geometry

5.1.3 Suspensions mounting points

The most important interfaces are the suspensions mounting points. A detailed analysis is required to have an overview of the most stressed areas of the car.

At the front, two connections for the lower arm and a single upper connection for the McPherson strut are included in the geometry. The strut mount assembly is realized through four ISO 4762 M5x25 screws while respectively three and two screws will be used for the front and rear lower arm mounts. Also in this case, ISO 4762 M5x25 screws are used. Figure 5-7 shows the three mounts previously described.

It is evident that the choice of adopting a McPherson solution for the front suspension system leads to greater roominess under the front hood. The McPherson strut mount is not affecting the available space since it substitutes a shock absorber mount and two upper arm mounts in a single connection. Nevertheless, this layout has several drawbacks, like the lower performance in camber recovery with respect to a double wishbone solution and the shock absorber piston rod deformation which can increase friction and hysteresis (Genta & Morello, 2008a, p. 148). These problems could be mitigated properly designing the kinematics of the suspension.

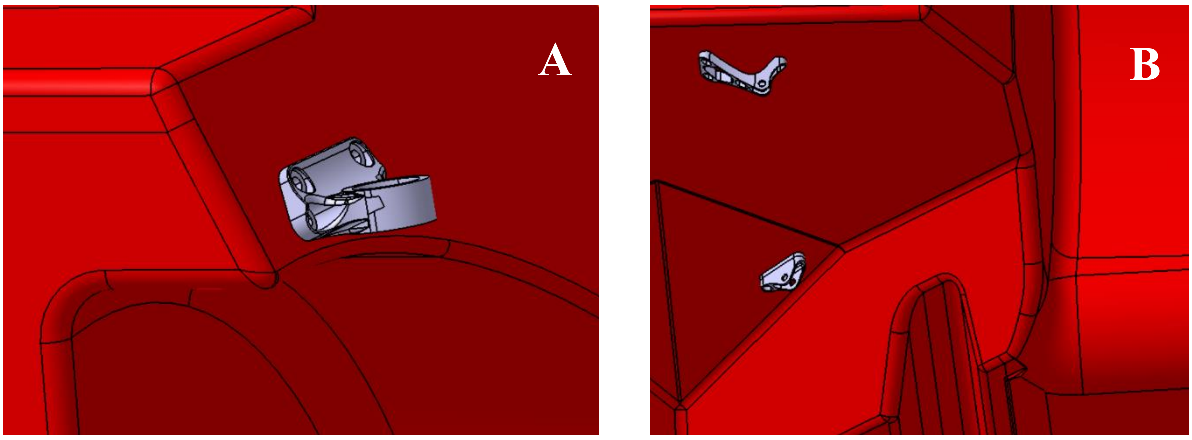

Figure 5-7 Front upper mount (A) and lower arms mounts (B)

At the rear axle the suspension is a double wishbone. Consequently, it has an upper and lower arm, a toe link and a shock absorber to be separately attached. To reduce the concentration of stress on the box walls, corner mounts will be used for upper and lower arm links. In Figure 5-8 the rear suspensions mounts are depicted.

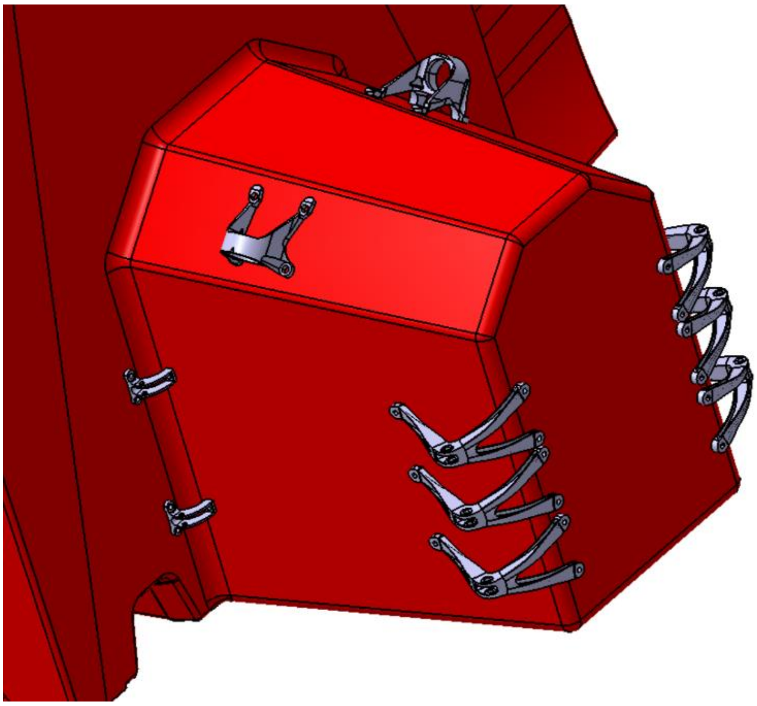

Figure 5-8 Rear suspensions mounts

In this case two types of standard elements are selected. For the shock absorber mount, subjected to high loads, four ISO 4762 M6x25 screws are chosen. On the contrary, for the mounts of the toe link and of the upper and lower arm, three screws ISO 4762 M5x20 are used.

5.2 Material Selection and Structural Analysis

MUC022 has a target mass of 70 kg which is a very low value even for a car characterized by these dimensions. This goal can be achieved switching from traditional materials (steel, aluminium, etc.) to composite materials and relative production methodologies.

The first part of this section is dedicated to a presentation of the materials adopted in the sandwich structure. For this purpose, also datasheets of pre-pregs and honeycomb core will be included in the dissertation. Additionally, since the number of layers and sandwich structure layout can be tuned region by region according to necessities, a preliminary ply layout concept will be introduced.

Nevertheless, it is important to remember that the optimization and the detailed selection of material layers is not the objective of this dissertation. Indeed, other TUfast Eco team members are directly involved in these tasks. However, the preliminary layout shown in the following is the solid base for future optimizations and is representative of the final structure behaviour.

The selection and allocation of the material in the different monocoque regions is the input for a FEM analysis which is used to validate the monocoque from structural point of view. The FEM simulations are essential both to assure the structural function of the monocoque, both to be compliant with SEM rules.

5.2.1 Material Selection

The monocoque laminate structure is based on the layout adopted for MUC019. It is mostly related to four layers of 200g/m^2 carbon fabric symmetrically arranged. Furthermore, in the majority of the surfaces, also an aluminium honeycomb structure is adopted to increase the stiffness performances of the laminate. In Figure 5-9 it is possible to see an example of sandwich structure with top and bottom CFRP skin and aluminium honeycomb core.

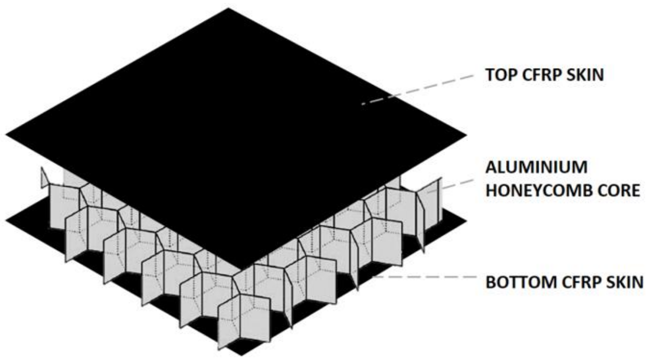

Figure 5-9 Structure of a composite sandwich panel (Mills, et al., 2020, p. 2)

Generally, single skin laminates are very strong, but the stiffness target is difficult to be achieved with a low thickness of the laminate. The core can be used to increase the thickness and, consequently, the stiffness of the component. In this way, a light core avoids the use of more material which would lead to an increase of mass and costs. This solution is similar to the concept behind the I-beam where the flanges are used to carry the majority of tensile and compressive loads. Analogously, in a sandwich laminate, the skins work similarly to flanges of an I-beam while the core can be associated to the web part of the I-beam (Gurit, n.d., p. 13). In Figure 5-10 an example of sandwich panel loading can be observed.

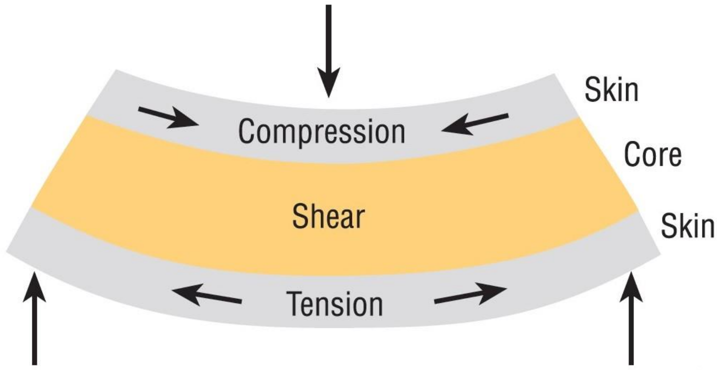

Figure 5-10 Sandwich panel loading (Gurit, n.d., p. 14)

It is worth noting that the core must be able to sustain compression, without premature failure to prevent the buckling of the thin skins (Gurit, n.d., p. 14). Regarding core material and typology, it is possible to use different kinds of solutions (thermoplastic honeycomb, wood, paper honeycomb, etc.), but the most appropriate for this application is the aluminium one. This latter is characterized by "one of the highest strength/weight ratios of any structural material" (Gurit, n.d., p. 43). Together with this strong point, and the relatively low price, it also presents some drawbacks, like the potential corrosion problems in salt environment and the lack of "mechanical memory". In fact, after an impact it can deform irreversibly, while the outer skins come back to the original position, causing and unbounding between skins and core material (Gurit, n.d., p. 43).

The selected core is called PAMG-XR1 5052 and has a thickness of 10mm. The datasheet is reported in Table 5-1.

Table 5-1 PAMG-XR1 5052 Datasheet (Plascore, n.d.)

Cell size	Nominal Density	Bare Compressive Strength		Plate Shear Strength "L" Direction		Plate Shear Modulus "L" Direction	Plate Shear Strength "W" Direction		Plate Shear Modulus "W" Direction
		Typical	Minimum	Typical	Minimum	Typical	Typical	Minimum	Typical
mm	kg/m³	MPa	MPa	MPa	MPa	GPa	MPa	MPa	GPa
3.2	50	2.14	1.48	1.55	1.07	0.34	0.85	0.62	0.18

With regard to pre-pregs, a woven fabric layout is selected. It is obtained "by the interlacing of warp (0°) fibres and weft (90°) fibres in a regular pattern or weave style" (Gurit, n.d., p. 34). The selection of a weave style allows to control the drape (so the capacity of the fabric to "follow" the shape of a surface), surface smoothness and stability. Between the different typologies of weave styles, the Twill is selected. In the Twill weave style "one or more warp fibres alternately weave over and under two or more weft fibres in a regular repeated manner" (Gurit, n.d., p. 34). This layout is selected because allows to reduce crimp, to increase surface smoothness and to slightly increase mechanical properties (Gurit, n.d., p. 34).

In particular, the selected carbon fibre pre-preg is called T300 and it is supplied by Toray. In Table 5-2 the composite properties are reported.

Table 5-2 T300 Datasheet (Toray, 2018)

Property	Value	Unit of measure	Test method
Tensile Strength*	1820	MPa	ASTM D-3039
Tensile Modulus*	140	GPa	ASTM D-3039
Tensile Strain	1.26%	-	ASTM D-3039
Compressive Strength*	1470	MPa	SACMASRM1R-94
Flexural Strength*	1790	MPa	ASTM D-790
Flexural Modulus*	123	GPa	ASTM D-790
ILSS	94.1	MPa	SACMASRM1R-94
In Plain Shear Strength	95	MPa	ASTM D-3518
90° Tensile Strength	76	MPa	ASTM D-3039
*Normalized to 60% fiber volume. Cured with #2500 epoxy at 130 °C			

As already described, the basic stack sequence is a sandwich structure with the core material at the centre and two layers of T300 per side. The outer skins are oriented at 45° and 90° symmetrically to improve laminate mechanical capability in multiple directions. Nevertheless, this sequence cannot be used everywhere since complex geometry regions cannot host the honeycomb core. Indeed, the honeycomb is not present on the door opening and windshield contour. Additionally, also the tunnels have not the honeycomb core. This lack is counterbalanced by reinforcements where additional carbon fibre is placed to create a stiff monolithic structure. Four more layers of T300 are symmetrically added on these areas (always oriented at 45° and 90°). "A" pillars are a particularly critical region for stiffness and strength, therefore they are also reinforced with the additional four layers.

Thanks to the Altair HyperMesh model, which will be introduced in section 5.2.2, it is possible to have an estimation of the final monocoque mass. Indeed, a mass of **9.335kg** is expected. It is worth noticing that this value does not take into account the additional mass given by inserts and related fastening products, like helicoils.

5.2.2 Structural Analysis

The structural analysis, realized through HyperMesh FEM software is required to validate the geometry and the design of the monocoque. In particular, OptiStruct solver is used for the simulation. In order to obtain reliable results, the model implemented in the software should replicate the design feature of the real car. For this purpose, suspensions links are exactly replicated using steel tubes modelled as rod elements. Indeed, they are used only to replicate the actual force direction to the vehicle body. The McPherson strut is modelled using a RBE2 element and the same happens for the suspension mounts. Additionally, RBE2 elements are used to create the suspension knuckle, where forces and constraints are applied in most of the cases.

The outer surface is modelled using a mix of square and triangular elements of 5mm, but it is further adjusted thanks to the mesh edit functions offered by the software. In this way, the quality index of the mesh can be optimized, increasing the reliability and the quality of the simulation outcomes. In Figure 5-11 a detail of the rear geometry mesh is reported.

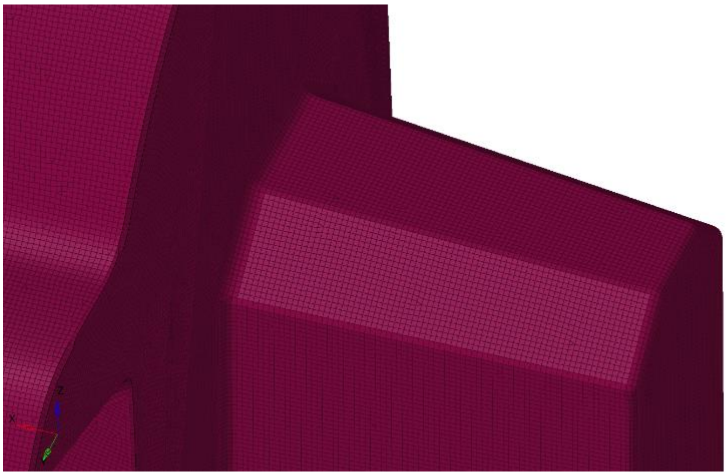

Figure 5-11 Rear geometry mesh (detail)

Regarding the properties of the model, it is worth mentioning the PCOMPP element property used to create the plies of the laminate. For each layer, the thickness and the orientation of the fibres must be specified. On the contrary, PROD is selected to reproduce the rod behaviour of the suspension links.

RBE3 elements are used to create the so called “spider” structures, able to share the force applied on a master node to the connected slave nodes. RBE3 elements do not influence structural rigidity and are used to apply the distributed load for the rollover and bending test. An example of “spider” structure is shown in Figure 5-12 where RBE3 elements are used to apply the rollover force to a portion of the roof.

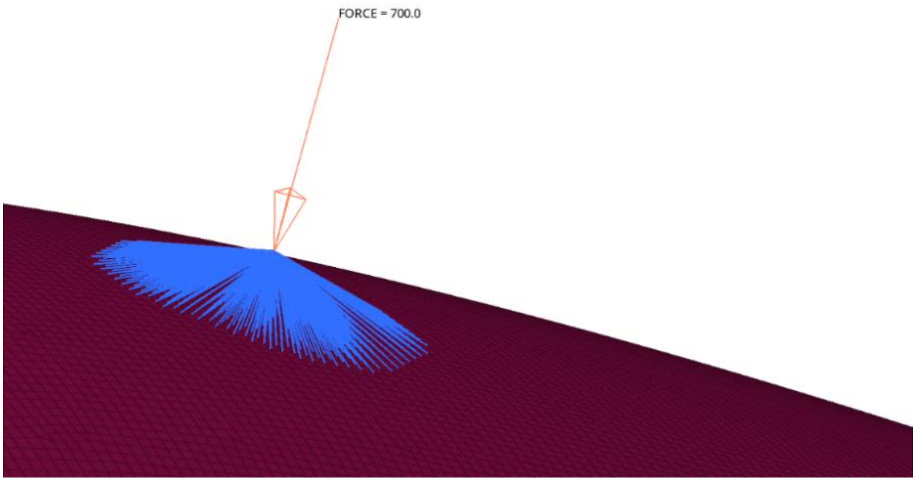

Figure 5-12 RBE3 elements for rollover force application

The setup of the model is shown in Figure 5-13. The replication of the exact final suspension kinematics is fundamental to carry on a proper simulation. The same happens in real test-bench experiments, where the suspensions are installed, substituting springs and rubber elements with stiff components, to assure the suspension transmits the loads during the test in the same way they act in real life conditions.

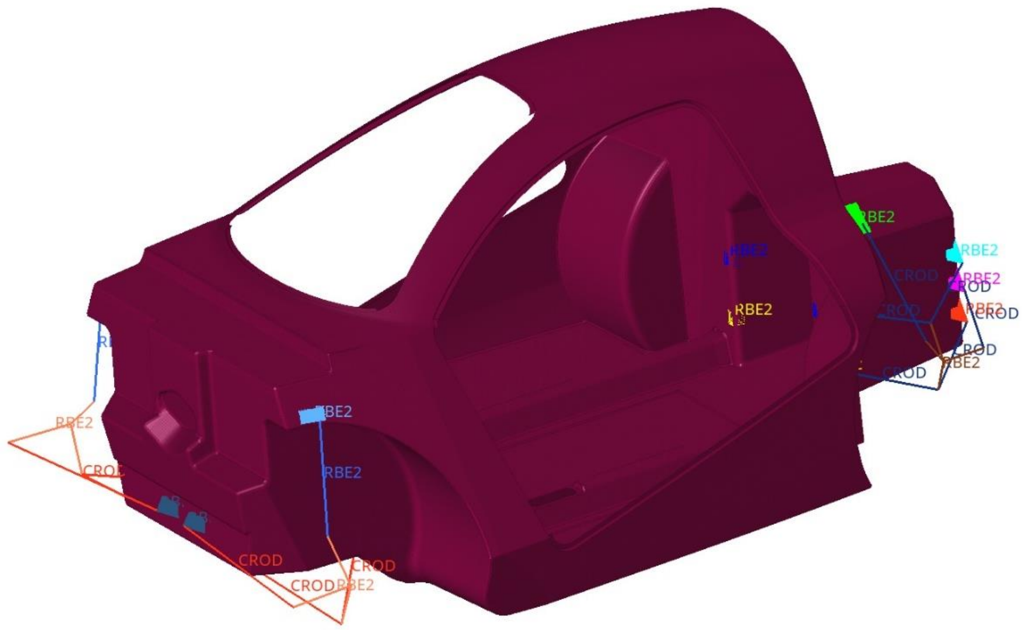

Figure 5-13 FEM simulation setup

The load cases are selected to analyse both strength and stiffness behaviour. Three critical cases are selected for the strength evaluation: Front Bump, Rear Bump and Rollover. On the other hand, talking about stiffness, the main important behaviours to be analysed are Torsion and Bending cases. In all the mentioned conditions, proper constraints must be selected to reproduce faithfully the real situation or experiment.

A) Front and Rear Bump

In the case of Front and Rear Bump, it is not convenient to set the constraints directly on the wheel hubs, instead, the "Inertia Relief" function is selected. In this case, the constraints are replaced by a counterforce applied to the centre of gravity of the passenger compartment which prevents the car from accelerating. In this way, a more realistic behaviour can be modelled. In Table 5-3 the load case of Front and Rear Bump is summarized.

Table 5-3 Front and Rear Bump load cases

Front Bump

	Front Left	Front Right	Rear Left	Rear Right
Loads	2280N (z direction)	-	-	-
Constraints	Inertia Relief			

Rear Bump

	Front Left	Front Right	Rear Left	Rear Right
Loads	-	-	2115N (z direction)	-
Constraints	Inertia Relief			

As explained in section 2.3.2, the Tsai-Wu criterion is adopted for the evaluation of the failure. In all the cases, the "Composite Failure" option is selected, and the reported quantities are referred to the layer with the maximum value (closer to failure) in the sandwich structure. In Figure 5-14 the Composite Failure map of the front bump case is represented.

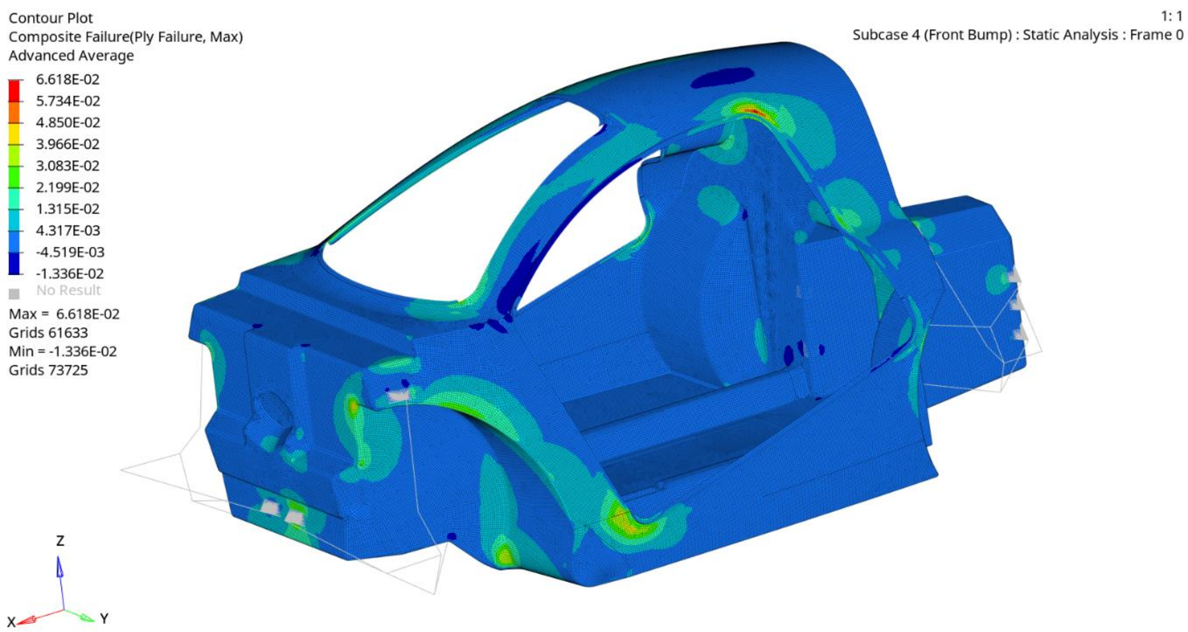

Figure 5-14 Front Bump Composite Failure

Considering the failure happens when the Composite Failure value reaches 1, it is evident the passenger cell is far from this condition in the case of a Front Bump. Similarly, in the case of a Rear Bump, the failure is far since the maximum value reported in the simulation is $5.3 \cdot 10^{-2}$, confirming the result obtained in the Front Bump load case. This last result is visible in Figure 5-15.

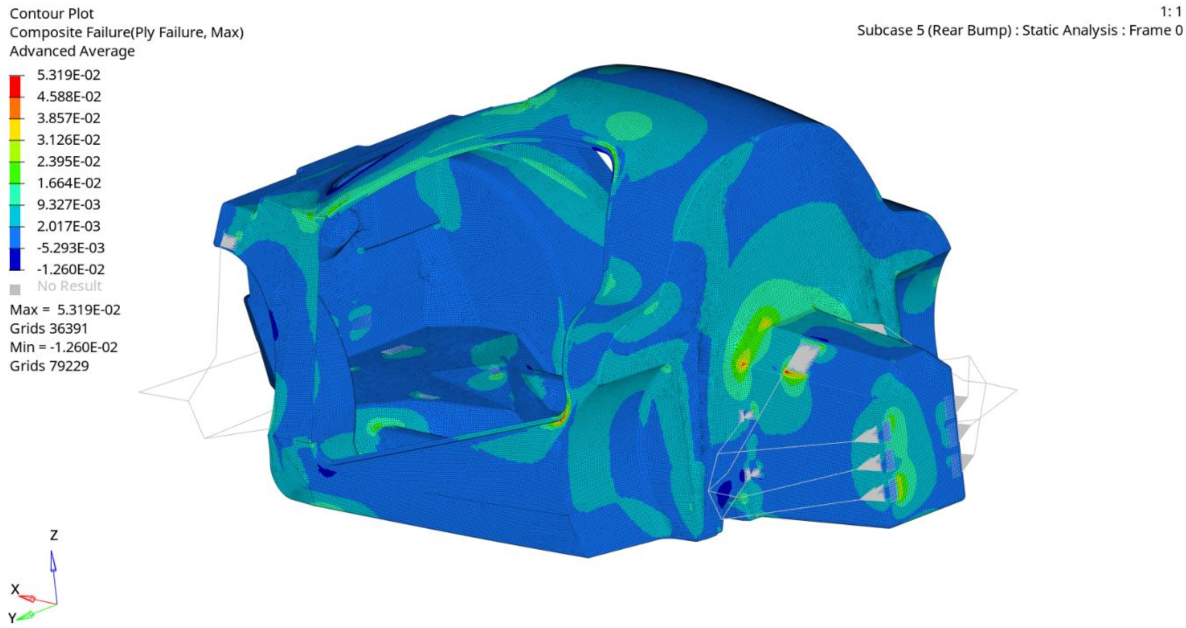

Figure 5-15 Rear Bump Composite Failure

It is particularly evident that one of the most critical regions in the case of Rear Bump is the interface region between the suspension box and the rest of the monocoque. In this area, the big change in geometry could lead to stress concentration but, thanks to the edge fillet introduced between the box and the wall and because of the low level of load at which the car is subjected, this geometry variation does not represent a problem.

In order to analyse the behaviour of the structure, the Composite Stresses can be evaluated. The stress map, expressed in MPa, of the Front Bump load case is reported in Figure 5-16. First of all, it is possible to highlight that the stress peaks are generally low and usually concentrated in specific areas. The most stressed points are the front left suspension attachment points, since the force is applied on the front left wheel hub, and some areas around the door opening contour. Indeed, the change of geometry in this area creates some stress concentration regions like in the upper rear corner of the door opening. In this part, a reinforcement is already present, but it could be supported, in the future evolution of the ply book, by other reinforcement plies.

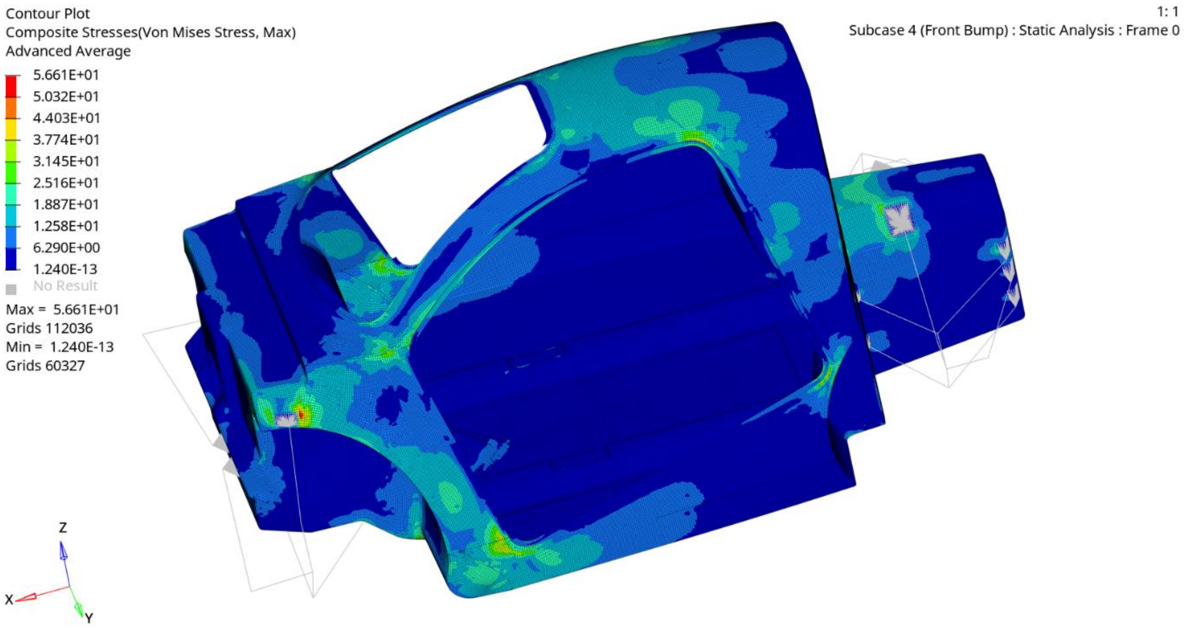

Figure 5-16 Front Bump Composite Stresses

B) Rollover

The other case, relevant from strength point of view, is the Rollover condition. As explained in section 3.1.2, 700N should be sustained by the roof without deformation or failure. Therefore, this load case can be seen as a direct implementation of the rule previously described. The Inertia Relief is used as constraint also in this situation. The overall load case setup is summarized in Table 5-4.

Table 5-4 Rollover load case

Rollover	
Loads	-700N (z direction) applied on the master node of the top spider structure
Constraints	Inertia Relief

Figure 5-12 shows the top spider structure and the 700N force while Figure 5-17 reports the result in terms of Composite Failure. As expected, the most critical area is the one in which the load is applied. Additionally, also some regions around the windshield and door opening contour are characterized by relatively high Composite Failure value. Nevertheless, also in this case, the passenger cell is far from failure with a peak value of $1.6 \cdot 10^{-2}$ which is representative of a condition far from criticalities. Analogously, also the stresses are generally low in the whole passenger cell with a peak value around 25 MPa.

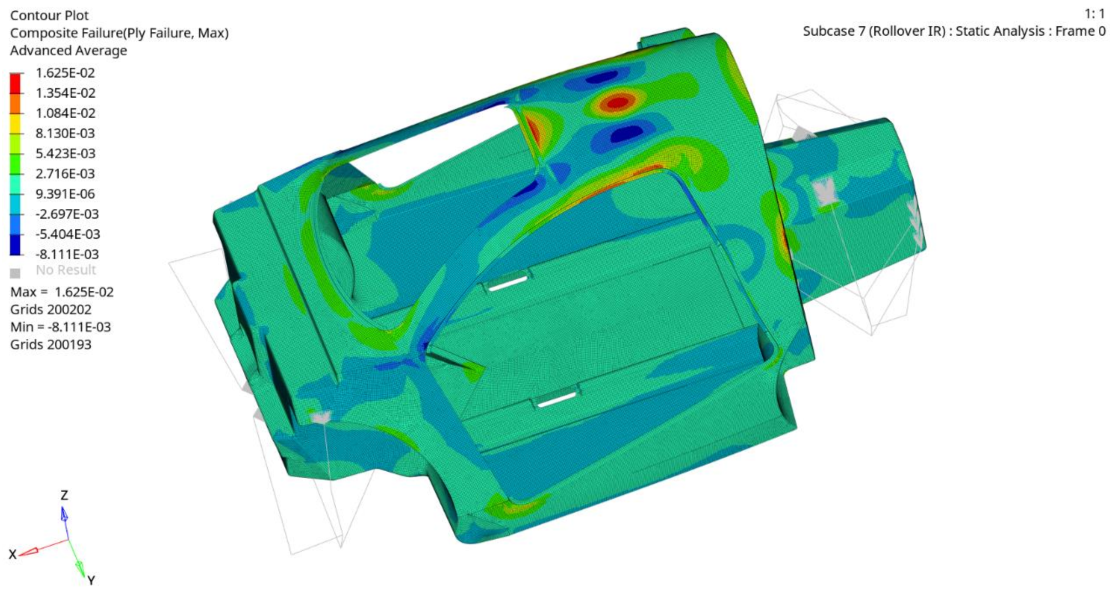

Figure 5-17 Rollover Composite Failure

C) Torsion

The following step is the analysis of the structure stiffness. The analysis of the stiffness allows to understand the level of deformation of the body during normal use conditions. The most common methods for the evaluation of body stiffness are the torsional and bending analysis. They are usually performed in FEM environment or by means of experimental tests. Generally, the stiffness results are influenced by the assembly stage of the vehicle, and, for this reason, different tests could be done to evaluate the stiffness contribution of the windshield and rear window, of movable parts, interiors, etc. In the case of MUC022 a single test will be performed since the windshield is not glued to the car and because of the lower number of modules to be mounted on the vehicle with respect to a traditional passenger car. The simulation in FEM environment is designed to reproduce the experimental test in terms of constraints and force application. In the case of Torsion, the rear cross beam of the test bench is connected to the wheel hubs. This beam is constrained to block all the displacements (xyz) on one end and the vertical movement (z) on the other end of the beam. At the front cross beam, the point of application of the force is left free while the other end is constrained to impair the vertical displacement (z) plus another direction (x or y). In this way, the rear cross beam can rotate around y axis while the front cross beam around the x axis (Morello, Rosti Rossini, Pia, & Tonoli, 2008b, p. 458). In Table 5-5 a summary of loads and constraints for the Torsion test is reported while in Figure 5-18 a top view of the model allows to observe the load case setup.

Table 5-5 Torsion load case

Torsion

	Front Left	Front Right	Rear Left	Rear Right
Loads	1000N (z direction)	-	-	-
Constraints	-	yz	z	xyz

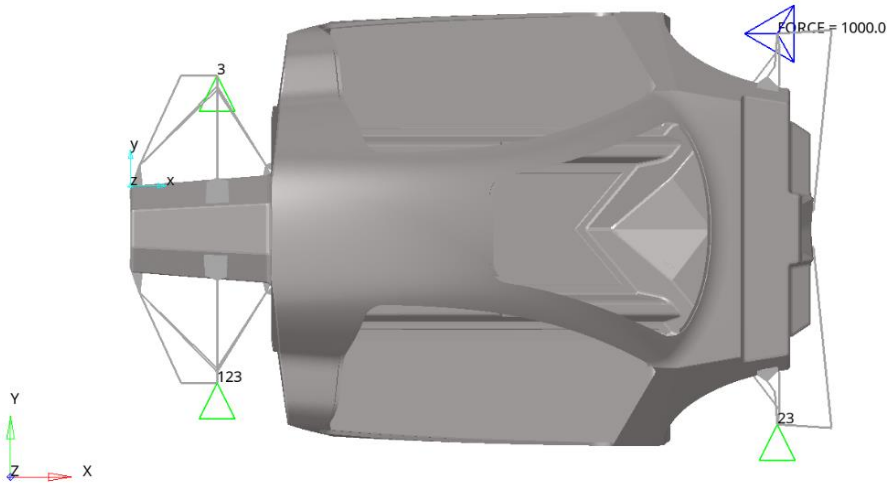

Figure 5-18 Torsion forces and constraints

The computation of the torsional stiffness of a structure is dependent on the displacement. Indeed, "the torsional stiffness is defined as the ratio between the torque load M_t and the relative rotation $\Delta\theta$ between the front and the rear axle" (Morello, Rosti Rossini, Pia, & Tonoli, 2008b, p. 458). This definition is summed up by Formula (5-1).

$$K_t = \frac{M_t}{\Delta\theta} \tag{5-1}$$

The relative rotation is directly computed from the displacement value at the level of the hub. For this purpose, the displacement of the structure in z direction, reported with a scaling factor which enhance the deformation of the monocoque, is shown in Figure 5-19. The scale on the left refers to the deformation in millimetres.

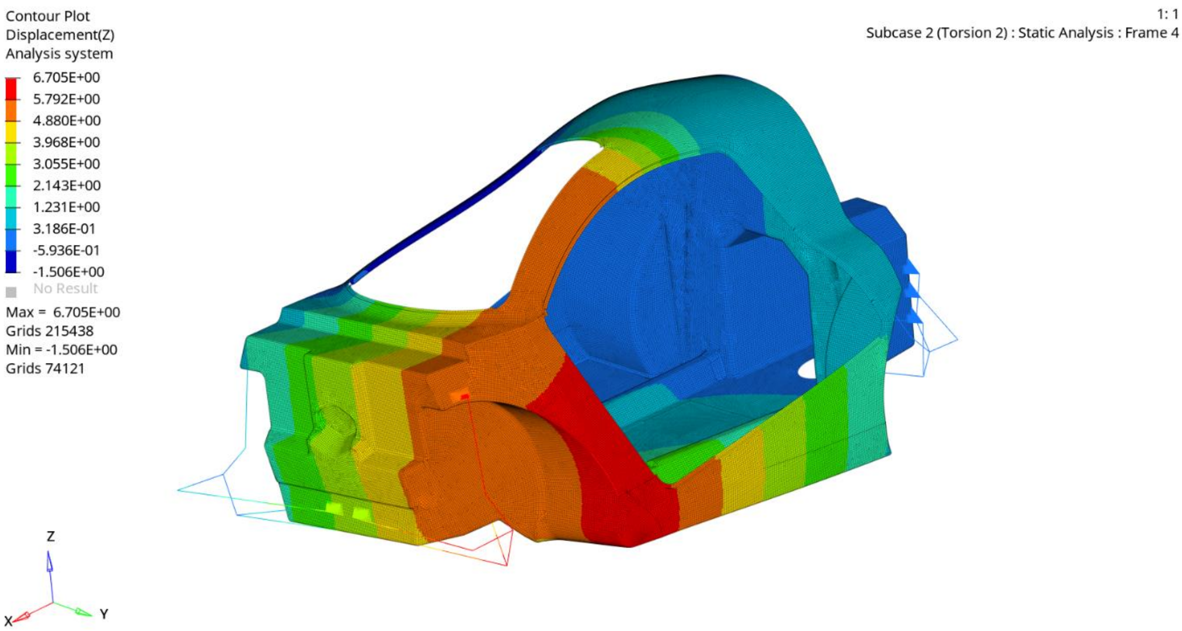

Figure 5-19 Torsion z displacement

The displacement of the front left wheel hub is 6.56mm while the other wheel hub displacements are null because of constraints. Since the torsional stiffness result is very low in absolute value if compared with passenger cars, a useful way to compare the outcomes according to vehicle type and category, is referring to the torsional stiffness divided by the mass of the structure.

The torsional stiffness referred to monocoque mass is computed according to Formula (5-2).

$$K_{t,mass} = \frac{M_t}{arctan\left(\frac{(z_l+z_r)_{front}}{t_1}\right)+arctan\left(\frac{(z_l+z_r)_{rear}}{t_2}\right)} \cdot \frac{1}{m_{monocoque}} = 8.22 \cdot 10^4 \; \frac{N \cdot mm}{kg \cdot rad} \qquad (5\text{-}2)$$

where t_1 and t_2 are respectively the front and rear track while $m_{monocoque}$ is the mass of the monocoque previously introduced.

D) Bending

A similar procedure can be followed for the computation of the bending stiffness. In the case of bending performances evaluated at the test bench, the four ends of the cross beams at the front and at the rear are connected to the bench. Nevertheless, it is allowed the rotation of the body around the two axes corresponding to the two axles. The load is applied through a cross beam in contact with the sills of the vehicle. This latter is usually placed at the middle of the wheelbase. It is worth mentioning that wood or similar materials can be used to distribute the load on the sills, with the purpose of avoiding stress concentration (Morello, Rosti Rossini, Pia, & Tonoli, 2008b, p. 458).

Also in this case, the real test in traduced in FEM simulation. The load is applied by means of RBE3 elements which simulate the presence of the cross beam in the middle of the wheelbase. Figure 5-20 reports the test layout in FEM environment.

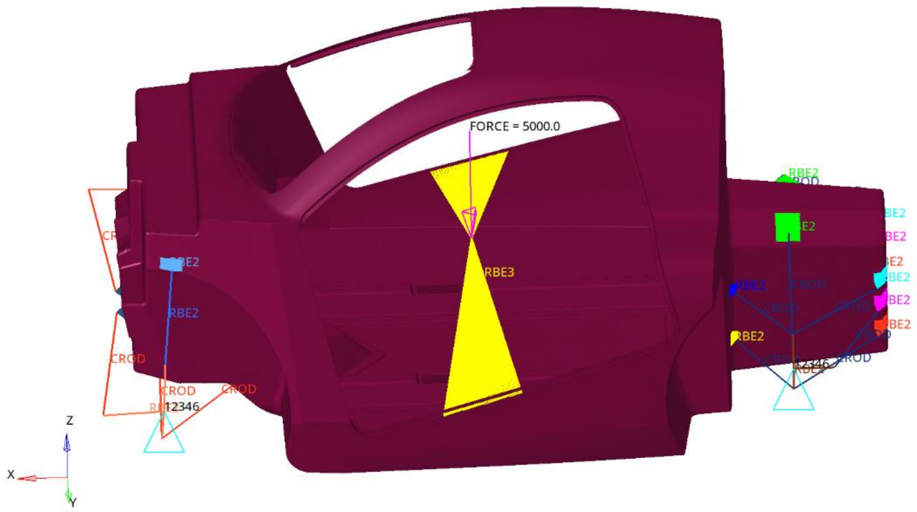

Figure 5-20 Bending load case model

Four constraints (one for each wheel hub) are applied to simulate the condition previously described. Therefore, only the rotation around the y axis is left free. A 5000N force is applied in the master node of the rigid structure simulating the beam. In Table 5-6 a summary of the load case is displayed.

Table 5-6 Bending load case

	Bending			
	Front Left	**Front Right**	**Rear Left**	**Rear Right**
Loads	-5000 N (z direction) in the master node of the spider simulating the central cross beam			
Constraints	xyz + x and z rotation	xyz + x and z rotation	xyz + x and z rotation	xyz + x and z rotation

The bending stiffness is defined as the ratio between the vertical force F and the resulting displacement Δz of the section where the load is applied. The following formula is used in case of experimental evaluation of the bending stiffness but can be adapted to a FEM analysis. (Morello, Rosti Rossini, Pia, & Tonoli, 2008b, p. 458).

$$K_b = \frac{F}{\Delta z} = \frac{F}{z_F - (z_f \cdot d_2 + z_r \cdot d_1)/l} = 1.72 \cdot 10^3 \frac{N}{mm} \tag{5-3}$$

where

- z_F is the displacement of the central cross beam used to apply the force;
- d_1 is the distance front axle-cross beam;
- d_2 is the distance rear axle-cross beam;
- l is the wheelbase;
- z_f is the vertical displacement of the front axle;
- z_r is the vertical displacement of the rear axle.

z_f and z_r are included in the formula to compensate the compliance of the test bench. Obviously, they are null in this case. d_1 and d_2 are both 775mm since the beam is placed in the middle of the wheelbase. z_F value is equal to 2.94mm and is directly derived from the simulation. The deformation of the monocoque after the Bending test is displayed in Figure 5-21. A scaling factor is used to enhance the passenger cell deformation.

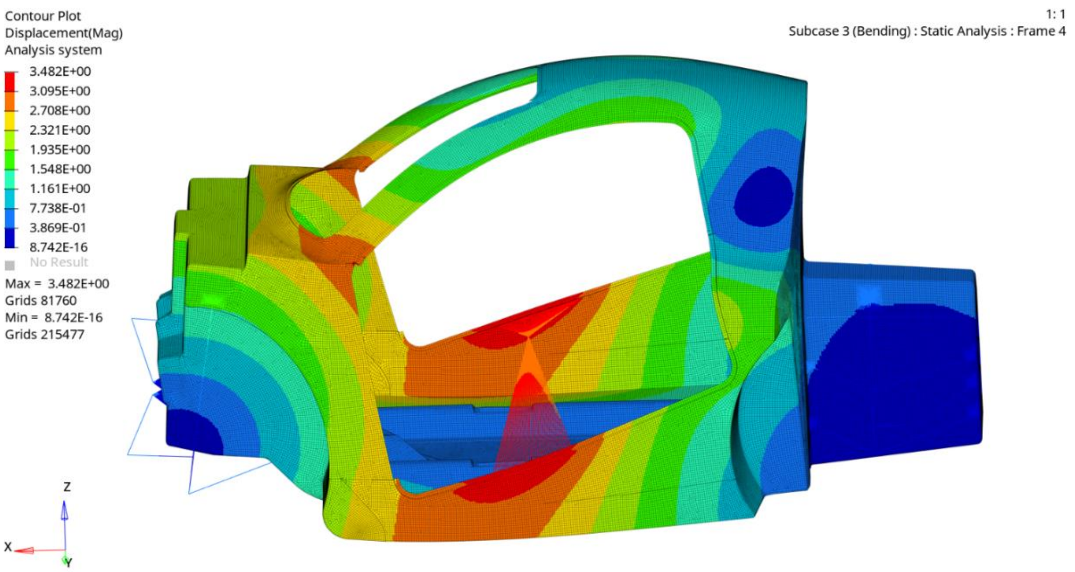

Figure 5-21 Bending deformation

5.3 Manufacturability and Moulds Design

The design must be validated also through the selection of a proper production process. The designed part has to respect manufacturability standards to be effectively produced. The manufacturing process and the assembly techniques are presented in this section.

5.3.1 Production Process and Moulding Layout

The manufacturability evaluation and production process selection are essential steps during the design of a product. In the case of MUC022 several techniques have been evaluated for the realization of the car. Generally, polyurethane (PU) moulds are milled according to the negative of the final product and directly laminated in case of non-structural parts. Nevertheless, it is not usually possible to reach high temperature directly with the use of PU moulds. For this reason, CFRP tools are generally preferred for monocoque production phase. They must reproduce the negative of the monocoque to be laminated. For the production of CFRP tools, PU moulds, designed as the positive of the vehicle, should be used. Also in this case, the temperature resistance and the strength of PU moulds is a limiting factor to be evaluated in relation to the necessities of the carbon fibre moulds curing cycle. For this evaluation, the density of the PU material is usually assessed as discerning factor. On the other hand, the CFRP fabrics for tool production are usually dedicated products with a density around 600g/m^2. As previously mentioned, different production layouts could be implemented in relation to performance and cost targets. A first possibility is the production of the final monocoque in two parts to be joined together by means of glue or bolts. This solution has a big advantage in terms of reduction of complexity, but the final mass is generally higher and the joining point in the structure creates a weak point, worsening structural performances. For these reasons, this option was discarded. Another possibility is the creation of the monocoque in a single part but exploiting several CFRP moulds joined together and separately extractable. In this way, a moulds combination can be found to avoid undercuts which, inevitably, characterize a solution with a single mould. Figure 5-22 shows the main steps characterizing this solution.

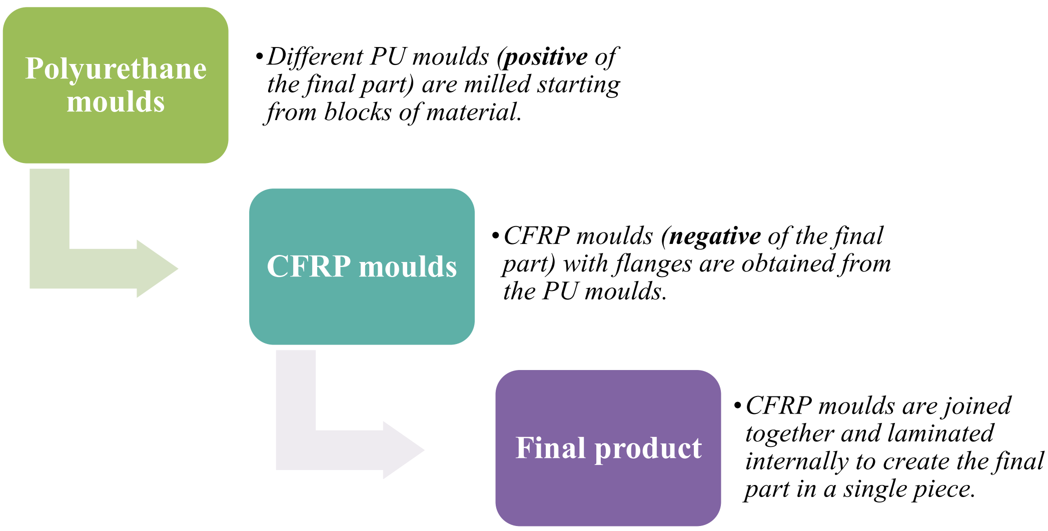

Figure 5-22 Production process steps

In this way, the final part is lighter and without problems of material continuity since the passenger cell would be a stand-alone structure. Consequently, this solution was selected as production process and the geometry adapted to its requirements.

Indeed, draft angles more than 2-3° are required to properly extract the moulds. Furthermore, to simplify the machining and to enhance the flexibility of the design, the PU moulds can be made up of different elements. In fact, detachable panels can be joined to the main PU moulds by means of screws and pins to realize small draft angles or undercuts. This is the typical solution adopted for the lamination of the flanges around CFRP moulds.

CFRP moulds present flanges which are used to locate bolts and pins necessary to join the different tools. Once they are bolted together, a big mould reproducing the negative of the car is obtained. This latter will be then laminated according to predefined ply book directives. The result is then prepared and put in the autoclave where the curing cycle can be performed. The last step regards the extraction of the CFRP moulds which can be removed singularly.

In Figure 5-23 it is possible to see a picture of the blocks used for the milling of one of the PU moulds of MUC019.

Figure 5-23 Polyurethan blocks used in MUC019 project (TUfast, 2018)

The blocks in PU material are sold according to standard dimensions. After PU mould design, the blocks are selected in relation to the geometry and, before milling, they are glued together to prepare the base for the machining.

The CFRP moulds can be realized following several carbon fibre lamination procedures as explained in section 2.3.3. The VAP® process is a valid option since it is cheaper than pre-pregs, but it is more challenging in case of complex surfaces. In general, also considering the final surface quality, pre-pregs must be preferred if the budget allows to. Therefore, in the case of MUC022, the pre-preg methodology is selected also for the realization of the CFRP tools.

A description of the splitting layout of the monocoque is required to highlight the design features introduced to comply with the manufacturing process. The monocoque is divided in 7 moulds, defined following the best compromise between complexity and surface geometry. In particular, the front is divided in an upper and lower mould, while the rear is realized in a single mould. Furthermore, there are two side moulds, a roof mould and a floor mould. Figure 5-24 is useful to visualize the splitting planes used to derive the 7 moulds.

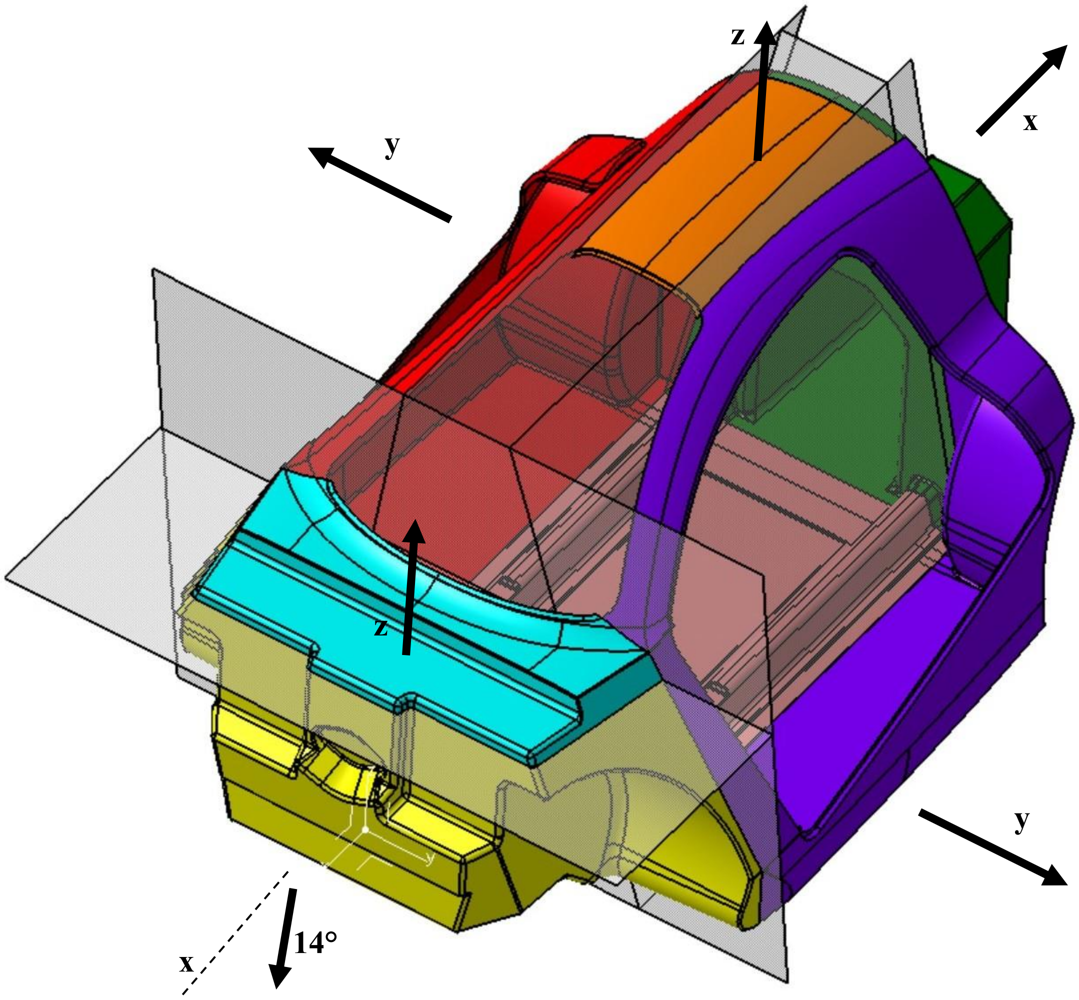

Figure 5-24 Moulds split (front)

Together with the planes of the moulds, also the extraction direction should be defined. In Figure 5-24 the directions are represented by means of black arrows. They are generally aligned with the xyz axes of the vehicle reference system. Only the front lower mould presents a specific direction (14° with respect to x axis) to maintain a more articulated geometry without the need of creating additional draft angles and inclined surfaces. The extraction direction of the floor is according to z axis as depicted in Figure 5-25.

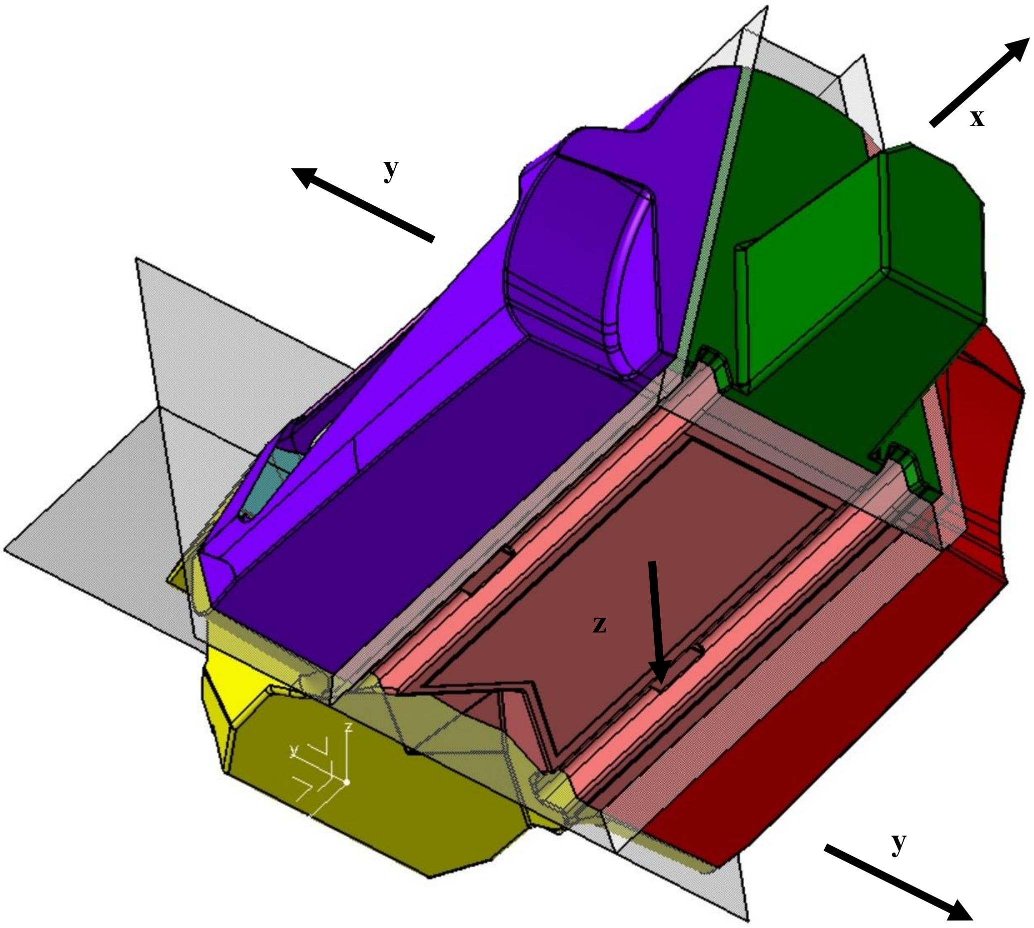

Figure 5-25 Moulds split (rear)

The geometry of the monocoque is directly influenced by the necessity of creating draft angles for the correct extraction of the CFRP moulds. An example is the rear wheelhouse which is part of the side mould. Since it must be extracted in y direction, the wheelhouse has a conical shape towards the exterior of the car in order to create a draft angle. The same happens for the rear suspension box which is characterized by inclined planes with the purpose of facilitating the rear mould extraction in x direction. Additionally, the two tunnels enlarge at the rear of the car for the same reason.

The floor of the car is not completely flat since the part of the bottom surface belonging to the side mould requires a draft angle. Indeed, it present an inclination of 3° as it is possible to observe in Figure 5-26. Moreover, it is important to specify that the moulds split layout is strongly influenced by the necessity of realizing a vehicle width which reduces passing from the bottom of the car to the top part. This shape variation leads to the definition of sloped planes for the side moulds.

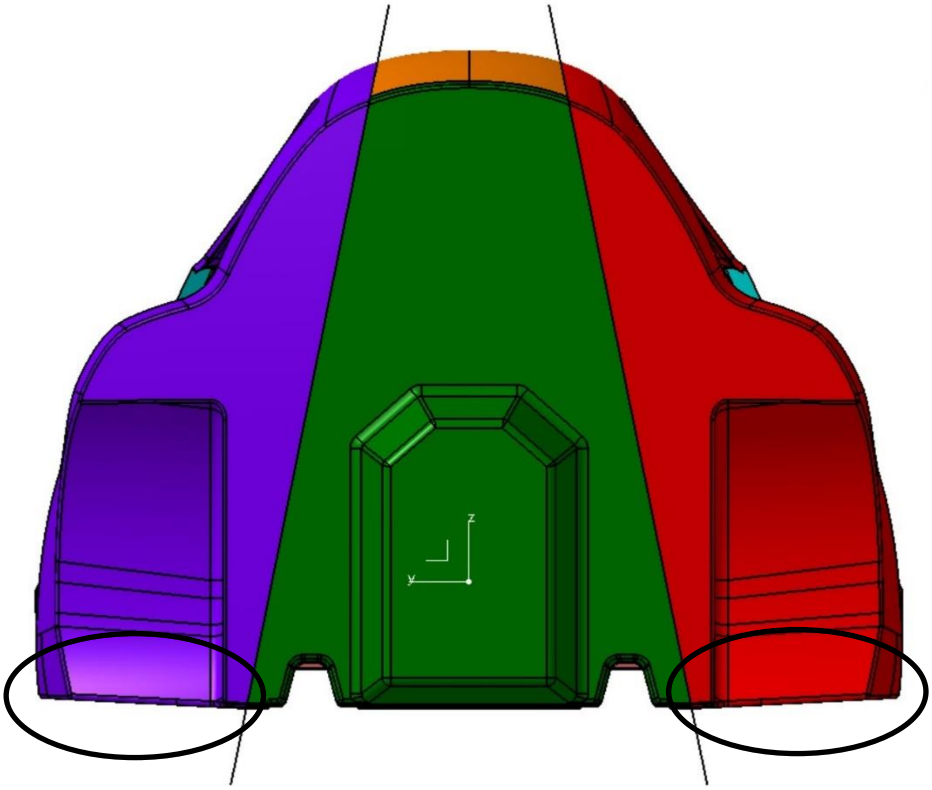

Figure 5-26 Rear moulds split

5.3.2 Interfaces and Standard Components Selection

The management of the interfaces with the various components and systems of the vehicle is a crucial step since, if previously included in the moulds design, allows to simplify and improve the assembly of the various parts. More than 50 interfaces are designed together with the related joining techniques and standard components. One of the most important interfaces, the one with the suspension system, was already introduced in section 5.1. In the case of the suspension mounts, the advanced state of development of this system allowed to precisely select the location and the dimension of the holes on the monocoque. On the contrary, for many other modules, a complete design was not ready during the interface freeze period; therefore, a detailed study with the various sub-teams was required to define holes which can flexibly fit the final components design.

Three main joining techniques will be used for the connection of the different parts. They follow the setup of MUC019:

- Hitsert2® + carbon fiber insert;
- Bolts + aluminium insert;
- Helicoil® + aluminium insert.

An insert in the sandwich structure is required to avoid stress concentration in the composite, in particular in the case of critical connections like suspensions mounts. The use of inserts is usually coupled with other products, designed to offer threaded connections.

The first technique (Hitsert2® + carbon fiber insert) is used in case of connections where a low amount of force is developed. It is the case of control panels, fenders and belly pans. The carbon fiber insert is associated with a product by Böllhoff called "Hitsert2®". This latter is a thread insert which is thermally installed into the part. It is heated and, during the insertion, the plastic around the product is plasticized (Böllhoff, n.d.). Figure 5-27 shows a section view of Hitsert2® joined with a component.

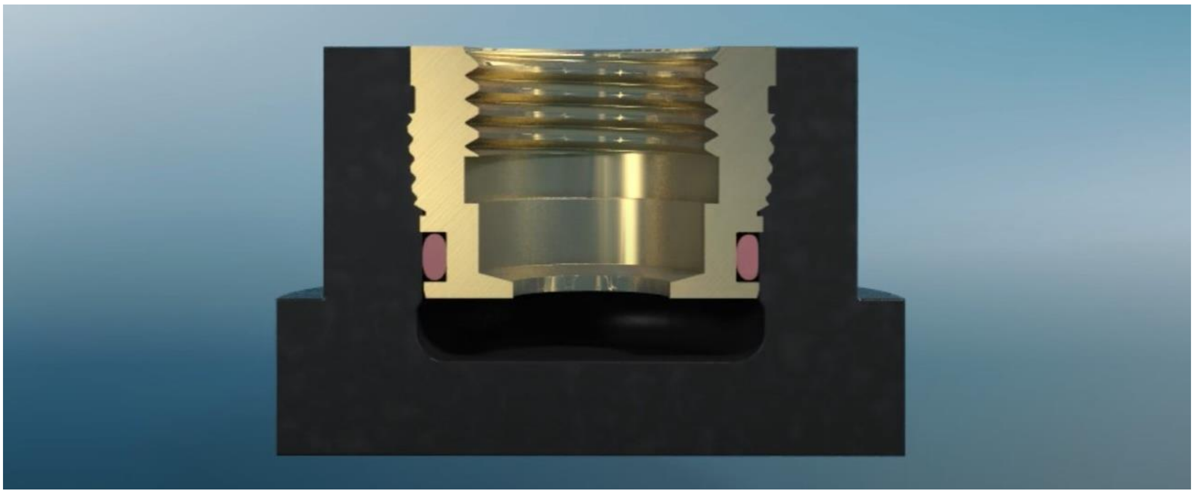

Figure 5-27 Hitsert2® (Böllhoff, 2013)

The second joining option is realized through a bolt coupled with an aluminium insert. Aluminium inserts are used instead of carbon fiber inserts when the load at which the composite is subjected is higher. It is the case of suspension mounts, steering system attachment regions, brake pedal, etc.

The third joining option is used, also in this case, when a high load is expected but where there is no space to place the nut and to properly screw it. It is the case of the lower screws of the front upper suspension mounts. In this case there is no space for the head of the bolts so the "Helicoil®" product by Böllhoff is used together with an aluminium insert. The Helicoil® is used as reinforcement where low strength materials, like aluminium, are used. In order to insert it, a threaded hole is required. In Figure 5-28 the Helicoil® Classic Free Running is shown.

Figure 5-28 Helicoil® Classic Free Running (Böllhoff, n.d.)

Generally, if the space allows to place a bolt instead of a Helicoil®, it is always preferred since the complexity of the manufacturing process is reduced and the performances of the connection improved. This is due to the fact that the bolt is compressing the sandwich structure of the laminate, reducing the probabilities of delamination.

The need of designing all the interfaces and related holes at this level of development, is due to the manufacturing technique adopted for the creation of the holes of the monocoque. In fact, the lamination is performed around a pin positioned where the hole should be. In this way, it is possible to avoid a subsequent cut which would interrupt the material continuity. Furthermore, in this way it is possible to precisely locate the hole and the relative insert. Obviously, the PU moulds must already include the holes locations through the presence of holes in the mould where pins are inserted. These latter are then matched with draw bushes laminated inside the CFRP mould. So doing, the location is "transferred" from the first mould to the second one.

The pins and draw bushes standard dimensions should be selected to choose the correct holes depth in the PU mould. Only specific dimensions are available depending on the producer and standards prescriptions. In particular, draw bushes are based on DIN 172 while the pins on DIN 7979 D/ISO 8735 A.

5.3.3 Polyurethane Moulds Design

The seven PU moulds are designed using CATIA V5 in the "Part Design" mode. They are derived from the monocoque model through links between CAD files available thanks to CIM database. The holes defined during the interface design are included in the foam models. They are obtained directly exploiting the location and direction of the bolt defined in the monocoque file. In Figure 5-29 the roof mould is reported. This latter is exploiting 3 detachable panels for the creation of the CFRP mould flanges. It is also possible to observe the holes for the connection of camera, GPS and for cable routing.

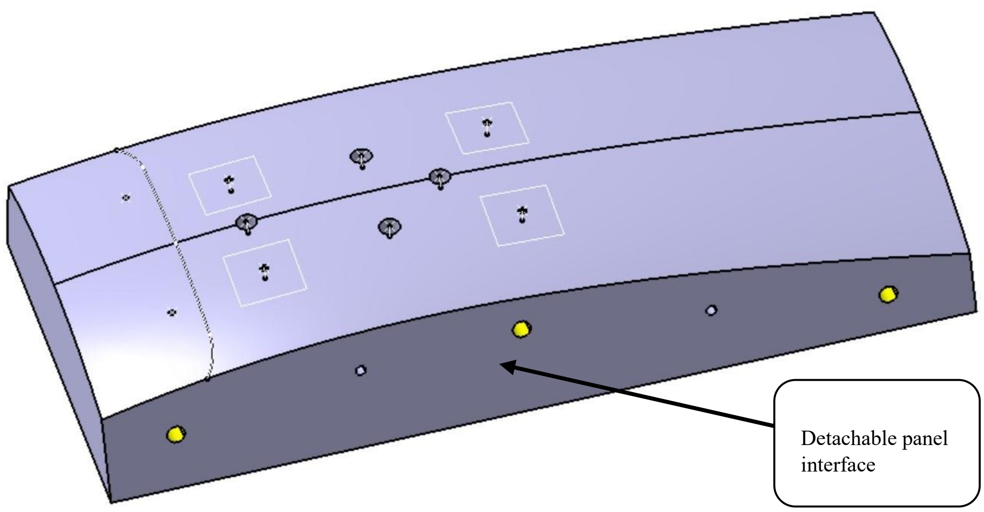

Figure 5-29 Roof mould

The panels to be joined to the mould are made up of PU material and are connected through screws and pins. The pins have a diameter of 8mm while the screws are of M10 type. For the connection of the screws, a threaded element between mould and screw should be inserted. They are called "Mubux" and are characterized by an external and internal thread. The outer one is connected to the threaded hole directly present on the PU mould while the internal one is used to screw the M10 screw for the connection of the panel. The Mubux (and relative hole) technical drawing is depicted in Figure 5-30. As reported in the picture, the external thread on the mould should be a M14 to host a M10 Mubux.

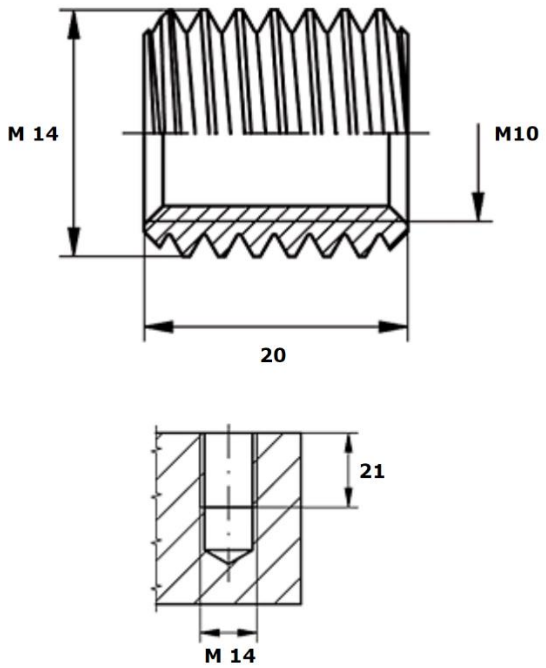

Figure 5-30 Mubux and related hole technical drawing

The other particularity of the mould design regards the presence of the so called "scribelines". They are profiles, realized as changes in geometry or as small steps, used to put in evidence a specific curve which indicates exactly where a cut of the final part must be realized. In the case of MUC022 they are used to indicate the contour of the door opening and of the windshield. Additionally, a scribeline, with an ellipse shape, is included in the lower part of the suspension box. This is done to have a backup option in case the lamination of the rear suspension box is not feasible without a close access point. Indeed, in case of problems, the scribeline can be used as reference to create an opening in this area. The scribeline is created in CAD environment as a simple curve and it is realized by the milling machine according to the possibilities of the tool. In Figure 5-31 it is shown the rear moulds with the scribeline for the backup opening. This mould, because of the rear suspensions connections, presents a high number of holes and interfaces.

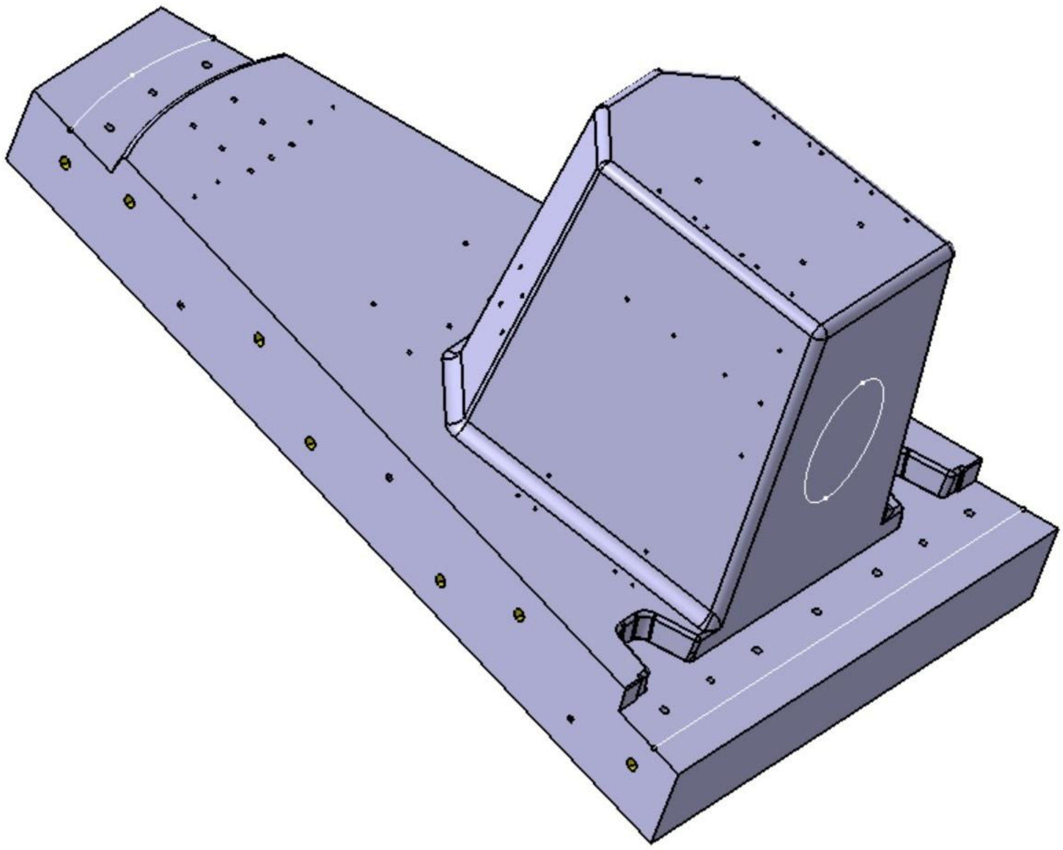

Figure 5-31 Rear mould

For the realization of the holes on the CFRP moulds flanges, a sequence of 1 pin every 5 bolts is selected. Indeed, for the assembly of the 7 CFRP moulds, bolts are required to assure a stiff connection. However, they are not enough to guarantee a proper alignment, therefore, pins are introduced. To obtain the location of these holes in the final CFRP tools, they must be included also in the PU moulds. In particular, these holes are located in the areas around the PU mould body when the flanges are realized directly using the mould. On the contrary, these series of holes are on the detachable panels when these latter are used to create the flanges. This contour of bolts and pins is placed at 30 mm from the part itself and, as for the detachable panels connection, the pins for alignment have a diameter of 8mm while the bolts are M10. In Figure 5-32 it is possible to observe the front lower mould. In this case a detachable panel is placed on the upper part while the other flanges are realized exploiting the plane of the mould itself. Also this part is characterized by a high number of interfaces because of the connections on the front firewall and because of the presence of the front suspension system.

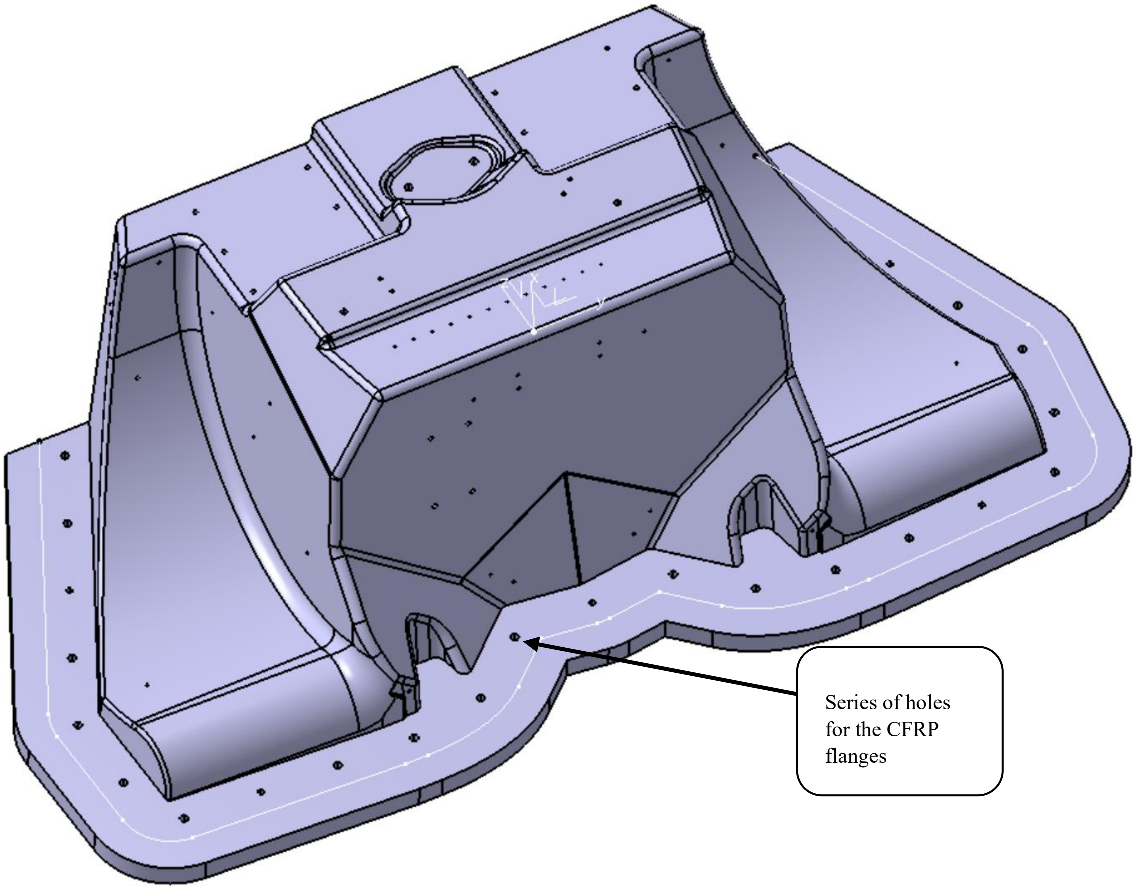

Figure 5-32 Front lower mould

6 Conclusion

6.1 Summary

The relation between car body and efficiency is investigated in this research. This is driven by motivations linked to the current automotive trends, which are mainly related to reduction of fuel consumption and optimization of battery electric vehicles. This research effectively started with the preliminary analysis of the rules of the competition, included in Chapter 3. The requirements coming from Shell must be matched with the efficiency targets in terms of weight and aerodynamics which influence the product final design. On the other hand, also the constraints set by structural requirements are an important input for the design process, since they fix boundaries during the concept decision phase. For this purpose, a preliminary evaluation of the loads on the structure has been developed.

The solution to the problem of the creation of an efficient body structure is presented and discussed in terms of aerodynamics, structural integrity and manufacturability. To reach these objectives, a concept decision phase is required to have an overview of the product in terms of systems layout and location. Indeed, the monocoque is interfacing with all vehicles modules and must be designed around their necessities. The two main outcomes of the work, the outer body shell and the monocoque, have been shown and described in detail to point out the validity of the methodology behind the research. The outline of the vehicle is mostly influenced by aerodynamics. Additionally, all the already stated boundary constraints have been considered and assessed during the CAD model creation to comply with the rules. The style of the car does not represent a priority, but it is taken into account to offer a lean and futuristic appearance. The design of the outer body shape has been validated through an aerodynamic analysis and related simulation (CFD). To give strength to the result, a comparison with the old model has been carried out, pointing out the differences and the improvements. About the half of the aerodynamic resistance has been eliminated thanks to the new design.

From the outer body concept, a layout for the body split has been selected and implemented through the division in the three modules: front, monocoque and rear. The most important and challenging part, the monocoque, is derived according to packaging directives and structural requirements. The structure has to guarantee the right accessibility while assuring stiffness and strength. The design has been validated through a FEM analysis which shows results in line with expectations, confirming the feasibility of the solution. Finally, the manufacturing process is designed and described. The manufacturability is assured through the creation of draft angles and shapes in line with production passages. The interfaces setting and related standard elements selection is described in the last part of the dissertation, showing the details of the final PU moulds.

In conclusion, it is possible to affirm that the goal related to the optimization of the car body in favour of efficiency is reached. The mass of the monocoque is in line with the expectations and the aerodynamic drag strongly reduced. At the same time the rules are respected, and the structural integrity of the vehicle assured.

6.2 Outlook

The research described in this dissertation goes beyond the creation of the vehicle body for the MUC022. Indeed, the outcomes of this research can be transferred to similar projects, optimizing the body structure by means of the same methodology and approach.

At the same time, the results shown in this work can be a starting point for future improvements. The assembly process will be developed on the basis of the body layout introduced in this research, can be an important source of information to define protocols and standardized solutions to be recovered for new TUfast Eco models. Analogously, bad practices can be categorized to be avoided in the future.

The aerodynamic results are already appreciable but there is room for future improvements. Indeed, with the setup of a dedicated simulation sub-team, more detailed iterations can be exploited for an improved optimization and validation of the outer body surfaces.

The monocoque geometry and the stacking sequence layout introduced in this work represent a starting point for other studies focused on the optimization of the plies and on the creation of a detailed ply book. A further reduction of monocoque mass can be achieved while maintaining, or improving, the stiffness and strength targets.

An advanced modification of the geometry could lead to a simplification of the ply layout, reducing the reinforcement regions and, consequently, further reducing the monocoque mass. This goal can also be achieved coupling the geometry modification with a variation of rear suspension setup. A redesign of the rear monocoque region, with a potential enhancement of rear packaging flexibility, could be obtained passing from a double wishbone to other suspension types.

At the end of this work, the described solutions will be implemented by TUfast Eco Team for the creation of the real car. Furthermore, modifications could be developed in the near future to improve, or adapt, the design to unplanned manufacturing requirements. After the assembly of the car, a testing period will be exploited to further refine the final outcome and to compensate for eventual production defects.

7 List of Figures

8 List of Tables

9 List of Abbreviations

CAD	Computer-Aided Drafting
CAE	Computer-Aided Engineering
CAM	Computer-Aided Manufacturing
CFD	Computational Fluid Dynamics
CFRP	Carbon Fiber Reinforced Plastic
DIN	Deutsches Institut für Normung
FEM	Finite Element Method
FIA	Fédération Internationale de l'Automobile
MUC	Munich Urban Concept
LED	Light Emitting Diode
PU	Polyurethane
RBE2	Rigid Body Element type 2
RBE3	Rigid Body Element type 3
SAE	Society of Automotive Engineers
SEM	Shell Eco-marathon
VAP	Vacuum Assisted Process
VIP	Vacuum Infusion Process

10 Bibliography

Auxibito. (n.d.). *Home*. Retrieved August 15, 2021, from Auxibito: Auxibito.in

Belingardi, G. (2021). *Lecture on Design of Lightweight and composite structures - Intro [Lecture slides]*. Politecnico di Torino, Turin.

BMW. (2013, July 29). *The BMW i3*. Retrieved 08 15, 2021, from BMW Group: https://www.press.bmwgroup.com/global/article/detail/T0143924EN/the-bmw-i3?language=en

Böllhoff (Director). (2013). *HITSERT® 2 – thread insert with sealing ring* [Motion Picture]. Retrieved August 22, 2021, from https://www.youtube.com/watch?v=vXWGyXbwCdE

Böllhoff. (n.d.). *Thread creation*. Retrieved August 22, 2021, from boellhoff: https://www.boellhoff.com/tr-en/products-and-services/special-fasteners/thread-inserts-amtec.php

Böllhoff. (n.d.). *Thread reinforcement*. Retrieved August 22, 2021, from Böllhoff: https://www.boellhoff.com/gb-en/products-and-services/special-fasteners/thread-inserts-helicoil.php

Chunguang, W., Shiquan, G., Mingyu, S., Zhirong, J., & Baomin, H. (2019, February 3). Comparative Study of Vortex-Induced Vibration of FRP Composite Risers with Large Length to Diameter Ratio Under Different Environmental Situations. 24. doi:https://doi.org/10.3390/app9030517

Composyst. (n.d.). *VAP® stands for Vacuum Assisted Process.* Retrieved August 16, 2021, from Composyst: https://www.composyst.com/en/vap/#layup

Daimler. (2021a, August 24). *The new EQS[1] : the main points at a glance*. Retrieved from Daimler: https://media.daimler.com/marsMediaSite/en/instance/ko/The-15-biggest-innovations.xhtml?oid=49578620

Daimler. (2021b, April 15). *The new EQS: Aerodynamics*. Retrieved August 16, 2021, from Daimler: https://media.daimler.com/marsMediaSite/en/instance/ko/The-new-EQS-Aerodynamics.xhtml?oid=49581781

Daimler. (2021c, April 15). *EQS*. Retrieved August 16, 2021, from Daimler: https://media.daimler.com/marsMediaSite/instance/ko.xhtml?relId=1001&fromOid=48613391&resultInfoTypeId=172&styleId=5001&viewType=grid&sortDefinition=PUBLISHED_AT-2&oid=48613391&thumbScaleIndex=1&rowCountsIndex=5#toRelation

D'Ambrosio, S. (2020). *Lecture on Propulsion systems and their applications to vehicles - Engine-vehicle matching [Lecture slides]*. Politecnico di Torino, Turin.

Federation Internationale de l'Automobile. (2018, September). Guide and installation specification for Hybrid & Hybrid Pro devices in racing competition.

Genta, G., & Morello, L. (2008a). *The Automotive Chassis Volume 1: Components Design.* Springer. doi:10.1007/978-3-030-35635-4

Genta, G., & Morello, L. (2008b). *The Automotive Chassis: Volume 2: System Design.* Springer. doi:10.1007/978-3-030-35709-2

Gurit. (n.d.). *Gurit Guide to Composite*. Retrieved August 16, 2021, from Gurit: https://www.gurit.com/prepregs

Hucho, W.-H. (Ed.). (1987). *Aerodynamics of Road Vehicles.* Butterworth-Heinemann Ltd.

Mills, A. J., Hamilton, A. W., Gillespie, D. I., Andonovic, I., Michie, Craig, . . . Tachtatzis, C. (2020). Identifying Defects in Aerospace Composite Sandwich Panels Using High-Definition Distributed Optical Fibre Sensors. 13. doi:10.3390/s20236746

Morello, L., Rosti Rossini, L., Pia, G., & Tonoli, A. (2008a). The Automotive Body - Volume I: Components Design. Springer. doi:10.1007/978-94-007-0513-5

Morello, L., Rosti Rossini, L., Pia, G., & Tonoli, A. (2008b). *The Automotive Body: Volume II: System Design.* Springer. doi:10.1007/978-94-007-0516-6

Nettles, A. T. (1994, October 1). Basic Mechanics of Laminated Composite Plates. *NASA Reference Publication 1351*. Alabama, United States: NASA.

Performance Composites. (n.d.). *Vacuum Infusion Process (VIP) Guide*. Retrieved August 16, 2021, from Performance Composites: https://www.performancecomposites.com/about-composites-technical-info/125-resin

Plascore. (n.d.). *PAMG-XR1 5052 Aluminum Honeycomb (datasheet)*.

Rimac (Director). (2020a). *Rimac Nevera Monocoque - Daniele Giachi, Director of Vehicle Engineering and Chief-Engineer* [Motion Picture]. Retrieved from https://www.youtube.com/watch?v=QdxM4GOzXxI

Rimac. (2020b, December 21). *Media Galleries*. Retrieved August 15, 2021, from Rimac Automobili: https://www.rimac-automobili.com/media/gallery/?category=manufacturing&type=image

Scattina, A. (2020). *Lecture on Body and interiors components design - Materials and technologies [Lecture slides]*. Politecnico di Torino, Turin.

Scopione. (n.d.). *"Carbon Fiber" Terminology*. Retrieved August 16, 2021, from Scopione: https://scopione.com/terminology/

Shell. (2020). SHELL ECO-MARATHON 2021 OFFICIAL RULES CHAPTER 1. Retrieved from https://www.makethefuture.shell/en-gb/shell-eco-marathon/global-rules

Shell. (n.d.). *2020 Virtual Programme*. Retrieved August 24, 2021, from Make the future: https://www.makethefuture.shell/en-gb/shell-eco-marathon/virtual-programme

Shell. (n.d.). *How it works*. Retrieved August 15, 2021, from Make the future: https://www.makethefuture.shell/en-gb/shell-eco-marathon/how-it-works

Shell. (n.d.). *Track competitions*. Retrieved August 15, 2021, from Make the future:

https://www.makethefuture.shell/en-gb/shell-eco-marathon/competitions

Sudarisman. (2009, December). *Flexural Behaviour of Hybrid Fibre-Reinforced Polymer (FRP) matrix composites*. (Doctoral dissertation, Curtin University).

Thermo Analytics. (n.d.). *CAE Coupling*. Retrieved August 15, 2021, from Thermo Analytics: https://www.thermoanalytics.com/cae-coupling

Toray. (2018, April 13). *T300 Technical Datasheet*. Retrieved August 20, 2021, from toraycma: https://www.toraycma.com/products/carbon-fiber/

Trans-Textil GmbH. (n.d.). *VAP®: Membrane-assisted low-pressure infiltration*. Retrieved August 16, 2021, from Trans-Textil: https://www.trans-textil.de/en/applications/vap-process/

Tsai, S. W., & Wu, E. M. (1972, August). A General Theory of Strength for Anisotropic Materials.

TUfast. (2018). [Polyurethane blocks used in MUC019 project]. Retrieved from TUfast database

TUfast. (2018, November 2). *TUfast Eco Team Twitter account*. Retrieved August 15, 2021, from Twitter: https://twitter.com/tufast_eco/status/1058388668027715585

TUfast. (2019). *muc019*. Retrieved August 15, 2021, from TUfast Eco: https://tufast-eco.de/project_muc019=en.html

TUfast. (n.d.). *About TUfast*. Retrieved August 15, 2021, from TUfast Racing Team: https://tufast-racingteam.de/about-tufast/

Volkswagen. (2018, June 30). *XL1 (Archive)*. Retrieved August 16, 2021, from Volkswagen Newsroom: https://www.volkswagen-newsroom.com/en/images/albums/xl1-archive-2096

Volkswagen. (n.d.). *XL1*. Retrieved August 16, 2021, from Volkswagen Newsroom: https://www.volkswagen-newsroom.com/en/xl1-3588